

Soils Developed in Granitic Alluvium near Merced, California

U.S. GEOLOGICAL SURVEY BULLETIN 1590-A



Soils Developed in Granitic Alluvium near Merced, California

By J.W. HARDEN

U.S. GEOLOGICAL SURVEY BULLETIN 1590-A

SOIL CHRONOSEQUENCES IN THE WESTERN UNITED STATES

DEPARTMENT OF THE INTERIOR
DONALD PAUL HODEL, Secretary

U.S. GEOLOGICAL SURVEY
Dallas L. Peck, Director



UNITED STATES GOVERNMENT PRINTING OFFICE, WASHINGTON : 1987

For sale by the
Books and Open-File Reports Section
U.S. Geological Survey
Federal Center, Box 25425
Denver, CO 80225

Library of Congress Cataloging-in-Publication Data

Harden, Jennifer Willa, 1954—
Soils developed in granitic alluvium near Merced,
California.

(Soil chronosequences in the Western United States)
(U.S. Geological Survey Bulletin 1590-A)

Bibliography: p. A24-A26

Supt. of Docs. No.: I 19.3:1590-A

1. Soils—California—Merced River valley. 2. Soil
formation—California—Merced River valley. 3. Soil
chronosequences—California—Merced River valley. 4.
Granite—California—Merced River valley. 5. Alluvium—
California—Merced River valley. 6. Geology—California—
Merced River valley. 7. Geology, stratigraphic—Cenozoic.
I. Title. II. Series: Soil chronosequences in the Western
United States. III. Series: United States. Geological
Survey. Bulletin 1590-A.

QE75.B9 no. 1590-A
[S599.C2]

557.3s
[551.3'05]

86-600047

FOREWORD

This series of reports, "Soil Chronosequences in the Western United States," attempts to integrate studies of different earth-science disciplines, including pedology, geomorphology, stratigraphy, and Quaternary geology in general. Each discipline provides information important to the others. From geomorphic relations we can determine the relative ages of deposits and soils; from stratigraphy we can place age constraints on the soils. Field investigations and mineralogic and sedimentologic studies provide information on the nature and types of deposits in which soils form. As a result of our work, we have estimated rates of soil formation, inferred processes of soil formation from trends in soil development with increasing age, and obtained information on the types of weathering that occur in various areas. In return, soil development and soil genesis have provided data on the age of landforms, the timing and duration of sedimentation, and, in some cases, the history of climatic fluctuations.

Between 1978 and 1983, a coordinated and systematic study was conducted on soil development in different types of geologic deposits in the Western United States. The goals of this project, led by the late D.E. Marchand and subsequently by M.N. Machette, were to learn whether rates of chemical, physical, and mineralogic transformations could be determined from soil chronosequences; how these rates vary in different mineralogic and climatic environments; and how accurately soils can be used for such problems as estimating the ages of deposits, periods of landscape stability, and timing of fault movements. This series of reports presents data from several soil chronosequences of that project.

More than 100 analyses on more than 1,000 samples were performed on soils collected in the Western United States. Some results have appeared in various books, journals, and maps (for example, Harden and Marchand, 1977, 1980; Burke and Birkeland, 1979; Dethier and Bethel, 1981; Marchand and Allwardt, 1981; Meixner and Singer, 1981; Busacca, 1982; Harden, 1982a, b; Harden and Taylor, 1983; Machette, 1983; Machette and Steven, 1983; Busacca and others, 1984; Machette and others, 1984; Reheis, 1984). In the reports in this series, the basic field information, geologic background, and analytical data are presented for each chronosequence, as well as some results additional to the previous publications.

One of the most significant aspects of these chronosequence studies is that in every study area, many soil parameters change systematically over time, or with the age of deposits. As Deming (1943) emphasized, it is this recurrence of correlation in such different conditions that is most significant to geologic and pedologic studies. In relatively moist areas, such as coastal and central California, such soil properties as percent clay or reddening of soil colors change most systematically over time. In more arid regions, such as in the Bighorn Basin of Wyoming, calcium carbonate and gypsum contents best reflect the relative ages of the deposits. A few parameters—for example, elemental composition of sands or clays—appear to be comparable between areas so diverse in climatic setting.

Numeric age control has enabled us to estimate rates of soil development. In some places, we have been able to compare rates between different areas. For example, in central California, rates of clay accumulation were found to be most rapid during the initial stages of soil development; these rates declined with increasing age. The straightest lines for regression were on a log-log scale. In coastal California, rates of clay accumulation appeared to be much higher than in central California. This difference in rates could be due to parent material (the coastal soils that we studied were formed on reworked shale and sandstone, whereas central California soils were developed in granitic alluvium), and (or) the differences in rates could be due to eolian additions of clay. In the Bighorn Basin of Wyoming, rates of clay accumulation, as well as most other soil properties, increased linearly over time, with no apparent decrease in initial rates.

The data we present here suggest many opportunities for further interpretation. For example, we may learn how climate, vegetation, and mineralogy affect the rates of clay formation or organic-matter accumulation. In some study areas, we present data for rare-earth elements, which could be used to examine how each element reacts in different weathering environments. These examples are only a fraction of the possible future studies that could be conducted on the data presented here.

J.W. Harden
Editor

CONTENTS

Foreword	III
Abstract	A1
Introduction	A1
Geographic setting	A2
Geologic setting	A2
Previous work	A2
Origin of deposits and regional late Cenozoic stratigraphy	A4
Age control on alluvial units	A5
Post-Modesto deposits	A5
Modesto Formation	A5
Riverbank Formation	A7
Turlock Lake Formation	A9
China Hat Gravel Member of the Laguna Formation	A9
Provenance for Merced River deposits	A10
Evaluation of soil development	A10
Site selection and sampling criteria	A10
Assumptions and methods	A11
Trends of soil development with increasing age	A12
Major- and trace-element chemistry	A13
Relative rates of element loss	A13
Methods for an accumulation series of elemental oxides	A14
Methods for calculating loss percents of elemental oxides	A15
Resulting orders of rates of element loss	A17
Estimating rates of soil development	A17
Discussion	A20
Summary	A22
References cited	A24
Supplementary tables	A27

FIGURES

1. Map of central California, showing location of study area A3
2. Geologic map showing late Cenozoic deposits along the Merced River A6
3. Profiles of Merced River terraces, showing sample localities A9
- 4-7. Plots of:
 4. Ratio of pyroxene to zircon grains in the very fine sand fraction of C horizons of Merced soils A11
 5. Etching scale of hornblende and zircon grains from the very fine sand fraction of Merced soils A11
 6. Examples of soil properties that develop over long timespans and for the initial timespans A13
 7. Examples of soil properties that show changes after 100 ka A14
8. Chart showing examples of method for deriving an accumulation series for relative rates of element loss or gain A15
- 9-12. Plots of:
 9. Element percent loss from A and B horizons for three size fractions versus best-estimate age A18
 10. Rates of soil-property development for three timespans A19
 11. Clay content versus age A22
 12. Example of estimating age from soil development A23
13. Map of study area in central California, showing locations of sample sites A29

TABLES

1. Generalized map units and taxonomic classes of soils of the Merced chronosequence **A4**
2. Age controls for alluvium in the northeastern San Joaquin Valley **A8**
3. Variation of rates of element loss from the A-horizon silt-plus-clay fraction, with age uncertainties considered **A16**
4. Order of rates of element loss from size separates **A19**
5. Tests for constraining rates of soil development for late Cenozoic deposits **A20**
6. Tests for constraining rates of soil development for Holocene deposits **A21**
7. Tests for constraining rates of soil development for Pleistocene deposits **A23**
8. Comparison of Pleistocene and Holocene rates of soil development from tables 6 and 7 **A23**

SUPPLEMENTARY TABLES

1. Field descriptions **A28**
2. Physical properties **A34**
3. Extractive chemical analyses **A37**
4. Mineralogy **A42**
5. Total chemical analyses of the fine (less than 47 μm) fraction by X-ray fluorescence **A45**
6. Total chemical analyses of the less-than-2-mm fraction by X-ray fluorescence **A49**
7. Total chemical analyses of the fine (less than 47 μm) fraction by instrumental neutron activation **A53**
8. Total chemical analyses of the less-than-2-mm fraction by instrumental neutron activation **A60**

Soils Developed in Granitic Alluvium near Merced, California

By J.W. Harden

Abstract

Terrace and fan deposits along the Merced River in the San Joaquin Valley, Calif., have been approximately dated and range in age from about 0.2 to 3,000 ka. Soils were sampled on nine deposits to establish a soil chronosequence in an area with a Mediterranean climate, grassland vegetation, and sandy granitic parent material. Soil samples were analyzed for several morphologic, chemical, physical, and mineralogic properties, many of which vary systematically with age. Properties showing the most systematic changes over time include: (1) field descriptions of clay films, total texture (texture plus wet consistence), rubification (color hue plus chroma), and dry consistence; (2) depletion or concentration of Ca, Mg, Na, Fe, Al, and Ti relative to Zr, the most stable constituent; and (3) other physical and extractive-chemical characteristics, including clay mineralogy, dithionite- and oxalate-extractable Fe content, and total (titratable) soil acidity. Changes in soils over the 3,000-ka age span demonstrate that significant chemical differentiation, mineralogic transformations, and morphologic changes occurred as a result of soil development. The high correlation of soil characteristics with age provides a means to use the soils for correlating and dating late Cenozoic deposits.

INTRODUCTION

Alluvium in the northeastern San Joaquin Valley, Calif., offers an opportunity to study soils in an exceptionally well dated, widely spanned age sequence. Nine principal units of terrace and fan deposits range in age from about 0.2 to 3,000 ka; the ages of many of these deposits have been established or approximated by radiometric dating. Deposition of each unit was relatively rapid; major depositional events were separated by periods of stream

entrenchment and slow sedimentation (hiatuses). Older, nested terrace and fan deposits are isolated above modern stream channels and flood deposits, and as a result, the ages of many of these deposits (particularly the Pleistocene deposits) closely approximate those of the surfaces and soils. In this study, soils along the Merced River were sampled in relatively flat, grass-covered areas, and a soil chronosequence was established; that is, the soils differ in age but appear to have formed under similar conditions of climate, vegetation, slope position, and parent material (Jenny, 1941).

Both the soils and geology in the Merced area have been mapped and studied in detail by Arkley (1962a, b) and Marchand and Allwardt (1981); their work is carefully reviewed here to evaluate radiometric ages and site-specific data that affect interpretation of the soil chronosequence. For example, uncertainty of age assignments is analyzed in this report, and soil-development rates are estimated by considering the uncertainties in radiometric ages (and their relation to surfaces and soils). These rates are estimated for several soil parameters, including morphologic, bulk or total chemical, and extractive-chemical characteristics. The morphologic characteristics have been reported previously (Harden, 1982a) but are reexamined in this report to provide a more complete discussion of the soils. Other data are presented here for the first time.

The wide age range represented by the chronosequence of this study permits an evaluation of the time dependence of soil (and soil property) development. Some soil characteristics, such as color hue and chroma, clay mineralogy, and the morphologic soil-development index (Harden, 1982a), change systematically over time. Other properties, including clay films and percent loss of certain elements from size separates, change significantly in the older Pleistocene and Pliocene soils. Another set of characteristics, including organic-carbon content and dry consistence, change systematically in the younger Holocene and latest Pleistocene soils.

Acknowledgments.—Innumerable people played important roles in the planning, excavation, analytical, and interpretative stages of this work. My project leader, the late Denis Marchand, conducted the geologic investigations and guided and supported this study throughout most of its history. M.J. Singer, A.J. Busacca, R. Meixner, and Peter Janitzky not only conducted many of the soil analyses but also contributed many ideas and tests in the planning and execution of the work. E.M. Taylor was fundamental in all of the data compilation and contributed many ideas toward data analysis and future studies. C. Terhune and S. Walker spent countless hours in organizing the data presentation. M.N. Machette accepted and succeeded in the difficult task of continuing leadership of this work after the loss of Marchand. R. Mark contributed many ideas to the methods of data analysis and helped identify limitations that might be overcome in future work. G. Dembroff helped with some of the calculations. In conjunction with my doctoral dissertation, R.J. Arkley, Hans Jenny, H.E. Doner, and Clyde Wahrhaftig were helpful in their guidance and encouragement of this work. B.F. Atwater encouraged consideration of the effects of age uncertainties, which clearly strengthened the arguments and their validity. K.L. Pierce helped to clarify many of the main points of the manuscript, and J.C. Tinsley encouraged presentation of these ideas. Last, I thank the landowners of my excavation sites, without whom I could not have proved worthy of spending wisely the taxpayers' money: thanks go to the J.J. Stevinson Corp., M. Cotta, F. Moiser, R. Jones, C. Matheson, R. Armstrong, M. MacNeilson, L. Roedner, A. Spence, Mrs. A. Arkelian, Turlock Lake State Park, and the Circle J Ranch.

GEOGRAPHIC SETTING

The Merced River heads in the Sierra Nevada and flows through the Sierran foothills and the eastern San Joaquin Valley before joining the lower San Joaquin River to the west (fig. 1). The Sierra Nevada, glaciated several times during the Pleistocene, is underlain by granitic and dioritic rocks. Glacial outwash of the Merced River is the parent material for most of the soils discussed in this study; with the possible exception of Holocene alluvium, it is composed of granitic debris and minor mafic minerals derived from the metamorphic terrane of the foothills.

The study area has a Mediterranean climate in which most of the rain (mean annual precipitation, 30 cm) falls during the cool winters. Because evapotranspiration is low during the rainy season, rainfall is effective in penetrating and leaching the soil. During the dry summers, the soils are readily desiccated by evapotranspiration. The effective wet-dry cycles constitute a xeric soil-moisture regime (Soil Survey staff, 1975). The mean annual temperature near the study area is about 16 °C, and the soil-temperature regime is thermic (Soil Survey staff, 1975).

GEOLOGIC SETTING

Previous work

In the 1950's, R.J. Arkley mapped the soils in much of the northeastern San Joaquin Valley (Arkley, 1954, 1962b) and began to elucidate the relation between soil development and the surficial geologic deposits in this area (table 1). Arkley (1962a, p. 3) differentiated soils developed in "recent alluvium, young alluvium, moderately old alluvium, high terrace gravels, and very high terrace gravels," and proposed a glacial origin for the deposits along the major streams heading in the Sierra Nevada. Davis and Hall (1959) used Arkley's mapping and designated three Pleistocene formations, which they named, from youngest to oldest, the Modesto, Riverbank, and Turlock Lake Formations.

The influence of Quaternary glaciations in the Sierra Nevada on deposition in the valley became widely recognized when Arkley (1962b), Wahrhaftig and Birman (1965), and Janda and Croft (1967) compared the glacial sequence of the Sierra (Blackwelder, 1931, 1932; Birman, 1954, 1957, 1964; Matthes, 1960; Birkeland, 1964) with the alluvial, glaciogenic sequence of the valley. Glacial deposits are not well preserved on the west slope of the Sierra, but similar (major unit) time stratigraphies and rock compositions are found in deposits along glaciated river drainages in both the Sierra Nevada and the San Joaquin Valley. Janda and Croft also used (1) the stratigraphy of subsurface cores in a confined basin, (2) available radiometric ages correlating valley units with glacial deposits, and (3) the regional similarity of glaciated river drainages in the northeastern San Joaquin Valley to link the origin of alluvial fans to glaciation in the Sierra Nevada. Janda (1965, 1966) and Janda and Croft (1967) subdivided the Modesto and Turlock Lake Formations on the basis of erosional unconformities and buried soils; with extensive fieldwork and limited age control, they proposed a sedimentation model of several cyclical, climatically induced periods of alluviation separated by periods of nondeposition and soil formation.

Helley (1966) extended Janda's (1966) model to the unglaciated Chowchilla River basin in the San Joaquin Valley. Helley's stratigraphy is strikingly similar to that of the glaciated river basins nearby, and he concluded that alluviation in the Chowchilla drainage nearly coincides with alluviation in these glaciated river drainages. Helley further inferred that sedimentation over much of the San Joaquin Valley was probably induced by changes in erosion rates, landscape stability, and precipitation patterns of climatic origin which also were manifest as cycles of Sierra Nevada glaciation.

In the late 1970's, D.E. Marchand mapped the late Cenozoic deposits between Bakersfield and Stockton (including the Merced area) and established a widespread regional time stratigraphy that emphatically supports a climatic control on sedimentation in the eastern San Joaquin Valley. Marchand used the soil maps by Arkley (1962b), Ulrich and Stromberg (1962), and Huntington (1971) to examine soil differences in relation to geomorphic landform

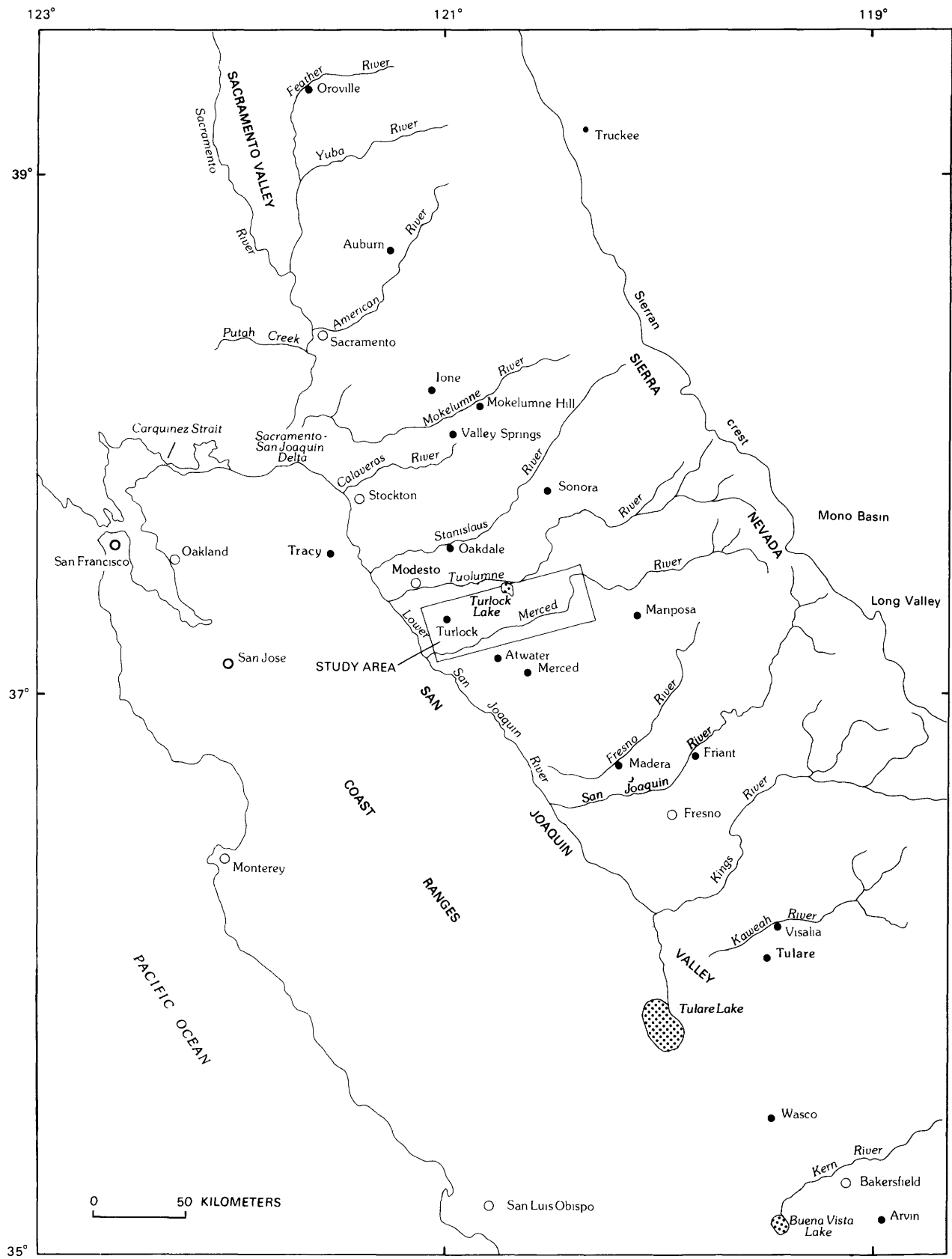


Figure 1. Central California, showing location of study area.

Table 1. Generalized map units and taxonomic classes of soils of the Merced chronosequence

[Units and approximate ages from Marchand and Allwardt (1981). Soil series from Arkley (1984). Taxonomic subgroups from Soil Survey staff (1975)]

Unit	Approximate age (ka)	Soil series	Taxonomic subgroup
Post-Modesto deposits-----	0.2-3.0	Grangeville, Hanford-----	Typic xerorthent.
Modesto Formation			
Upper member-----	10	Hanford, Honcut-----	Do.
Lower member-----	40	Greenfield-----	Typic haploxeralf.
Riverbank Formation-----	100-300	Snelling-----	Do.
Turlock Lake Formation			
Upper member-----	600	Montepellier-----	Do.
China Hat Gravel Member of the Laguna Formation.	3,000	Corning (acid variant)----	Utic palexeralf.

differences. From detailed mapping of the geology on large-scale maps (Marchand, 1976b, c, d, e, f, g) and from additional radiometric ages (Marchand and Allwardt, 1981), Marchand (1977) (1) concurred with the sedimentation models of Arkley (1962a), Helley (1966), and Janda and Croft (1967); (2) subdivided the Pleistocene formations into even more units than Janda and Croft (1967) had recognized; and (3) extended the climatic model of sedimentation to correlate with other climatic histories recorded in continental and marine records. Marchand (1976b, c, d, e, f, g) separated as many as 24 mappable units but fewer time-stratigraphic units, 9 of which were sampled for this soil-chronosequence study. Although Marchand used soils to help recognize and map the alluvial deposits, each of the nine units chosen for this study was also recognized on the basis of (1) geomorphic expression of terrace and fan surfaces, (2) buried soils and unconformities, and (3) regional extent along different river systems within the eastern San Joaquin Valley. Thus, major regional rather than local control of sedimentation was identified.

The late Cenozoic history and chronology of the San Joaquin Valley as defined by Marchand (1977) and Marchand and Allwardt (1981) were used in this study for the chronology of Merced River deposits in this study. Some new ages are available and have been added to this report. Most of the radiometric ages reported here were determined on deposits correlated with those along the Merced River. Discussions of regional geology and age control are included below; in addition, more site specific details are discussed for the Merced area, in the context of the regional mapping.

Origin of deposits and regional late Cenozoic stratigraphy

Throughout the eastern San Joaquin Valley, tectonic uplift and tilting and cyclical patterns of sedimentation have created a sequence of nested

Quaternary alluvial terraces that are incised into older units near the Sierran foothills and open into alluvial fans to the west. Successively younger fans spread westward over older fans; thus, many alluvial units grade westward from surface to subsurface expression (Marchand and Allwardt, 1981). Tectonic uplift and tilting of the Sierra Nevada are shown by depositional and erosional gradients in Tertiary and Quaternary units that increase with increasing age (Marchand, 1977; Huber, 1981). Westward shift of fan apices in the Quaternary units over time suggests relative subsidence of the valley, a tectonic trend demonstrated by Croft (1968, 1972) in subsurface lacustrine deposits.

Although tilting and uplift of the Sierra Nevada have occurred during the late Cenozoic, several lines of evidence support a climatic control on pulses of alluviation in the eastern San Joaquin Valley. Janda and Croft (1967, p. 175) discounted eustatic control on deposition because alluvial units are found along the Kings and Kaweah Rivers, which drain internally into the Tulare Lake basin; similar stratigraphies in open and closed drainages indicate that sedimentation was not controlled by eustatic fluctuations in sea level. Janda and Croft discounted a tectonic origin for alluvial-fan deposition for the following two reasons. (1) Quaternary alluvium predates the last major tilting of the Sierra Nevada, which occurred before deposition of the Turlock Lake Formation. More recently, however, Huber (1981) argued that tectonic deformation has continued and even accelerated during the late Cenozoic, although he also supported a glacial origin of alluvium in Sierran drainages in the San Joaquin Valley. (2) No major unconformities were recognized in the San Joaquin

¹More recently, Atwater and others (1987) proposed that the Tulare Lake basin was not closed during parts of early and middle Wisconsin time.

Basin subsurface to indicate episodic subsidence that would have caused the episodic alluviation found upstream.

As Marchand (1977) and Marchand and Allwardt (1981) indicated, a climatic control of sedimentation is supported by several features. (1) Unweathered granitic silt and very fine sand resembling glacial rock flour are found at the bases of deposits in glaciated drainages (Arkley, 1962a; Janda, 1965) whereas coarse sand and gravel, also typical of glacial outwash, commonly overlie the silt near fan apices. (2) At least two alluvial units, the upper member of the Modesto Formation and the upper unit of the Turlock Lake Formation, are nearly contemporaneous with glacial events. A minimum age for the Tioga glaciation in the Sierra Nevada (Adam, 1967) and ages for the end of the main stage of the Wisconsin glaciation of midcontinental North America (Frye, 1973, p. 277) approximately correspond to the minimum age for the upper member of the Modesto Formation. The upper unit of the Turlock Lake is contemporaneous with the end of marine oxygen-isotope stage 16, a time characterized by glacial conditions (Shackleton and Opdyke, 1976). (3) Uranium-trend ages (Rosholt, 1978, 1980; J.N. Rosholt, written commun., 1978, 1980, 1982) also coincide with the marine record for oxygen-isotope stages (Shackleton and Opdyke, 1976) of the end of glacial conditions.

Age control on alluvial units

The soils in this study compose the following time-stratigraphic units, from youngest to oldest²: post-Modesto deposits; the upper and lower members of the Modesto Formation; the upper, middle, and lower units of the Riverbank Formation; the upper unit of the Turlock Lake Formation; and the China Hat Gravel Member of the Laguna Formation (fig. 2; table 2). Most of the age information is from Marchand and Allwardt (1981), except for some uranium-trend ages reported more recently (J.N. Rosholt, written commun., 1982) and some new ¹⁴C ages obtained by B.F. Atwater (unpub. data, 1984).

Uncertainties in the ages (table 2) are associated both with the regional correlations of units and with local conditions at the sampling sites. Any available ages must be related to the geomorphic surface at the site of soil sampling. Subdivision of the formations is especially subject to uncertainty in the ages; for example, in some areas, multiple terraces in a major unit could represent only a local phenomenon, such as recent aggradation, and thus make regional correlation invalid. A strong argument for subdividing alluvial units on a regional scale is that similar numbers of subunits occur along the major Sierran streams. For example, three surfaces are commonly associated with

the Riverbank Formation; this regionwide repetition of stratigraphy suggests a regional rather than a local control of sedimentation.

A major problem with identification and age assignment of subunits is that they must be correlated by using soil and geomorphic characteristics, which may not differ significantly for the age span considered. A good example of this problem occurs along the Tuolumne River (see Marchand and Harden, 1978), where four subunits or phases all have Hanford soils developed on them within the upper member of the Modesto Formation. Marchand and I distinguished these subunits throughout the quadrangle, but unless all four terrace levels are adjacent to each other, the differentiation is ambiguous, as we indicated by queries on our map. The uncertainty of stratigraphic assignment and correlation with dated localities varies among the different soil-sampling localities. Age control is discussed below, and sampling localities are considered for each stratigraphic unit to assess the reliability of age estimates (table 2).

Post-Modesto deposits

Post-Modesto alluvial deposits are divided into four units, all of which were mapped by Marchand and Allwardt (1981) along major Sierran streams in the northeastern San Joaquin Valley. Post-Modesto IV deposits, not sampled for this study, generally consist of unvegetated alluvium of channels and point bars. Post-Modesto III (PM3) deposits, which form part of the modern flood plains, are 2 to 3 m above the modern stream channels (figs. 2, 3). Although no datable material has been found within post-Modesto III deposits, very mature oak trees on the surface suggest that this surface is more than a few years old. Although I estimated that post-Modesto III deposits are 0.2 ka old (table 2), the surface could be as old as about 3 ka on the basis of the age of post-Modesto II (PM2) deposits, or as young as a few years if there has been recent aggradation on the surface.

Post-Modesto II deposits, extensive along the Merced River near Snelling, form a surface about 3 to 5 m above the modern channel (fig. 3). Marchand and Allwardt (1981, p. 63-64) reported ¹⁴C and U-Th ages that range from about 2 to 4.5 ka, but the dated deposits are situated near Oroville and Stockton. A very conservative maximum age of 8.3 ka (sample Beta-2787) was provided by B.F. Atwater (written commun., 1983) on wood fragments in San Joaquin River deposits below the post-Modesto II surface near the mouth of the Tuolumne River. A more reasonable age estimate for post-Modesto II deposits is about 3 ka (table 2), but the post-Modesto II surface and soil could be younger if covered more recently by flood deposits.

Modesto Formation

The Modesto Formation is divided into two members (Marchand and Allwardt 1981). The upper member, which may include as many as four phases of alluvial filling and incision, may be as old as about 27 to 29 ka at its base and as young as 8 or 9 ka at its

²The U.S. Geological Survey's convention of discussing units in the order of decreasing age is not followed here because this report focuses on the genesis of soils rather than on the evolution of geologic units.

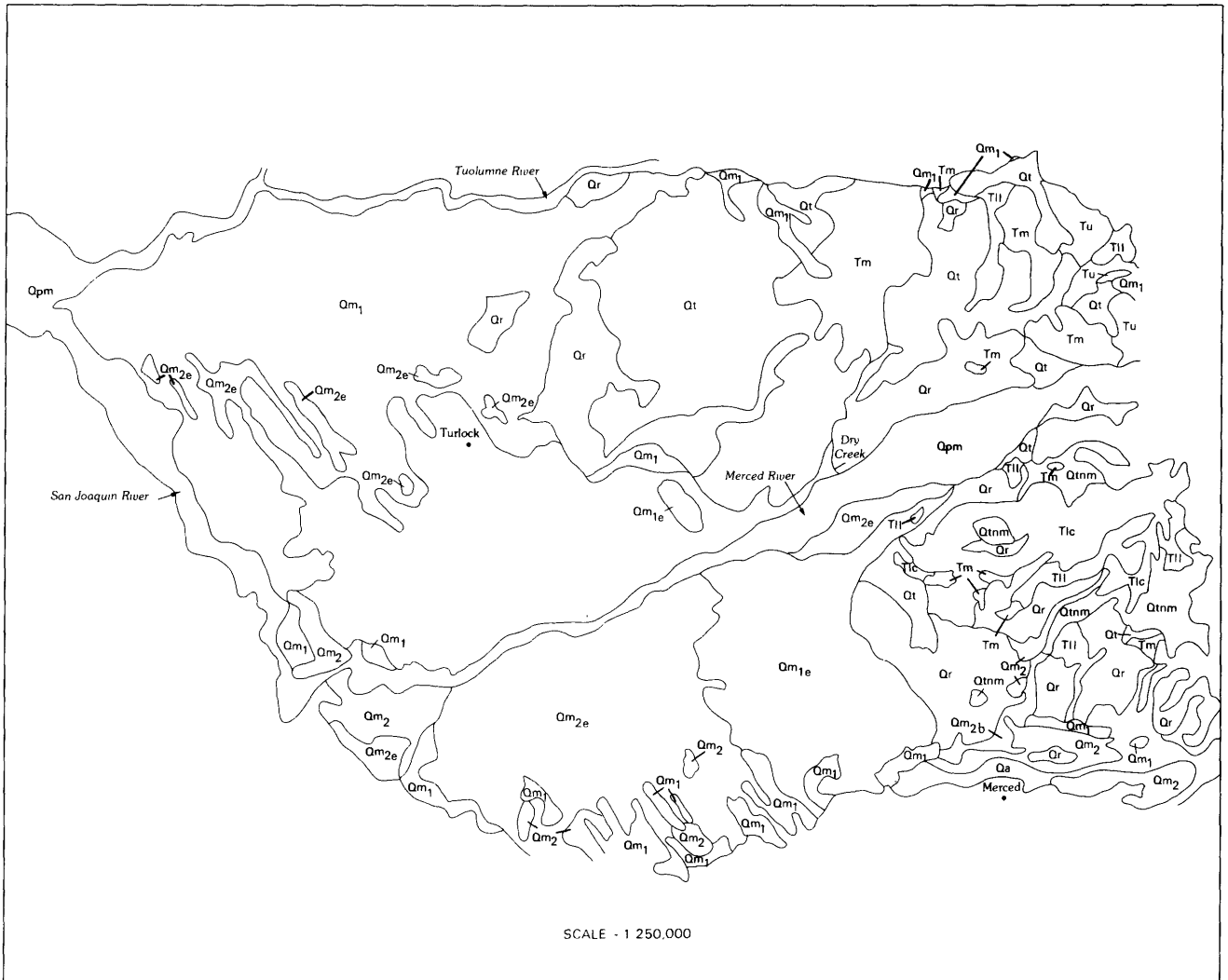


Figure 2. Geologic map showing late Cenozoic deposits along the Merced River. Geology compiled from Marchand (1976a, b, c, d) and Marchand and Allwardt (1981).

surface. The upper member appears to be correlative with the Tioga glaciation, which ended before about 9.8 ka (Adam, 1967), and with the end of marine oxygen-isotope stage 2 of Shackleton and Opdyke (1976). The minimum constraining age of 8.23 ka is based on charcoal in San Joaquin River deposits that are set into the upper member at the toe of the Tuolumne River fan (table 2). The maximum constraining age of 31.24 ka is based on ^{14}C data on charcoal in deposits beneath the same late Modesto fan (table 2). Marchand and Allwardt (1981, p. 57) also cited a constraining (maximum) uranium-series age of about 29 ka by E.L. Begg on bone in basin alluvium mapped by Marchand and Allwardt as the lower unit of the Modesto Formation.

Both soil-sampling localities in the upper member of the Modesto Formation display features which suggest that the surface and soil are within the younger end of the age range of this unit. Site M31 is only 3 m above the modern stream channel (much like

post-Modesto II deposits), and its elevation appears to be somewhat low for the longitudinal profile of the terrace (fig. 3). The surface of site M46 is located along the projected profile of upper-member terraces (fig. 2), but the terrace is incised into, and somewhat younger than, the extensive eolian phase of the upper member (table 1). Both sites M31 and M46 were assigned an age of 10 ka, which corresponds to the closing phase of the glacial stage, but the surface and soils could be anywhere from about 8.2 to 14 ka (table 2).

The age of the lower member of the Modesto Formation is somewhat ambiguous. Marchand and Allwardt (1981, p. 57) referred to the uranium-series age of 29 ka determined by E.L. Begg as a minimum age for the lower member. Atwater and others (1986), in their recent work on the Tulare Lake bed, tentatively correlated it with an early phase of the Tioga glacial deposits of the late Wisconsin glaciation and estimated an age of about 20 to 26 ka. Marchand

EXPLANATION

Qpm	Post-Modesto deposits (Holocene)
	Modesto Formation (Pleistocene)-- Consists of:
	Upper Member-- Divided into:
Qm ₂	Alluvial deposits
Qm _{2e}	Eolian deposits
Qm _{2b}	Basin deposits
	Lower Member--Divided into:
Qm ₁	Alluvial deposits
Qm _{1e}	Eolian deposits
Qr	Riverbank Formation (Pleistocene)
Qt	Turlock Lake Formation (Pleistocene)
Qtnm	North Merced Gravel (Pleistocene or Pliocene)
	Laguna Formation (Pliocene)-- Consists of:
Tlc	China Hat Gravel Member
Tll	Lower part
Tm	Mehrten Formation (Pliocene and Miocene)
Tu	Sedimentary and volcanic rocks, undivided (Tertiary)

Figure 2. Continued

and Allwardt (1981, p. 57) reported a uranium-trend age (Rosholt, 1980) of 95 ± 45 ka on an early Modesto terrace, but this age has been modified because of new calibrations. The revised uranium-trend ages are 42 ± 16 ka for the alluvial terrace (sample M12, fig. 3) and 43 ± 34 ka for the alluvial fan farther downstream (sample M14 of J.N. Rosholt, written commun., 1982). If deposition of the major Sierran streams coincided with the later parts of glacial events, then deposition of the lower member might have coincided with the later part of isotope stage 4, at about 65 ka (Shackleton and Opdyke, 1976). A tentative age of 40 ka was used for terrace deposits of the lower member of the Modesto Formation (table 2), which corresponds to the ages determined by J.N. Rosholt and is in the central part of the estimated age range from 20 to 70 ka.

Riverbank Formation

The Riverbank Formation was divided by Marchand (1976a, b, c, d, e, f; 1977) into three units. The upper unit is separated in the subsurface from the middle and lower units by a disconformity and a buried soil (Marchand and Allwardt, 1981, p. 40). The upper unit was correlated with oxygen-isotope stage 6, on the basis of Marchand's model of sedimentation (Marchand, 1977) and on uranium-trend ages for soil sample R9 of this report (see fig. 3; table 2); its age of 140 ± 40 ka generally coincides with the end of marine oxygen-isotope stage 6 at about 127 ka (Shackleton and Opdyke, 1976). This uranium-trend age, however, does

not overlap the 260 ± 60 -ka uranium-trend age of sample R10 from the middle unit of the Riverbank Formation (table 2), which is compatible with the end of marine oxygen-isotope stage 8 at about 250 ka (Shackleton and Opdyke, 1976). Hansen and Begg (1970) determined an open-system uranium-series age of about 103 ka on bone from within Riverbank deposits at the Teichert Quarry in the Sacramento Valley (Shlemon, 1967). Marchand and Allwardt (1981, p. 41) considered this bone to be within the middle unit but that this age should be regarded only as a minimum for the middle unit. Subsequent uranium-trend data on the unit adjacent to the Teichert Quarry yield an age of 120 ± 40 ka (J.N. Rosholt, written commun., 1982). Because the uranium-trend age corresponds to late Riverbank ages along the Merced River, and because this age does not overlap ages within the middle unit, I believe that the Teichert unit correlates with the upper unit of the Riverbank. In this case, the uranium-series age determined by Hansen and Begg would be a minimum for all units of the Riverbank Formation.

Separation and correlation of the upper and middle units of the Riverbank Formation pose problems in the Snelling area, where the soils were sampled. Sampling sites are from Marchand and Allwardt's (1981) "reference section" for the three subunits, but topographic distribution in the study area may be less clear cut than their geologic map indicates. Topographic profiles of the Riverbank terraces (fig. 3) demonstrate that the upper unit is about 2 to 3 m above the middle unit. Because stream profiles appear to converge below the Merced River-Dry Creek confluence, the surfaces near the sampling sites are difficult to separate. The surfaces of sites R9 and R33 appear to be typical of those of stream profiles of the upper unit, but samples R2, R10, and R32, mapped on the middle unit, occur at low elevations for the middle unit and could be from either the middle or upper unit. One of Marchand's (1977) mapping criteria for subdivision of the Riverbank Formation is that the middle unit is more extensive than the upper and lower units. Apparent convergence of the terrace at sites R2, R10, and R32 with an extensive Riverbank surface along Dry Creek (fig. 2) supports Marchand's original claim that this terrace is one of the middle unit. Differentiation of the Riverbank units is a critical argument for interpreting the soil data because the soils of this study do not notably differ between the middle and upper units. These soils may be similar because they are developed in similar-age deposits, or the rate of soil development in this area may have declined after about 100 to 300 ka. If the sampling sites from the upper and middle units of the Riverbank are actually on the same unit, their age is bracketed by 103 ka as a minimum (U-series age on bone) and by 305 ka as a maximum (oldest U-trend age on the upper and middle units of the Riverbank). These two units, however, were assigned ages of 130 and 250 ka, respectively (table 2), on the basis of the later parts of oxygen-isotope stages 6 and 8 and on J.N. Rosholt's dating.

A minimum age for the lower unit of the Riverbank Formation appears to be provided by a uranium-trend age of about 260 ka on the middle unit; the maximum age is limited by a K-Ar age of about

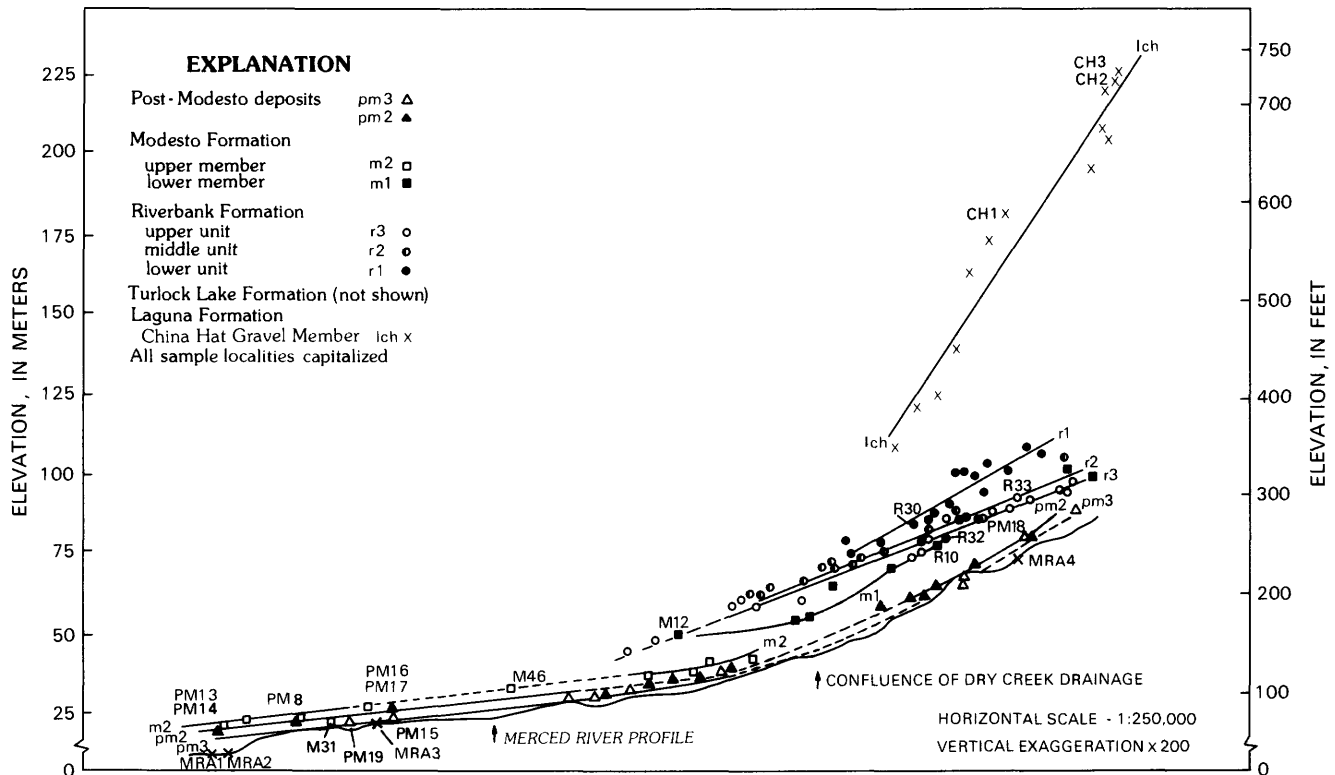


Figure 3. Profiles of Merced River terraces, showing sample localities (see supp. table 1).

615 ka (Janda, 1965, 1966; Dalrymple, 1980) on ash within the Turlock Lake Formation, and by a uranium-trend age of 570 ± 50 ka for the upper unit of the Turlock Lake. Marchand (1977) and Marchand and Allwardt (1981) correlated the lower unit with oxygen-isotope stage 10 but suggested that this unit could also correlate with stage 12. A tentative age of 330 ka was used for this study (table 2) to generally coincide with the later part of marine oxygen-isotope stage 10 of Shackleton and Opdyke (1976).

Turlock Lake Formation

At least two units compose the Turlock Lake Formation; they are separated by a well-developed buried soil at exposures near the town of Friant and in roadcuts near Turlock Lake (Marchand and Allwardt, 1981, p. 26-27). This study includes soil samples from only the upper unit of the Turlock Lake because there are no surface exposures of the lower unit. Janda (1965, 1966) found a pumiceous ash at the base of, and conformable with, the upper unit of the Turlock Lake. This ash, now called the Friant Pumice Member of the Turlock Lake Formation, provides a maximum age for the deposit and has a K-Ar age of 615 ± 31 ka (Dalrymple, 1980). In addition, uranium-trend ages of about 570 and 610 ka (table 2), may indicate ages for about the upper 3 m of the deposit and thus for the surface and soil.

Sampling sites for soils of the upper unit of the Turlock Lake Formation are located along the Tuolumne River where the deposits and surfaces are well defined by mapping criteria. The surface of the upper unit of the Turlock Lake is dissected, and although samples were collected on relatively flat topographic highs, the soils could have been partly eroded. Janda (1965) proposed that dissection of the surface occurred during deposition of the Riverbank Formation, and so the soils of the Turlock Lake deposits would have developed for a few hundred thousand years before dissection and partial erosion occurred.

China Hat Gravel Member of the Laguna Formation

The China Hat Gravel Member of the Laguna Formation, the oldest unit in the study area, occurs as a remnant of a late Tertiary gravel deposit of the Merced River near the town of Snelling (fig. 2). The gradient of the China Hat deposits along the Merced River is considerably steeper than those of younger alluvial units (fig. 3), and paleochannels in the China Hat Gravel Member have a more southerly trend than those in younger alluvial units (Marchand, 1977, p. 39-41).

A maximum age for the China Hat Gravel Member is provided by a vertebrate fauna of latest Hemphillian age (3,000-4,000 ka) from the underlying

Miocene and Pliocene Mehten Formation (Marchand and Allwardt 1981, p. 19). Wahrhaftig and Birman (1965, p. 314, table 2) and Marchand and Allwardt (1981, p. 19) correlated the China Hat Gravel Member with the Pliocene Tuscan Formation in the Sacramento Valley, which includes the Nomlaki Tuff Member, dated at about 3,300 ka near its base. Marchand and Allwardt (1981, p. 19) also correlated the China Hat with gravel deposits in the Kings River, which contain basalt clasts about 3,800 ka old (Huber, 1981, p. 1194). Furthermore, Marchand and Allwardt (1981, p. 19) and Busacca (1982) discussed a magnetic reversal discovered by K.L. Verosub within the Laguna Formation in the Sacramento Valley and tentatively assigned it to the Gilbert Reversed/Gauss Normal Polarity Chrons boundary, at about 3,400 ka. For this study, an age of 3,000 ka was used for the surface; this age is constrained between about 730 ka (magnetic reversal within the younger North Merced Gravel) and 4,000 ka (Hemphillian fossil in the next oldest unit, the Mehten Formation) (table 2).

Soils found in the China Hat deposits were sampled on the flat, relatively uneroded tops of surface remnants. Mima-mound topography (Nikiforoff, 1941) is ubiquitous across the terrace surface, and soils were sampled at the tops of the mounds. Soil excavations revealed many filled animal burrows of different ages, as evidenced by varying degrees of redness, hardness, and clay-film development (see supp. table 1). Gopher activity probably played an important role in the formation of these mounds (Arkley and Brown, 1954). Concentric collapse features were also observed all along a depression (intermound area), suggesting collapse related to chemical loss or to ground-water dissolution (Nikiforoff, 1941).

As discussed above, there are considerable uncertainties in the dating of these surfaces. The uncertainties in both age estimates of the surfaces and in variation of the soils are shown schematically by horizontal and vertical error bars in figures 6, 7, 10, and 11.

Provenance for Merced River deposits

Deposits along the Merced River were chosen for this study to limit the variation in mineralogy of the soil parent material. The Merced River drains about 600 km² of granitic terrane of the Sierra Nevada and about 150 km² of metamorphic and marine sedimentary rocks of the Sierra Nevada foothills.

Holocene alluvium along the Merced River has a larger component of mafic minerals than do older alluvial units, apparently in relation to a climatic control of erosion in the Merced River drainage basin. Janda (1966) discussed the relation of erosion rates in the Sierra Nevada and foothills to the origin of alluvium along the major Sierran streams. Under glacial conditions, most of the erosion and, thus, the sediment supply is from the glaciated headwaters of major Sierran streams. Under interglacial conditions and, possibly, during transitions into or out of glacial events, more erosion takes place in the Sierran foot-

hills, which is underlain mainly by metavolcanic and metasedimentary rocks.

Janda's (1966) conclusions are borne out by the higher content of mafic minerals in Holocene deposits along the Merced River.³ Some mineralogic and chemical trends of the soils developed in Merced River alluvium suggest that the Holocene deposits contain more metamorphic (foothill derived) debris in comparison with the older units. In general, metamorphic rocks of the foothills contain more pyroxene and less zircon than do granodiorites of the Sierra Nevada (Roger, 1966), and the pyroxene/zircon ratio of C horizons is much higher for Holocene (younger than 10 ka) than for older soils (fig. 4). Etching categories of some of the heavy minerals also indicate unusual characteristics of the Holocene soils. In older soils, increase in etching with age indicates systematic weathering of consecutively older units. Clinopyroxene and hornblende grains, however, are more etched in late Holocene than in early Holocene soils (fig. 5), a difference which may indicate that the late Holocene deposits have inherited etched grains from previously weathered sources. The Holocene soils also contain unusually large amounts of total Mg, exchangeable Mg and H, smectites, and oxalate-extractable and total Fe, and have high ratios of fine to total clay (see supplementary tables), which suggest reworking of previously weathered materials rich in ferromagnesian rocks of the foothills.

EVALUATION OF SOIL DEVELOPMENT

Site selection and sampling criteria

Sampling sites had to meet the following requirements to be included in this chronosequence study. Ideally, sites had not been cultivated, had 0- to 3-percent slopes, showed no active erosion, were on well-drained, sandy alluvium, and had a grassland vegetation. The requirement that excluded the largest area was cultivation. Most of the eastern San Joaquin Valley is intensely cultivated, typically including grading of surfaces, plowing of the upper half-meter of soil, and addition of large amounts of fertilizers, herbicides, and other soil amendments. All sampling sites in the study area were free from major grading, some sites had been farmed lightly, and all sites had been grazed by livestock at some time in the historical past.

³Although alluviation along major streams may have coincided with Holocene glaciations in response to climatic fluctuations (Marchand and Allwardt, 1981), alluvial deposits in the valley were probably derived primarily from the metamorphic rocks in the foothills. Several late Holocene moraines are still confined to the high alpine areas on the west slope of the Sierra Nevada (Curry, 1969; Yount and others, 1982), and preservation of these moraines indicates that the granitic debris was not captured by western drainages.

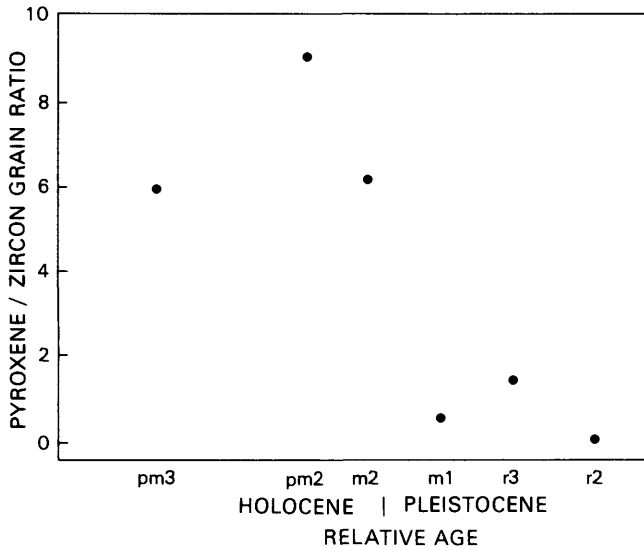


Figure 4. Ratio of pyroxene to zircon grains in the very fine sand fraction of C horizons of Merced soils. See table 2 for map units; data listed in supplementary table 4.

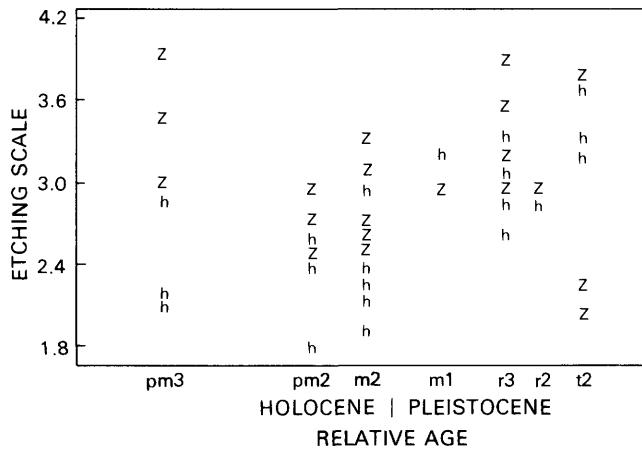


Figure 5. Etching scale of hornblende (h) and zircon (Z) grains from the very fine sand fraction of Merced soils. Etching scale after Gillam and others (1977).

Another requirement that excluded many potential sites was internal (vertical) drainage. Many soils in the Central Valley have hardpans cemented by carbonates, iron oxides, or silica that greatly affect the movement of soil water. Such hardpans may have formed as a result of initial stratification or drainage boundaries in the soil parent material (Marchand, 1976a; Harden and Marchand, 1977). Soils with hardpans were avoided in this study so as to compare only well-drained soils. All sites were sampled on topographic highs with slopes of 0 to 3 percent.

Further requirements of uniform vegetation and uniform parent-material texture were generally met, as outlined in figure 2 and generalized below for the

study area. Sampling pits were excavated by backhoe or by hand, or sampled along a roadcut or bluff (in which case the site was dug at least a meter inward from the exposed vertical cut). Soils were sampled at least to the depth of the B3 (BC) horizons. Soils were described in the field (Soil Survey staff, 1962) and analyzed for several chemical, physical, and mineralogic properties; most of the analyses were described in detail by Singer and Janitsky (1986):

<u>Soil-forming factor</u>	<u>Description</u>
Climate-----	Xeric moisture regime (mean annual precipitation, 30 cm), thermic temperature regime (mean annual temperature, 16 °C).
Vegetation-----	Perennial, annual grasses, scattered oaks (<u>Quercus lobata</u>).
Topography-----	Topographic highs, 0- to 3-percent slopes.
Parent material---	Sand-loamy texture, granitic composition.
Age (ka)-----	0.2-3,000

Assumptions and methods

Some important limitations affect the interpretation of a soil chronosequence. Soil-forming factors other than time differ among the sampling sites, and so the differences in soils would be due not only to age but also to differences in other factors. If the variations in other factors is random within the chronosequence, then trends with increasing age are dominated by time rather than by other factors. For example, if precipitation at the sampling sites increased covariantly with age, then soil differences are due not only to age but also to the precipitation gradient. In the study area, precipitation increases slightly with the age of these soils, but this effect is thought to be minimal. Random differences in soil-forming factors (other than time) among the sampling sites might be an important source of soil variations, and accounting for these variations is likely to improve the age trends.

A similar complexity in a chronosequence is climatic change over time; older soils might have undergone more variations in climate, as well as drier or wetter climates, in comparison with younger soils. In the study area, soils older than those of the upper member of the Modesto Formation underwent at least one full glacial-to-interglacial cycle, and successively older soils underwent successively more cycles—an attribute of cumulative frequency and not necessarily one of differences in inherent precipitation. Because Holocene soils were developed only in Holocene, interglacial climates, important climate-related differences may exist between Holocene and pre-Holocene soils.

Reference to soil processes and pathways of soil development may be misleading if only chronosequence data are considered. For example, a soil property such as clay content may change systematically with age, but older soils may have had clay forming in place, whereas younger soils may have received clay from flood deposits. In addition, the systematicness of a plot of a soil property versus age does not necessarily reflect a continuous process. Because the deposits in this study were apparently generated during similar (late) phases in a climatic cycle, stepwise functions or some other pathway of soil development (such as the "soil-forming intervals" proposed by Morrison, 1967) would not be evident simply from age plots of soil properties. As Yaalon (1975) emphasized, the use of chronosequences to decipher pathways of soil genesis would be improved by smaller increments between the ages of deposits. The rates of soil or soil-property development are useful, but only as an empirical measure of cumulative processes. In figures 6, 7, and 9 through 12, the term "age" rather than "time" is used on the x-axis to emphasize this shortcoming.

Uncertainty in the numerical ages affects the correlation between soil properties and age; this uncertainty is large in most cases (a factor of 2 is typical). The uncertainty, expressed as a percentage, differs between age groups and generally is not centered about the best-estimate ages, and so the errors are not symmetrical. Several different graphical and numerical approaches are used to represent age uncertainties and their bearing on interpretation.

Laboratory-measurement error is small in comparison with the natural soil variation represented by replicate soils on a given terrace (Harden, 1982b; Singer and Janitzky, 1986). As a result, by analyzing replicate soils on given deposits, soil variation encompasses the smaller laboratory error.

Trends of soil development with increasing age

Some soil properties develop rapidly or regularly within a given age interval, before or after which the properties decline or do not develop with age, or show irregular age trends (figs. 6, 7). Possible intermittent action of soil processes over long timespans results in a time dependence of soil-property development. Soil properties are discussed below according to the processes that may be time dependent, although such time dependence is hypothetical and limited by the numerous assumptions discussed above.

Clay content, rubification (figs. 6A, 6B), iron oxide content (fig. 7C) and the soil-development index (explained in detail for these soils by Harden, 1982a) increase throughout the 3,000-ka age span of these soils. These four properties increase most strikingly at first, then increase more slowly during later stages (older units) of soil development. Soil-property curves are bowl shaped if plotted against age on a log scale, and straighten when plotted as log (soil)-log (age) functions. Development of these properties is clearly nonlinear over such long timespans.

For young (as old as 10 ka) deposits of the Merced area, organic-matter content increases with

soil age. Soils of this age range can be differentiated on the basis of their carbon content and by darkening and thickening of the A horizons, represented by melanization (fig. 6C). Although all soil characteristics vary somewhat, owing to stratification of the alluvium, strata in the upper meter are mixed by biotic (animals and plant roots) and mineralogic (swelling of grains) processes and weather fluctuations (freeze-thaw, shrink-swell). After about 10 ka, organic-carbon content and melanization generally decline irregularly with age, possibly in relation to a decline in soil fertility and in response to the climatic changes that are inherent in the trends of older soils.

After stabilization of the surface, soil structure forms (see supp. table 1), and peds become harder or firmer as binding agents develop, such as sesquioxides and organic matter. Buildup of binding agents is evident from the increase in hardness as measured by dry consistence of soils younger than about 100 ka (fig. 6D). Most of the structure and hardness in young (Holocene) soils develop in the A horizons, whereas in older (Pleistocene) soils, further changes occur mostly in the B horizons. After about 100 to 600 ka of soil development, consistence and structure apparently reach a maximum state of development, whereafter structure and consistence generally decline unsystematically. Commensurate with the development of consistence and structure in these soils, bulk density begins to increase within a few hundred years of surface stabilization, and then reaches a maximum after about 100 to 300 ka (see supp. table 2).

Properties related to clay formation⁴ and translocation and to soil acidity develop most noticeably in soils older than about 100 ka. Although the total clay content increases in both young and old soils (fig. 6B), morphologic evidence for increase in clay content is unclear until sometime between about 10 and 100 ka, as indicated by increases in clay films (fig. 7B) and total texture. Soil acidity, indicated by pH lowering in figure 7D, develops mostly between about 600 and 3,000 ka.

Most physical and morphologic properties appear to be unaffected by mineralogic differences in the parent materials, as evidenced by smooth, systematic age curves through the Holocene to Pleistocene. Some soil parameters, however, particularly those measured by chemical analyses, appear to be highly sensitive to the mineralogic differences between deposits. Age trends of dithionite-extractable Fe (fig. 7C) demonstrate the difference between Holocene and pre-Holocene deposits. Most chemical analyses must be evaluated separately for these two age groups because the parent materials differ. Although the total-chemical analyses are discussed below only for Pliocene and Pleistocene age ranges, the same processes clearly must have occurred during the Holocene as well (there have been considerable

⁴Increase of kaolinite content over time suggests that this clay mineral is forming in these soils (see supp. table 4).

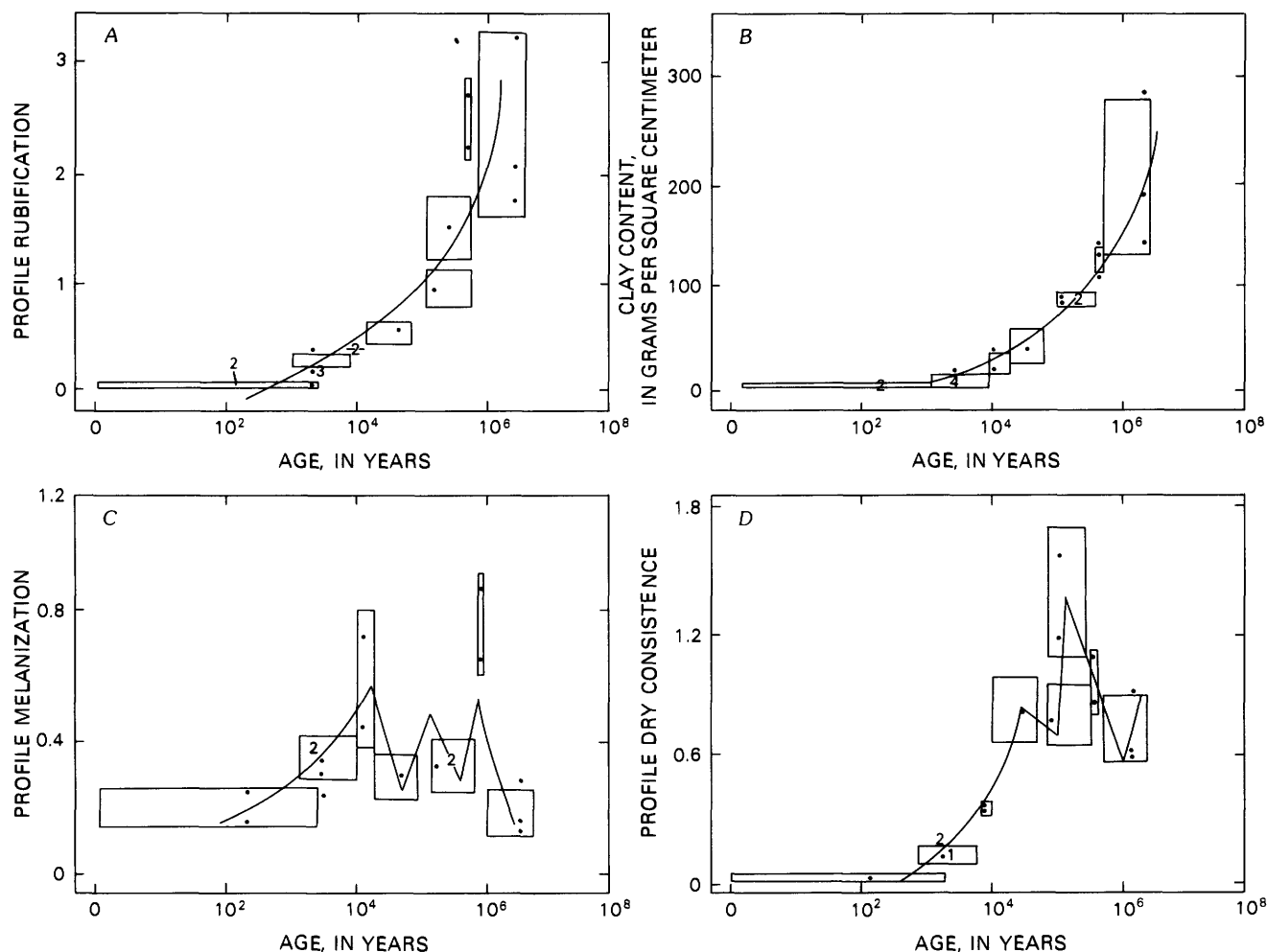


Figure 6. Examples of soil properties that develop over long timespans (A, B) and for initial timespans (C, D). A, Rubification. B, Clay content. C, Melanization. D, Dry consistence. Points and numbers indicate number of samples and best-estimate ages. Vertical

dimension of boxes indicates one standard deviation for replicate soil profiles on same surface; horizontal dimension indicates total age uncertainty (table 2). Field properties in figures 6A, 6C, and 6D from Harden (1982a).

transformations in the youngest Pleistocene soil, which shows no evidence of reworked, preweathered parent material).

major-elemental composition of the A-horizon silt plus clay are used to demonstrate the methods used for data interpretation.

Major- and trace-element chemistry

Two size fractions, 2 mm (whole soil) and silt plus clay (fine), were separated and analyzed for total amounts of major and trace elements. Major elemental oxides were determined by X-ray fluorescence (see supp. tables 5, 6), and trace elements were determined by instrumental neutron activation (see supp. tables 7, 8). The composition of the sand fraction was also determined by calculating the difference between the whole-soil and fine fractions. Samples chosen for analysis generally include the lowermost A1 horizon, the B horizon containing the most clay, and the lowermost C horizon. Trends in

Relative rates of element loss

The concentrations of major elements change profoundly over the 3,000-ka age span of these soils. Greater understanding of these changes requires that actual losses or gains of an element be distinguished from apparent changes caused by the opposite loss or gain of other constituents. Two methods were devised to determine the losses and gains of elements over time. The first method, referred to as the accumulation-series method, examines elemental ratios over time; the second method, referred to as the net-loss method, uses Merrill's (1906) loss equation, in which a stable constituent and a standard are defined for

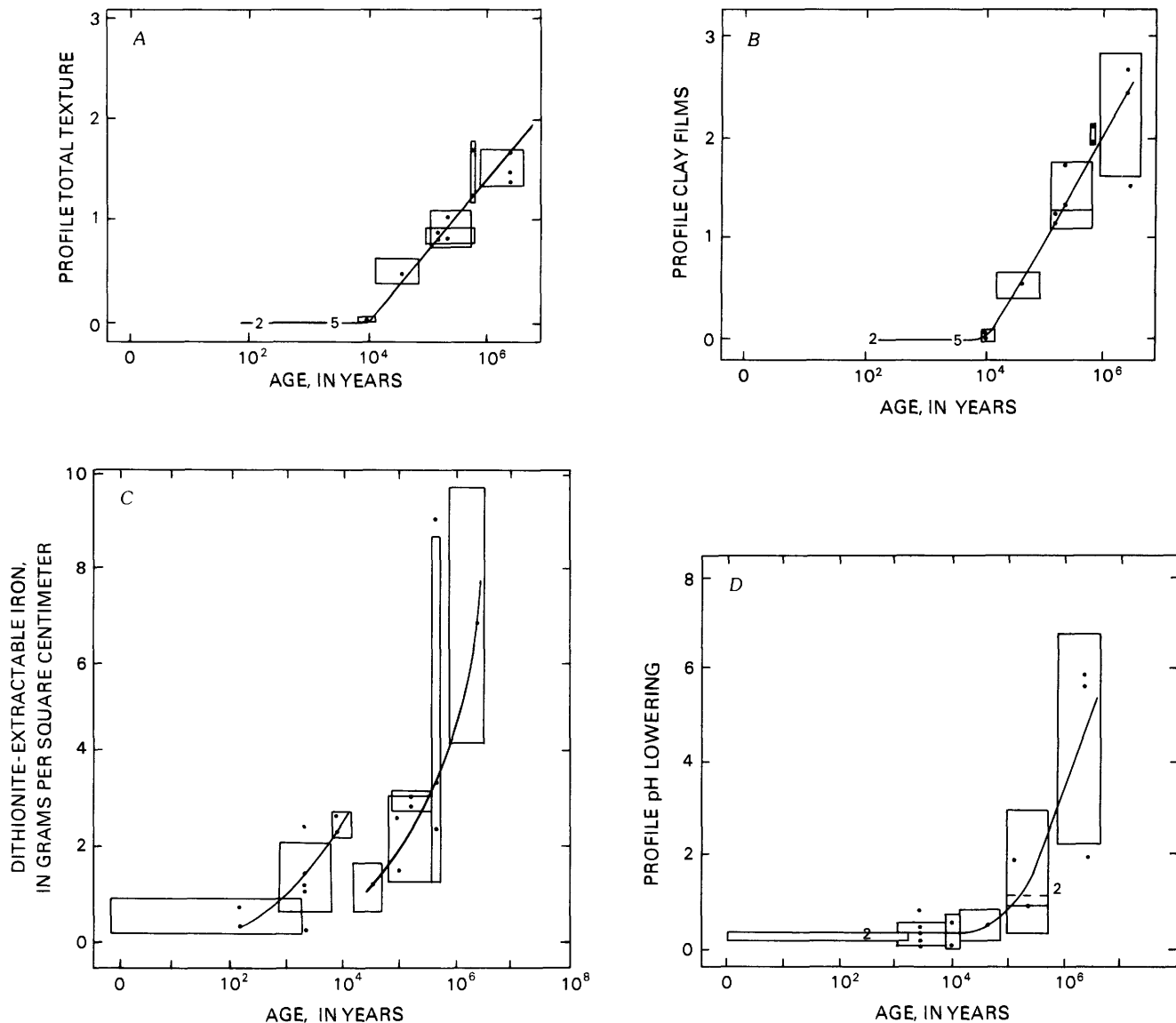


Figure 7. Examples of soil properties that show changes after 100 ka. A, Total texture. B, Clay films. C, Dithionite-extractable Fe. D, pH lowering. Vertical dimension of boxes indicates one standard deviation for replicate soils on deposit; horizontal dimension of box indicates total age uncertainty (table 2). Field properties in figures 7A and 7B from Harden (1982a).

calculating actual losses (positive values) or gains (negative loss values) of other constituents. Both methods allow for net loss or net gain of elements.

Methods for an accumulation series of elemental oxides

In the accumulation-series method (fig. 8), a ratio of two elements is tested for significant increases or decreases with age. The order of

accumulation or depletion of elements is obtained by comparing the concentration of each element to that of every other element in a ratio and by tabulating the consecutive order of accumulation or depletion. The term "accumulation" is used here because it can mean net gain or only apparent gain by loss of other constituents. Net depletion or dilution by other elements can also cause relative accumulations. Rank correlation is used to test the age trends in which elemental ratios and age are both ranked from low to high categories. The (ranked) elemental ratio is then regressed against the (ranked) age. In this case, only the relative age

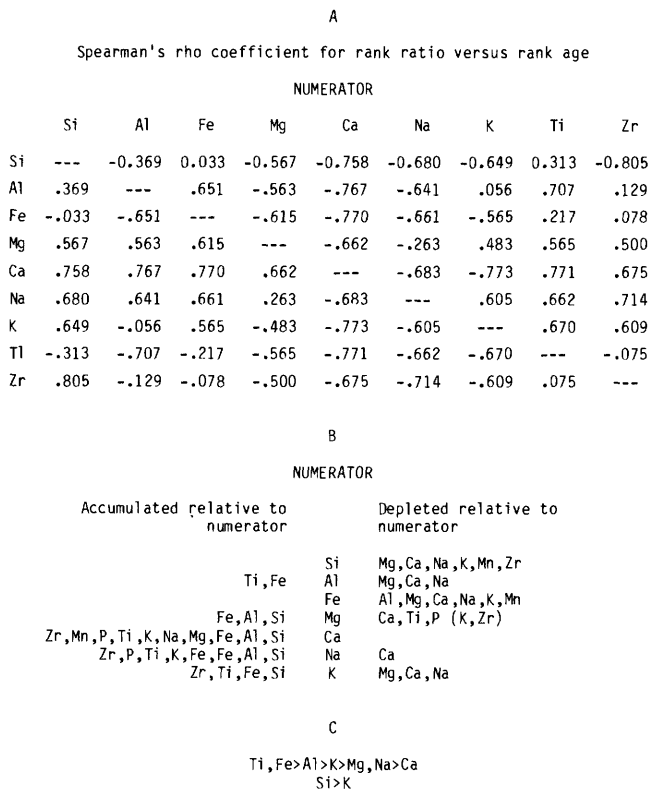


Figure 8. Example of method for deriving an accumulation series for relative rates of element loss or gain. A, Element ratios for A-horizon fine fraction, ranked and regressed against ranked age for Spearman's rho correlation. B, Element ratios listed as accumulated or depleted if significant at 5-percent-confidence level ($r \geq 0.66$). Numbers in parentheses, significant at 5- to 10-percent-confidence level. C, Series tabulated for relative rates of accumulation, with highest rates to left or most depleted to right.

must be known to determine the relative rates of element loss. The resulting correlation, or Spearman's rho coefficient (Tate and Clelland, 1957), is then a test for whether or not the elemental ratio changes significantly with relative age. Figure 8 illustrates this procedure. If an elemental ratio increases significantly with age, then the element in the numerator is said to accumulate relative to the element in denominator. A decreasing ratio indicates the reverse; if the ratio does not change significantly over time, the trend is not considered to be pedologically significant.⁵

⁵A constant ratio would infer that the elements are lost or gained at the same rate. Typically, however, when ratios do not change significantly with age, there is considerable scatter in the regression. Such scatter is likely to be caused by parent-material variation; therefore, statistical tests consider only significant changes with age.

For the silt-plus-clay fraction of the A horizons, Spearman's rho coefficients were determined for each (ranked) elemental ratio versus (ranked) age. For each element, the correlations of its ratio to the other elements are evaluated. If the ratio changes significantly (at the 5-percent-confidence level), then the relative loss or gain is tabulated (fig. 8B) by listing decreases with age to the right and increases to the left of the numerator (center column, fig. 8B). Elements listed to the right may be lost more rapidly or gained more slowly than a given element; elements listed to the left are either lost more slowly or gained more rapidly than the given element. The accumulation series of all elements is then tallied with accumulated or concentrated constituents to the left of other elements. For the A-horizon silt-plus-clay fraction, Fe, Ti, Si, and Al increase, and the alkaline-earth elements are depleted, relative to Zr (a stable constituent; fig. 8C).

Methods for calculating loss percents of elemental oxides

Rates of element loss or gain can also be determined by using Merrill's (1906) loss equation, in which a stable or resistant species and an unweathered parent material are used as standards to monitor net changes in other constituents. For relative rates of element loss, the slopes of regression equations are used from correlating percent loss with age. Estimates of real percent loss can also be made, although many assumptions and limitations are used in these estimates.

Using the equation of Merrill (1906) for percent loss, and using Zr as the resistant species, Ca loss from the A horizons can be estimated as follows:

$$Ca \text{ loss} = \frac{Ca_{pm} Zr_A - Ca_A Zr_{pm}}{Ca_{pm} Zr_A}$$

where pm signifies the parent material and A the A horizon.

For this study, Zr was used as the resistant species, and sample M12 was used as the parent material for all soils. Zr appears to be the most stable constituent, as indicated by its concentration in sand separates relative to the decreases in most other elements (see supp. tables 5-8). This stability is commensurate with the consistently low etching index of zircon grains in soils of various age (see supp. table 4). Barshad (1964), Wild (1961), Sudom and St. Arnaud (1971), and Busacca (1982) also found that Zr and zircon grains in soils are relatively resistant to loss and mobility. Given the resistance of Zr, element percent loss can be estimated by using Zr as a resistant species and by using a soil standard that represents the parent material. The C1 horizon of a soil from the lower member of the Modesto Formation (sample M12, from 20.1- to 23.1-cm depth) was chosen as the parent material for all soils because most soils were not sampled deep enough to reach relatively unweathered C horizons.

Use of a single parent material has the following advantages: (1) all data are normalized to a given standard; and (2) when element loss is plotted against age, the slopes of the curves do not change if the standard is changed. Thus, the estimated rates are good approximations that will change only when age uncertainties are considered. The disadvantages of using a single sample for the parent material are that (1) minor variations in parent material are not represented by the calculation; and (2) the intercepts, or estimates of loss percents, are not so valid because they depend on the chosen parent material. Mineralogic and chemical compositions of parent materials are assumed to be similar for Merced soils older than Holocene. Any variations among parent materials are most likely random and thus will increase scatter in the regression analysis. Holocene soils are not included because of compositional differences, and soils from the middle unit of the Riverbank Formation are omitted to ensure the correct order of ages (relative age).

Uncertainty of age estimates is a more complex problem for regressions of percent-loss calculations. Whereas relative age is established by the sequence of terraces, quantitative age can be listed only as a range (table 2). Most significantly, the uncertainty varies among the different deposits (as indicated by boxes in figs. 6 and 7). To determine the extent to which this uncertainty in age affects the correlation between chemical losses and age, the ages of units were

allowed to vary within their constraints, and the resulting effects on regression were determined. If the slopes of the regressions maintain a similar order for all elements, then regression techniques can decipher relative rates of element loss by using best-estimate, assigned ages (table 2). Otherwise, relative rates of loss must rely on the accumulation-series method, using rank regression.

Ages of the different pre-Holocene units were varied for different regression analyses to test how age uncertainties affect the calculated rates of element loss. In table 3, these tests include various combinations of minimum and maximum ages, as well as the best-estimate age assignments listed in table 2. In general, the combinations chosen include those of maximum constraints on young ages with minimum constraints on old ages for finding maximum slopes, and the reverse (minimums for young and maximums for old) for minimum slopes. This technique is used in later sections of this report to estimate rates of soil development.

Regardless of the combination of possible ages used in regression (table 3), the order of slopes remains the same for percent loss. One exception is the order of Ca and Na loss, but these rates are so close that the differences are probably insignificant. For ordering the rates of loss, then, it is valid to use the relative order of slopes from regression of percent loss versus best-estimate age. Such regressions probably would be invalid if the relative age order were uncertain.

Table 3. Variation in rates of element loss from the A-horizon silt-plus-clay fraction, when age uncertainties are considered

[Ages used for trials: 1, best-estimate ages; 2 and 3, best-estimate ages with one young and one old constraint; 4 through 7, combined young, old, and best-estimate ages (see table 2). Rates vary by a factor of about 1.7. \bar{y} , standard deviation of predicted \bar{y} values.]

Trial-----	Age used for trial (ka)							Range in rates (trial)		
	1	2	3	4	5	6	7			
Map unit										
m1	40	70	40	20	70	20	70			
r3	130	130	130	130	130	103	250			
r1	330	330	330	330	330	250	440			
t2	600	600	600	600	600	570	615			
CH	3,000	3,000	1,000	4,000	4,000	4,000	1,000			
Element	Regression	Units								
Al (n=8)	Slope	percent/log ₁₀ yr	0.213	0.249	0.223	0.170	0.171	0.278	0.267	0.170 (4) to 0.278 (6)
	\bar{y} -intercept	percent loss	-1.05	-1.26	-1.09	-0.804	-0.805	-1.40	-1.36	
	$\frac{\bar{y}}{r^2}$.01 percent	.572	.651	.432	.506	.537	.517	.360	
	\bar{y}	percent loss	.11	.10	.13	.12	.12	.12	.14	
Ca (n=8)	Slope	percent/log ₁₀ yr	.412	.458	.460	.343	.340	.537	.588	0.340 (5) to 0.588 (7)
	\bar{y} -intercept	percent loss	-1.83	-2.10	-2.07	-1.44	-1.41	-2.50	-2.84	
	$\frac{\bar{y}}{r^2}$.01 percent	.740	.758	.633	.714	.730	.664	.605	
	\bar{y}	percent loss	.15	.15	.18	.16	.15	.17	.19	
Mg (n=8)	Slope	percent/log ₁₀ yr	.319	.354	.358	.266	.264	.418	.458	0.264 (5) to 0.458 (7)
	\bar{y} -intercept	percent loss	-1.25	-1.45	-1.45	-.949	-.927	-1.78	-2.05	
	$\frac{\bar{y}}{r^2}$.01 percent	.594	.606	.517	.574	.590	.540	.493	
	\bar{y}	percent loss	.16	.16	.18	.17	.16	.173	.18	
Fe (n=8)	Slope	percent/log ₁₀ yr	.124	.140	.136	.101	.099	.165	.173	0.099 (5) to 0.173 (7)
	\bar{y} -intercept	percent loss	-.452	-.545	-.526	-.326	-.312	-.676	-.738	
	$\frac{\bar{y}}{r^2}$.01 percent	.621	.656	.537	.582	.582	.585	.490	
	\bar{y}	percent loss	.06	.06	.066	.06	.063	.06	.07	
Na (n=8)	Slope	percent/log ₁₀ yr	.405	.459	.436	.333	.333	.521	.548	0.333 (4, 5) to 0.548 (7)
	\bar{y} -intercept	percent loss	-.208	-.239	-.222	-1.67	-1.65	-2.70	-2.90	
	$\frac{\bar{y}}{r^2}$.01 percent	.691	.736	.550	.650	.675	.603	.508	
	\bar{y}	percent loss	.167	.15	.20	.18	.172	.19	.21	

Regression lines and best-estimate ages were also used to order the rates of element loss in other size fractions of the A and B horizons (fig. 9; table 4).

Resulting orders of rates of element loss

The accumulation-series and net-loss methods generally agree on the relative order of element loss. For example, for the A-horizon fine fraction, the order is Ti, Fe > Al > K > Mn > Na > Ca by the accumulation-series method and Si > Zr > K > Mn > Na > Ca by the net-loss method. The major difference in these two methods is that the net-loss method lists fewer elements, because it relies only on the significance of ratios with Zr versus time. In general, alkaline-earth elements are lost more rapidly than sesquioxides. Al is added more slowly to this fraction than Fe, as a result of either faster Fe dissolution of the sand fraction or more rapid incorporation into the fine fraction, in comparison with Al. The poor correlation of Zr ratios seen in the accumulation series (fig. 8A) suggests that although there are distinguishable differences in losses of Ti, Al, and Fe based on interrelations of these elements, Zr may not serve as a good index for monitoring their net loss. Indeed, Zr may not be truly stable, and so small losses or even gains of Zr into the silt or clay fraction would make the ratio correlation indeterminate. Relative to Al, there is a net gain of Ti and Fe. The increase in dithionite-extractable Fe over time (fig. 7C) verifies that Fe tends to be sustained in this fraction. Mabee (1978) found that magnetite grains incorporate Ti into the soils sampled in this study, an observation that explains the influx of Ti into this fraction relative to Al and, possibly, Fe.

The order of element loss varies among size fractions and horizons (table 4) in relation to processes of dissolution, translocation, and size fractionation. In the sand fraction of B horizons (fig. 9; table 4), the order of element loss is: Zr (most resistant) < Si < Al, K < Na < Ca. Cementation of fine particles into sand-size grains is not evident in these soils, and so the elements in the sand fraction are an index of the relative retention of elements by primary mineral grains, or, in other words, an index of dissolution. Mineral grains generally release Ca, Mg, and Na more readily than Si, Al, and K, and (or) minerals rich in Ca, Mg, and Na are more easily weathered than those rich in Si, Al, and K. There may be a net gain of Ti and, possibly, Fe into the sands via the magnetic grains (Mabee 1978), but there is no systematic change over time of either element relative to Zr.

In contrast to the order of element loss from the sand fraction, the silt-plus-clay fraction of B horizons gains Al, Ti, Fe, and Si (table 4). These elements may be weathering from sand grains and upper soil horizons and reprecipitating in the B-horizon clays. Clay mineralogy (see supp. table 4) indicates a regular increase of kaolinite over time. Although the mineralogy explains the influx of Al into the fine fraction, there is no strong evidence for desilication of the illite-dominated parent material. The influx of Ti can be explained by incorporation into both magnetite and octahedral layers of clays (Barshad, 1953), possibly in the abundant vermiculite clays (see supp. table 4).

The relative order of element loss from the less-than-2-mm fraction in B horizons is generally similar to that in the sand fraction, where Zr > Fe > Al > Na > Ca > Mg (percent-loss method, table 4). If, indeed, there are net losses of Fe and Al in the less-than-2-mm fraction, they are due mostly to dissolution of sand grains, because there are net gains of these elements in the silt-plus-clay fraction. The relative loss of Ca and Na is similar to that in the sand but different from that in the fine fraction (percent-loss method, table 4), possibly owing to incorporation of Na into secondary compounds or minerals. Silica is lost more readily from sand than is Al (accumulation-series method, table 4), but the reverse is true for the fine fraction. Thus, enrichment of Al in the whole soil is due to rates of Al and Si enrichment of clays rather than to rates of Al and Si release from sands.

Several other studies have estimated the relative rates of element loss, and despite differences in their methodologies, their results are nearly identical to those of this study. Comparing fresh to weathered rock or less-than-2-mm soil, Steidtmann (1908) concluded that Al is concentrated (gained more rapidly or lost more slowly) at higher rates than Fe, although Goldich (1938) found the reverse to be true. Both of these reports found that Si is intermediate in rate of loss between the sesquioxides (Fe and Al) and Na, Mg, and Ca. Because Si constitutes more than 60 percent of the elemental analyses, volumes of Si loss could be substantial. Although the losses of Na, Mg, and Ca were greater than those of other elements, their relative order varied among the studies and was related in part to the composition of the parent rock. Colman (1982) found similar rates of accumulation or loss in basalt and andesite, where Ti > Fe > K > Al > Si > Mg > Na > Ca.

This study generally confirms the conclusions of other workers, although the approach differs somewhat. The previous work compared one weathered sample to the parent material, whereas in this study the element-loss series is based on five different-age samples plus a parent material. The advantage of comparing several different-age samples is evident in figure 9. Using only the oldest sample for the less-than-2-mm fraction (fig. 9), Ca is apparently lost more readily than Na or Mg; but using the rates of loss for all pre-Holocene soils, Mg is actually lost most readily. Another advantage of this study over previous ones is in the separation of the size fractions. As discussed above, the less-than-2-mm soil fraction demonstrates that Fe and Al are lost relatively slowly; analysis of the sand and fine fractions shows that these low rates are due both to slow release of Fe and Al from the sand fraction and to slow release and reprecipitation of sesquioxides in the silt-plus-clay fraction. Although mechanisms in these two size fractions are probably interdependent, comparison of the rates in separate fractions is a step closer to understanding the causes of chemical differentiation in soils.

Estimating rates of soil development

The number and age span of surfaces and soils and their associated ages invite calculations of soil-

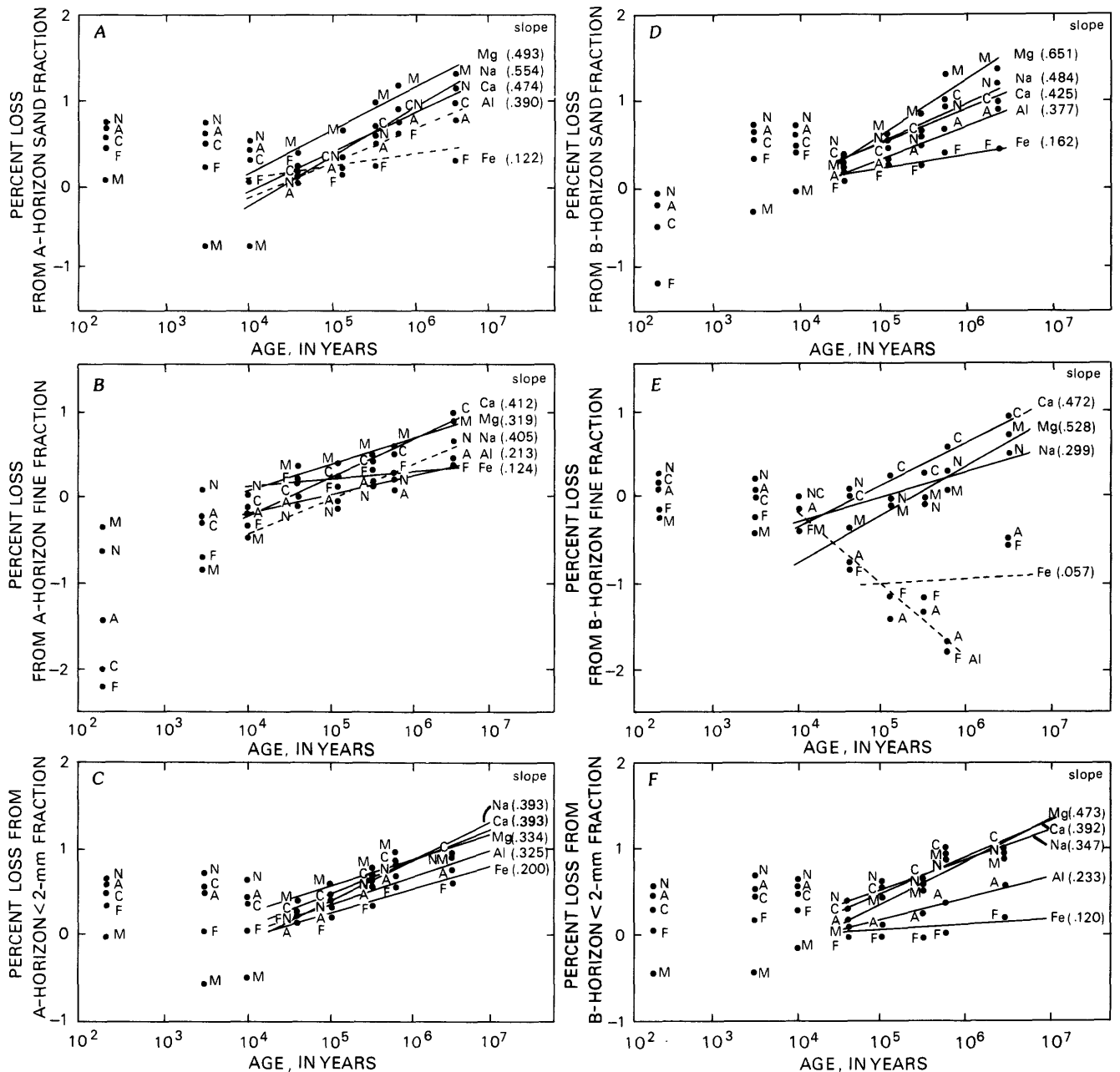


Figure 9. Percentage of element loss from A (A-C) and B (D-F) horizons for three size fractions versus best-estimate age. Using Merrill's (1906) loss equation (eq. 1), calculations used Zr for a stable index and sample M12-C1 for parent material. Linear regression was computed for all analyses, but values for each age

group (table 2) are averaged to show sample point. Dashed lines indicate regressions with less than 95-percent confidence (trial 1, table 3). Holocene soils are plotted but not used in regression because of differences in parent material. Positive slope, net loss; negative slope, net gain.

development rates, in which a given soil property is plotted or regressed against age. In addition, analysis of multiple soil profiles on a given-age surface provides a measure of soil variation. There are important limitations to these techniques, however, many of which have been identified or rectified in previous sections of this report. Probably the greatest limitation to estimating soil-development rates from

soil chronosequences is age uncertainties. As discussed in the preceding section, the effect of age uncertainties can be assessed by using different combinations of ages to calculate soil-development rates. Because some soil properties may change over wide or only narrow age ranges (for example, organic-carbon accumulation during the Holocene, or clay-film development during the Pliocene and Pleistocene),

Table 4. Order of rates of element loss from size separates

[Percent-loss method from Merrill's (1906) loss equation, using Zr as index and sample M12-C1 as parent material (see fig. 9 for regressions). Other elements were omitted because correlations with age were poor. Accumulation-series method as in figure 8]

Fraction	A horizon	B horizon
Percent-loss method		
Silt plus clay----	Zr<Fe<Al<Mg<Na<Ca	Al<Fe<Zr<Na<Ca<Mg
Sand-----	Zr<Fe<Al<Ca<Mg<Na	Zr<Fe<Al<Ca<Na<Mg
Whole soil-----	Zr<Fe<Al<Mg<Na,Ca	Zr<Fe<Al<Na<Ca<Mg
Accumulation-series method		
Silt plus clay----	Ti,Fe,Al<K<Mg,Na<Ca	Ti,Fe,Al<Si<Zr<K<Na<Ca
Sand-----	Ti,Zr<Si,Fe<Al<K<Ca	Ti<Fe,Si<Al,K<Na<Ca and Zr<Si
Whole soil-----	Ti<Fe<Si<Al,K<Na,Ca	Ti,Fe<Al<Si<K<Na,Ca and Zr<K

regressions of soil properties versus age are studied separately for the age spans 0-10, 0-3,000, 20-600, and 20-3,000 ka.

For soil properties that develop throughout the 3,000-ka age span of these surfaces, plots of soil property versus age are convex downward (fig. 10A), and of soil property versus the logarithm of age are bowl shaped (fig. 6B); the straightest curves are in log-log plots of soil property versus age (fig. 10A). Thus, linear regression must be applied only to log-log transformations for the wide (3,000 ka) age span. Seven trials of different age combinations suggest that rates using best-estimate ages are accurate within a factor of about 2 (fig. 10A; table 5). Minimum rates, obtained in trial 5 or 6, are obtained when minimum ages are used for young units and maximum ages for old units. Maximum rates (trial 2 or 3) correspond to a combination of maximum young and minimum old ages. Intermediate-age units in either of these cases may be assigned either best-guess or constraining ages.

Soil properties that develop primarily during the Holocene or Pleistocene age spans raise some important questions as to whether rates are linear or exponential. Properties that develop only during the Holocene or Pleistocene generally fit into linear curves, even when age uncertainties are accounted for. The seven combinations of ages have significant correlation coefficients for linear regressions of soil property versus age (figs. 10B, 10C; table 6). As in the trials for elemental analysis and the wide-range regressions (table 5), age uncertainties permit the rates to vary by a factor of about 2. If soil properties from the wide-range examples are plotted for only the Holocene or Pleistocene, the same properties appear to have linear rates, even though these rates are generally exponential over wider age spans. The exponential functions, then, might be approximated by linear segments along the curve (fig. 11). As would be

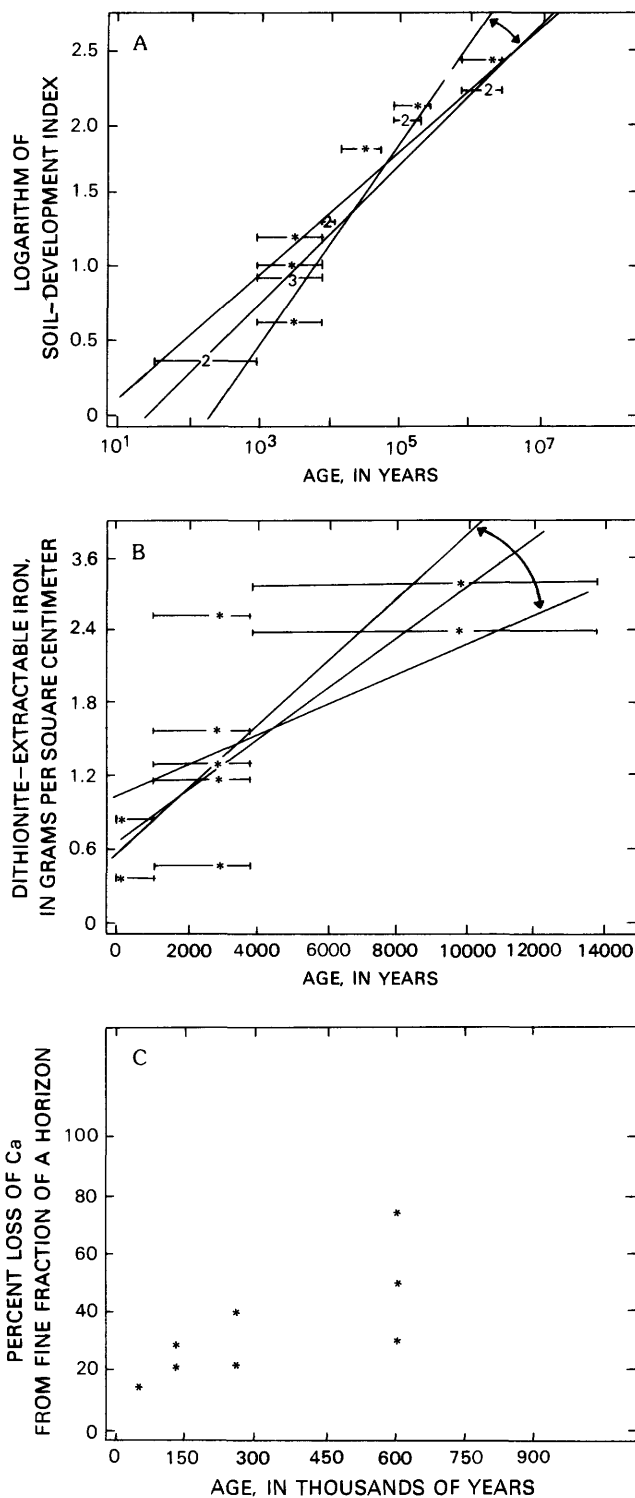


Figure 10. Rates of soil-property development for three timespans. **A**, Soil-development index. **B**, Dithionate-extractable Fe. **C**, Percent loss of Ca from A-horizon silt-plus-clay fraction. Points and numbers indicate samples at best-estimate age (table 1); error bars represent age uncertainty. Regression lines for constraining rates are from tables 5 through 7.

Table 5. Tests for constraining rates of soil development for Late Cenozoic deposits, when age uncertainties are considered

[Field properties from Harden (1982a). Rates vary by a factor of about 1.7. \bar{y} , standard deviation of predicted y values]

		Age used for trial (ka)							
Trial-----		1	2	3	4	5	6	7	
Map unit									
pmIII		0.20	1.00	1.00	1.00	0.05	0.05	0.20	
pmII		3.00	8.30	8.30	1.00	1.00	1.00	3.00	
m2		10.00	14.00	14.00	14.00	8.30	8.30	10.00	
m1		40.00	40.00	20.00	20.00	40.00	70.00	40.00	
r3		130.00	130.00	103.00	103.00	130.00	250.00	130.00	
r2		250.00	103.00	103.00	330.00	330.00	330.00	330.00	
t2		600.00	570.00	570.00	615.00	615.00	615.00	615.00	
CH		3,000.00	1,000.00	1,000.00	4,000.00	4,000.00	4,000.00	4,000.00	

Property	Regression	Units								Range in rate (trial)
Soil develop- ment index (SDI). (n=20)	Slope	log SDI/log yr	0.495	0.680	0.674	0.555	0.415	0.412	0.479	0.412 (5) to 0.680 (2)
	\bar{y} -intercept	log SDI x cm/100	-.731	-1.64	-1.59	-1.12	-.296	-.299	-.675	
	r^2	.01 percent	.931	.930	.908	.869	.950	.958	.932	
	\bar{y}	log SDI x cm/100	.173	.19	.21	.25	.16	.14	.18	
Rubification (rub). (n=18)	Slope	log rub/log yr	.107	.146	.146	.120	.089	.089	.104	0.089 (5, 6) to 0.146 (2, 3)
	\bar{y} -intercept	log rub x cm/100	-.271	-.465	-.459	-.358	-.177	-.176	-.259	
	r^2	.01 percent	.884	.879	.868	.826	.890	.889	.876	
	\bar{y}	log rub x cm/100	.06	.056	.06	.068	.054	.05	.057	
<2- μ m clay (n=20)	Slope	log g/cm ² /log yr	.454	.620	.617	.513	.381	.377	.440	0.377 (6) to 0.620 (2)
	\bar{y} -intercept	log g/cm ²	-.556	-1.37	-1.34	-.938	-.158	-.157	-.507	
	r^2	.01 percent	.937	.916	.902	.884	.950	.954	.933	
	\bar{y}	log g/cm ²	.16	.19	.20	.22	.14	.14	.17	

expected from exponentially decreasing functions, Holocene rates are 10 times higher than Pleistocene rates of the same soil properties (table 7). Although the exact form of the curves may not prove to be correct when more data are available, the data clearly show that initial rates are highest at first and drop off drastically within 100 ka.

The age combinations in tables 5 through 7 generally constrain the rates of soil (or soil property) development. They demonstrate that best-estimate ages are intermediate between minimum and maximum possible rates, and that rates based on best-estimate ages are accurate to within a factor of about 2. Although the linear rates documented for the Holocene and Pleistocene may not be representative for long-term processes, the straight, nonlogarithmic units are easy to interpret and compare with those from other studies, and they are probably reasonable approximations of short-term rates.

DISCUSSION

The systematic changes in the properties of Merced soils with age suggest that over intervals of thousands of years, some processes may act nearly continuously on soils, regardless of shorter term fluctuations and perturbations in soil-forming factors, such as paleoclimate or erosion. One question that should be addressed, however, is whether pre-Holocene soils formed as a result of modern soil-forming processes, or whether they are relict from past and different processes. If past processes were similar to modern ones, then "empirical" rates of soil-property development with age may be reasonable estimates of

the actual rates. If past effects of paleoclimate and vegetation on soil development can be accounted for, then soil-chronosequence studies can provide an onsite, empirical laboratory for such fundamental questions as how soil properties and rates of soil development differ with climate and time, how mineral-dissolution rates compare with those determined by laboratory and theoretical studies, and how soils might respond to such perturbations as cultivation, erosion, deposition, or changes in climate.

The changes in major-element (total) chemistry over time are generally systematic for most of the size fractions and soil horizons. The changes over time in the A horizons suggest that the geomorphic surfaces are somewhat stable and do not receive significant amounts of eolian materials, or that such processes are time dependent. It may be that the surfaces are being eroded, but erosion rates would have to be slow for chemical trends of the A horizons to change systematically with age. For example, if all the surfaces had vast erosion rates, then soils probably would not form. If individual soils were more eroded than others, then age trends would not be expected, especially in the A horizons. If these soils are being eroded slowly but continually, then the actual rates of soil development would be far greater than those documented by the chronosequence. Decreasing rates of various soil properties over time (table 8) could reflect geomorphic stability rather than the kinetics of mineral dissolution or other soil processes. Recent ¹⁰Be analyses of the soils sampled in this study (M.J. Pavich, written commun., 1984) suggest significant erosion of these surfaces. One argument for a kinetic origin of the decreasing rates of soil development is

Table 6. Tests for constraining rates of soil development for Holocene deposits, when age uncertainties are considered

[Field properties from Harden (1982a). Trial 7 is generally not significant at the 5-percent-confidence level]. Rates commonly vary by a factor of about 2.5. \underline{S} , standard deviation of predicted \underline{y} values]

Trial----- Map unit	Age used for trials (ka)							Range in rate (trial)		
	1	2	3	4	5	6	7			
pmIII	0.20	0.05	0.05	0.05	1.00	1.00	0.20			
pmII	3.00	3.00	8.30	1.00	3.00	8.30	8.30			
m2	10.00	14.00	14.00	14.00	8.30	8.30	8.30			
Property	Regression	Units								
Organic-carbon content.	Slope	g/cm ² /ka	0.036	0.023	0.030	0.018	0.048	0.042	0.038	0.18 (4) to 0.48 (5)
	\underline{y} -intercept	g/cm ²	.636	.669	.537	.713	.060	.488	.522	
	$\frac{\underline{y}}{\underline{z}}$.01 percent	.256	.225	.341	.168	.251	.277	.277	
	\underline{S}	mel x cm/ka	.22	.228	.21	.24	.22	.22	.22	
Melanization (mel). (n=10)	Slope	mel x cm/ka	3.83	2.54	2.68	2.19	5.10	2.87	2.58	2.19 (4) to 5.10 (5)
	\underline{y} -intercept	mel x cm	22.0	25.0	15.8	29.2	18.0	17.1	19.4	
	$\frac{\underline{y}}{\underline{z}}$.01 percent	.69	.662	.627	.592	.684	.308	.308	
	\underline{S}	mel x cm	9.4	9.80	10.3	10.8	9.5	14.0	14.0	
Dithionite-extractable Fe. (n=9)	Slope	g/cm ² /ka	.192	.127	.136	.110	.255	.155	.139	0.110 (4) to 0.255 (5)
	\underline{y} -intercept	g/cm ²	.744	.889	.445	1.09	.545	.465	.592	
	$\frac{\underline{y}}{\underline{z}}$.01 percent	.60	.576	.568	.512	.597	.306	.306	
	\underline{S}	g/cm ²	.61	.63	.63	.672	.610	.80	.80	
Dry consistence (dc). (n=8)	Slope	dc x cm/ka	3.27	2.14	2.53	1.85	4.34	2.46	2.21	1.85 (4) to 4.34 (5)
	\underline{y} -intercept	dc x cm	4.31	7.15	-3.32	11.1	.987	.544	2.56	
	$\frac{\underline{y}}{\underline{z}}$.01 percent	.18	.900	.805	.855	.916	.268	.268	
	\underline{S}	g/cm ²	3.78	4.18	5.8	5.2	3.8	.11	11.3	
Rubification (rub). (n=10)	Slope	rub x cm/ka	2.78	1.81	2.12	1.50	3.69	2.58	2.33	1.50 (4) to 3.69 (5)
	\underline{y} -intercept	rub x cm	11.1	13.5	5.25	16.7	8.29	4.11	6.23	
	$\frac{\underline{y}}{\underline{z}}$.01 percent	.644	.596	.700	.494	.637	.446	.446	
	\underline{S}	g/cm ²	7.5	8.03	6.9	9.0	7.6	9.4	9.4	
<2- μ m clay (n=10)	Slope	g/cm ² /ka	2.30	1.56	1.46	1.39	3.08	1.29	1.16	1.16 (7) to 3.08 (5)
	\underline{y} -intercept	g/cm ²	2.40	4.13	-.047	6.57	.056	2.52	3.57	
	$\frac{\underline{y}}{\underline{z}}$.01 percent	.730	.733	.46	.705	.732	.182	.182	
	\underline{S}	g/cm ²	5.11	5.08	6.6	5.3	5.1	8.9	8.9	
Soil development index (SDI). (n=10)	Slope	SDI x cm/ka	1.69	1.12	1.18	.966	2.25	1.25	1.12	0.966 (7) to 2.25 (5)
	\underline{y} -intercept	SDI x cm	.22	4.53	.540	6.4	1.47	1.17	2.20	
	$\frac{\underline{y}}{\underline{z}}$.01 percent	.845	.816	.764	.732	.841	.369	.369	
	\underline{S}	SDI x cm	2.6	2.87	3.3	3.5	2.7	5.32	5.3	

that studies on mineral weathering (Colman, 1982) typically document initially rapid rates, followed by slower rates.

The appropriateness of linear or nonlinear curve fitting is a difficult problem to overcome with these data. This study has shown that long-term exponential curves can be approximated by shorter term, linear segments (fig. 11); other chronosequence studies with narrow age spans may be approximated by linear rates for the same reason. In other words, such studies may actually demonstrate long-term nonlinear rates if older and (or) younger units were available for sampling.

Estimation of the ages of other deposits by using soil chronosequences is an important implication of this study, because so many soil properties change systematically with age. The age uncertainties of the chronosequence, however, are intrinsic to prediction of other ages. The clay content of Merced soils provides a good example for some methods and illustrates the problems with age prediction. When the clay content (\underline{y} -axis) is regressed against best-estimate age (\underline{x} -axis)

about the regression line, then the standard error of estimate \underline{S} , given by

$$\underline{S} = \frac{\underline{y} - \underline{y}_{\text{pred}}}{\underline{n} - 2}$$

(where $\underline{y}_{\text{pred}}$ is the predicted value of \underline{y} , and \underline{n} is the number of samples), is about 30 percent (see table 5). In other words, there is about 30-percent scatter about the regression line related to soil variation. This result is commensurate with estimates of the amount of soil variation on a single-age surface, as represented by the standard deviation divided by the mean for replicate soils on a given terrace (Harden, 1982b). When the axes are switched, however, so that age is the dependent variable (\underline{y} -axis), then \underline{S} more than doubles to about 70 percent (fig. 12). (Because the best-estimate ages are fixed without any uncertainties, this standard error cannot be related to inaccurate dating of the terraces.) The standard error, which is a rough estimate of how precise age estimates

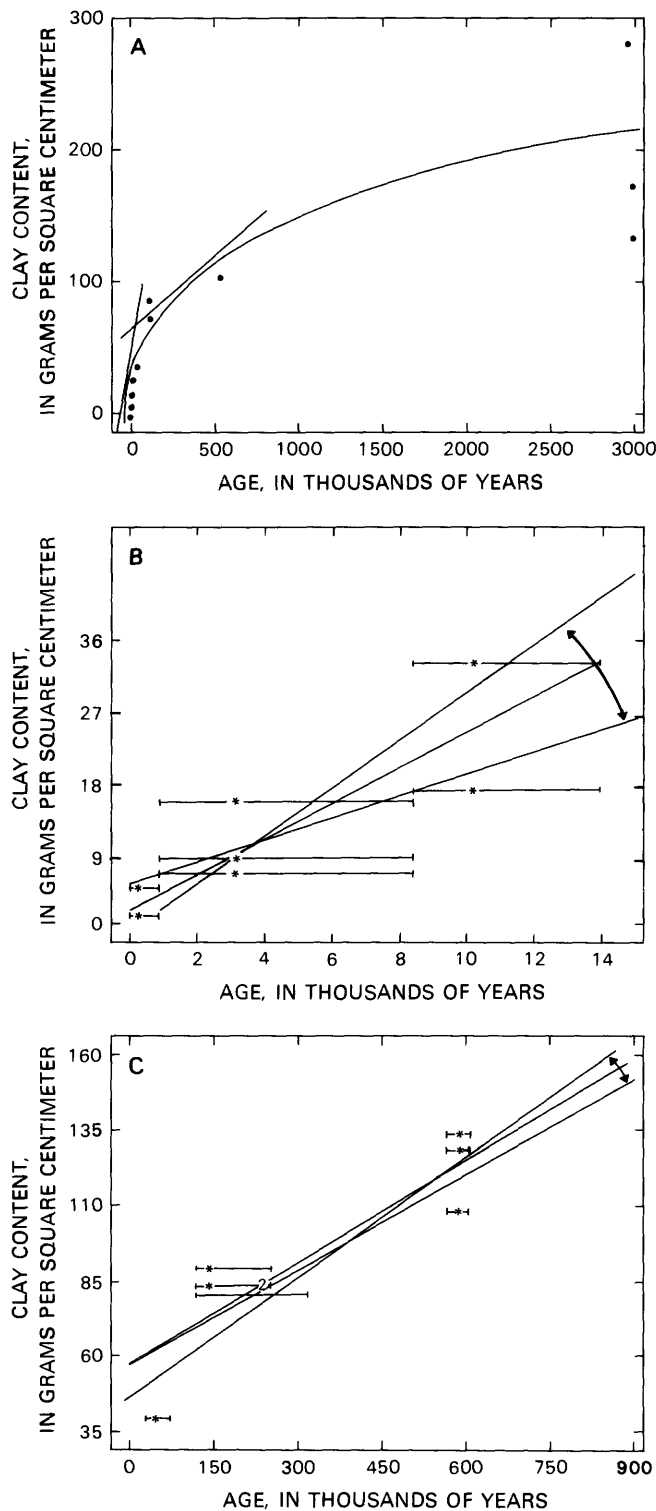


Figure 11. Exponential curve of clay content versus age, approximated by linear segments. **A**, Clay content versus log age for the timespan 3,000-0 ka. **B**, clay versus age for the timespan 10-0 ka. **C**, Clay versus age for the timespan 600-20 ka. Points and numbers indicate samples at best-estimate ages (table 2); error bars indicate constraining ages. Regression lines for rates are from tables 5 through 7.

by soils could be, suggests that a 100-ka-old deposit would be reported as being from about 40 to 160 ka old. More appropriate statistics are needed to consider the source of these errors. The standard error should increase when age errors are incorporated, but it might decrease when more appropriate statistics are used. Intuitively, because soil variation is typically about 30 percent, more appropriate statistics and sampling might improve the estimates to no better than about 30 percent for this clay function over the 3,000-ka age span.

Another aspect that should be considered for age prediction is the time dependence of different soil parameters. Although it is probably advantageous to use several soil properties for age estimates, a scheme must be devised for using properties that are limited to the Holocene or Pleistocene. One possibility is to use wide-range (0-3,000 ka) properties (table 5) for first-order estimates, and then to use Holocene and pre-Holocene parameters (tables 6, 7) for the appropriate soils. The more restricted age ranges, with their linear rates, might actually improve the precision of age estimates because then the standard errors are lower than in exponential functions.

SUMMARY

The soil chronosequence near the Merced River demonstrates that many soil properties develop systematically over time and that a significant association exists between soil properties and geologic age. Morphologic properties that develop most regularly with age over wide (3,000 ka) or narrower (10 ka to a few tens of thousands of years) age ranges include clay films, total texture (texture and wet consistence), rubification (color hue and chroma), dry consistence, and the soil-development index (Harden, 1982a), which combines the morphologic properties. Elements determined by total-chemical analysis that change most systematically with age include Ca, Mg, Na, Fe, Al, and Ti, as expressed in loss percent relative to Zr, which is assumed to be stable. Physical properties most indicative of age include clay percent, bulk density, and thickness or depth to C horizons; extractive-chemical analyses include dithionite- and oxalate-extractable Fe. Although many mineralogic properties (percentages and degree of etching) do not change systematically with age or cannot be measured precisely enough, these analyses help to interpret the significance of other trends.

Several of the methods for data analysis described in this report can be applied to similar studies. From total-chemical analysis, an accumulation series was developed to determine relative rates of element loss. This series can be used for soil chronosequences that lack radiometric age control but whose relative ages are well defined. Merrill's (1906) loss calculation was adopted for calculating the percent loss of an element from a given size fraction. Zr appears to work well as a stable index element. The selection of a single sample for the parent material of all soils appears to be appropriate for pre-Holocene deposits.

Table 7. Tests for constraining rates of soil development for Pleistocene deposits, when age uncertainties are considered

[Field properties from Harden (1982a). Rates vary by a factor of about 1.3. S_y , standard deviation of predicted y values]

Trial----- Map unit	Age used for trial (ka)							Range in rate (trial)
	1	2	3	4	5	6	7	
m1	40.0	20.0	20.0	20.0	70.0	70.0	70.0	
r3	130.0	130.0	250.0	103.0	130.0	103.0	250.0	
r2	250.0	330.0	330.0	330.0	103.0	103.0	250.0	
t2	600.0	615.0	615.0	615.0	570.0	570.0	600.0	

Property	Regression	Units								Range in rate (trial)
Total texture ($n=7$)	Slope	total texture x cm/ka	0.153	0.144	0.166	0.138	0.148	0.145	0.177	0.138 (4) to 0.177 (7)
	y -intercept	total texture x cm	51.5	50.5	38.1	53.4	59.8	61.7	37.7	
	r^2	.01 percent	.806	.774	.822	.754	.748	.744	.830	
	S_y	total texture x cm	18.7	20.2	17.9	21.1	21.4	21.5	17.5	
Clay films ($n=7$)	Slope	clay films x cm/ka	0.218	0.213	0.246	.204	.194	.190	.249	0.190 (6) to 0.249 (7)
	y -intercept	clay films	79.4	75.5	56.9	79.9	95.2	97.7	60.8	
	r^2	.01 percent	.830	.863	.923	.841	.655	.654	.837	
	S_y	clay films	24.6	22.0	16.5	23.8	34.9	35.0	24.0	
Rubification (rub). ($n=5$)	Slope	rub x cm/ka	.339	.329	.347	.322	.323	.319	.369	0.319 (6) to 0.369 (7)
	y -intercept	rub x cm	49.4	46.8	32.1	50.9	65.9	68.8	28.8	
	r^2	.01 percent	.942	.955	.926	.953	.825	.832	.900	
	S_y	rub x cm	25.6	22.4	28.9	23.0	44.4	43.5	33.6	
Soil develop- ment index (SDI). ($n=7$)	Slope	SDI x cm/ka	.212	.198	.225	.190	.207	.203	.244	0.190 (4) to 0.244 (7)
	y -intercept	SDI x cm	59.2	58.4	42.1	62.4	70.1	72.7	40.7	
	r^2	.01 percent	.762	.721	.154	.705	.728	.726	.779	
	S_y	SDI	29.4	31.9	29.9	32.8	31.4	31.6	28.3	
<2- μ m clay ($n=8$)	Slope	$g/cm^2/ka$.112	.108	.130	.103	.105	.102	.134	0.102 (6) to 0.134 (7)
	y -intercept	g/cm^2	57.8	65.5	44.8	59.0	64.5	66.2	46.1	
	r^2	.01 percent	.183	.774	.901	.743	.712	.694	.870	
	S_y	g/cm^2	15.1	15.4	10.2	16.4	17.4	17.9	11.4	
Dithionite- extractable Fe. ($n=8$)	Slope	$g/cm^2/ka$.0061	.0060	.0067	.0058	.0057	.0056	.0069	0.0056 (6) to 0.0069 (7)
	y -intercept	g/cm^2	1.40	1.31	.866	1.42	1.79	1.85	.924	
	r^2	.01 percent	.352	.353	.353	.349	.311	.314	.343	
	S_y	g/cm^2	2.1	2.13	2.13	2.13	2.19	2.19	2.14	

Table 8. Comparison of Holocene and Pleistocene rates of soil development from tables 6 and 7

[Field properties from Harden (1982a)]

Property	Units	Holocene rate	Pleistocene rate
Dithionite-extractable Fe.	$g/cm^2/ka$	0.110-0.255	0.0056-0.0069
Rubification (rub)-----	rub x cm/ka	1.5-3.69	.319-0.369
<1- μ m clay-----	$g/cm^2/ka$	1.16-3.08	.102-0.134
Soil-development index (SDI).	SDI x cm/ka	.966-2.25	.190-0.244

Long-term rates of soil development or some aspect of soil development, such as element loss or morphologic changes, can be estimated from these data. The variation between soils on the same age surface was represented by replication of soils on each terrace. Uncertainties in the ages of deposits can be considered by using minimum and maximum age constraints.

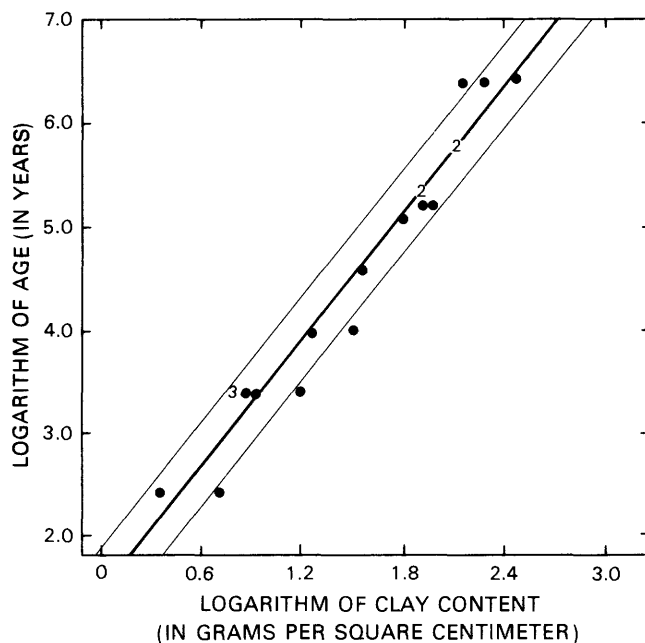


Figure 12. Example of estimating age from soil development. Points and numbers indicate number of samples. Heavy line, regression line; light lines, standard deviation of predicted y values about regression line.

REFERENCES CITED

- Adam, D.P., 1967, Late-Pleistocene and Recent palynology in the central Sierra Nevada, California, in Cushing, E.J., and Wright, H.E., Jr., eds., *Quaternary paleoecology*: New Haven, Conn., Yale University Press, p. 275-301.
- Arkley, R.J., 1954, *Soils of eastern Merced County*: University of California, Exploration Station Soil Survey, v. 11, 174 p.
- 1962a, The geology, geomorphology, and soils of the San Joaquin Valley in the vicinity of the Merced River, California, in *Geologic guide to the Merced Canyon and Yosemite Valley, California*: California Division of Mines and Geology Bulletin 182, p. 25-31.
- 1962b, Soil survey of the Merced area, California: U.S. Department of Agriculture, Soil Survey Serial 1950, no. 7, 131 p.
- 1963, Calculation of carbonate and water movement in soil from climatic data: *Soil Science*, 96, no. 4, p. 239-248.
- Arkley, R.J., and Brown, H.C., 1954, The origin of Mima mound (hogwallow) microrelief in the far western states: *Soil Science Society of America Proceedings*, v. 18, no. 2, p. 195-199.
- Atwater, B.F., Adam, D.P., Bradburg, J.P., Forester, R.M., Mark, R.K., Lettis, W.R., Fisher, G.R., Gobalet, K.W., and Robinson, S.W., in press, A fan dam for Tulare Lake, California, and implications for the Wisconsin glacial history of the Sierra Nevada: *Geological Society of America Bulletin*.
- 1964, Chemistry of soil development, chap. 2 of Bear, F.E., ed., *Chemistry of the soil*: New York, Reinhold, p. 1-70.
- Birkeland, P.W., 1964, Pleistocene glaciation of the northern Sierra Nevada north of Lake Tahoe, California: *Journal of Geology*, v. 72, no. 6, p. 810-825.
- 1974, *Pedology, weathering, and geomorphologic research*: New York, Oxford University Press, 285 p.
- Birman, J.H., 1954, Pleistocene glaciation in the upper San Joaquin basin, Sierra Nevada, pt. 6 of *Geomorphology*, chap. 5 of Jahns, R.H., ed., *Geology of southern California*: California Division of Mines Bulletin 170, p. 41-44.
- 1957, *Glacial geology of the upper San Joaquin drainage, Sierra Nevada, California*: Los Angeles, University of California, Ph.D. thesis, 237 p.
- 1964, *Glacial geology across the crest of the Sierra Nevada*: Geological Society of America Special Paper 75, 80 p.
- Blackwelder, Elliot, 1931, Pleistocene glaciation in the Sierra Nevada and Basin Ranges: *Geological Society of America Bulletin*, v. 42, no. 4, 865-922.
- 1932, *Glacial and associated stream deposits of the Sierra Nevada*: California State Mineralogist Annual Report 28, no. 3-4, p. 303-310.
- Burke, R.M., and Birkeland, P.W., 1979, Reevaluation of multiparameter relative dating techniques and their application to the glacial sequence along the eastern escarpment of the Sierra Nevada, California: *Quaternary Research*, v. 11, no. 1, p. 21-51.
- Busacca, A.J., 1982, *Geologic history and soil development, northeastern Sacramento Valley, California*: Davis, University of California, Ph.D. thesis, 348 p.
- Busacca, A.J., Aniku, J.R., and Singer, M.J., 1984, Dispersion of soils by an ultrasonic method that eliminates probe contact: *Soil Science Society of America Journal*, v. 48, no. 5, p. 1125-1129.
- Colman, S.M., 1982, *Chemical weathering of basalts and andesites—evidence from weathering rinds*: U.S. Geological Survey Professional Paper 1246, 51 p.
- Croft, M.G., 1968, *Geology and radiocarbon ages of late Pleistocene lacustrine clay deposits, southern part of San Joaquin Valley, California*, in *Geological Survey research, 1968*: U.S. Geological Survey Professional Paper 600-B, p. B151-B156.
- 1972, *Subsurface geology of the late Tertiary and Quaternary water-bearing deposits of the southern part of the San Joaquin Valley, California*: U.S. Geological Survey Water-Supply Paper 1999-H, p. H1-H29.
- Curry, R.R., 1969, Holocene climatic and glacial history of the central Sierra Nevada, California, in Schumm, S.A., and Bradley, W.C., eds., *United States contributions to Quaternary research*: Geological Society of America Special Paper 123, p. 1-47.
- Dalrymple, G.B., 1980, K-Ar ages of the Friant Pumice Member of the Turlock Lake Formation, the Bishop Tuff, and the tuff of Reds Meadow, central California: *Isochron/West*, no. 28, p. 3-4.
- Davis, S.N., and Hall, F.R., 1959, *Water quality of eastern Stanislaus and northern Merced Counties, California*: Stanford University Publications in the Geological Sciences, v. 6, no. 1, 112 p.
- Deming, W.E., 1943, *Statistical treatment of data*: New York, John Wiley, 261 p.
- Dethier, D.P., and Bethel, John, 1981, *Surficial deposits along the Cowlitz River near Toledo, Lewis County, Washington*: U.S. Geological Survey Open-File Report 81-1043, 67 p.
- Frye, J.C., 1973, Pleistocene succession of the central interior United States: *Quaternary Research*, v. 3, no. 2, p. 275-283.
- Gillam, M.L., Ensey, Chuck, Page, W.D., and Blum, R.L., 1977, Heavy mineral etching in soils from the Merced and Truckee areas, California, in Singer, M.J., ed., *Soil development, geomorphology, and Cenozoic history of the northeastern San Joaquin Valley and adjacent areas, California*: Soil Sciences Society of America-Geological Society of America joint field session, 1977, guidebook, p. 22-38.
- Goldich, S.S., 1938, A study in rock weathering: *Journal of Geology*, v. 46, no. 1, p. 47-58.
- Hansen, R.O., and Begg, E.L., 1970, Age of Quaternary sediments and soils in the Sacramento area, California, by uranium and actinium series dating of vertebrate fossils: *Earth and Planetary Science Letters*, v. 8, no. 6, p. 411-419.

- Harden, J.W., 1982a, A quantitative index of soil development from field descriptions: Examples from a chronosequence in central California: *Geoderma*, v. 28, no. 1, p. 1-28.
- 1982b, A study of soil development using the geochronology of Merced River deposits: Berkeley, University of California, Ph.D. thesis, 237 p.
- Harden, J.W., and Marchand, D.E., 1977, The soil chronosequence of the Merced River area, in Singer, M.J., ed., *Soil development, geomorphology, and Cenozoic history of the northeastern San Joaquin Valley and adjacent areas, California*: Soil Science Society of America-Geological Society of America joint field session, 1977, guidebook, p. 22-38.
- 1980, Quaternary stratigraphy and interpretation of soil data from the Auburn, Oroville, and Sonora areas along the Foothills fault system, western Sierra Nevada, California: U.S. Geological Survey Open-File Report 80-30, 57 p.
- Harden, J.W., and Taylor, E.T., 1983, A quantitative comparison of soil development in four climatic regimes: *Quaternary Research*, v. 20, no. 3, p. 342-359.
- Helley, E.J., 1966, Sediment transport in the Chowchilla River basin: Mariposa, Madera, and Merced Counties, California: Berkeley, University of California, Ph.D. thesis, 189 p.
- Huber, N.K., 1981, Amount and timing of late Cenozoic uplift and tilt of the central Sierra Nevada, California--evidence from the upper San Joaquin River basin: U.S. Geological Survey Professional Paper 1197, 28 p.
- Huntington, G.L., 1971, Soil survey of the eastern Fresno area, California: Washington, U.S. Department of Agriculture, Soil Conservation Service, 323 p.
- Janda, R.J., 1965, Quaternary alluvium near Friant, California, in *International Association for Quaternary Research Guidebook for Field Conference I, northern Great Basin and California*: Lincoln, Nebraska Academy of Sciences, p. 128-133.
- 1966, Pleistocene history and hydrology of the upper San Joaquin River, California: Berkeley, University of California, Ph.D. thesis, 425 p.
- Janda, R.J., and Croft, M.G., 1967, The stratigraphic significance of a sequence of noncalcareous brown soils formed on the Quaternary alluvium of the northeastern San Joaquin Valley, California, in Morrison, R.B., and Wright, H.E., Jr., eds., *Quaternary soils*: International Association for Quaternary Research Congress, 7th, Reno, Nev., 1967, Proceedings, v. 9, p. 158-190.
- Jenny, Hans, 1941, *Factors of soil formation*: New York, McGraw-Hill, 281 p.
- Mabee, 1978, The use of magnetite alteration as a relative age dating technique: Preliminary results: Boulder, University of Colorado, M.S. thesis, 183 p.
- Marchand, D.E., 1976a, Late Cenozoic stratigraphy and history of the northeastern San Joaquin Valley: Some early results of a regional study abs.: *Geological Society of America Abstracts with Programs*, v. 8, no. 3, p. 393-394.
- 1976b, Preliminary geologic maps showing Quaternary deposits of the northern Merced area, eastern San Joaquin Valley, Merced and Stanislaus Counties, California: U.S. Geological Survey Open-File Report 76-836, 12 p., scale 1:24,000, 8 sheets.
- 1976c, Preliminary geologic maps showing Quaternary deposits of the Merced area, eastern San Joaquin Valley, Merced County, California: U.S. Geological Survey Open-File Report 76-837, 12 p., scale 1:24,000, 7 sheets.
- 1976d, Preliminary geologic maps showing Quaternary deposits of the southern Merced area, eastern San Joaquin Valley, Merced and Madera Counties, California: U.S. Geological Survey Open-File Report 76-838, 12 p., 1:24,000, 7 sheets.
- 1976e, Preliminary geologic maps showing Quaternary deposits of the Chowchilla area, eastern San Joaquin Valley, Merced and Madera Counties, California: U.S. Geological Survey Open-File Report 76-839, 12 p., scale 1:24,000, 5 sheets.
- 1976f, Preliminary geologic maps showing Quaternary deposits of the Daulton area, eastern San Joaquin Valley, Madera County, California: U.S. Geological Survey Open-File Report 76-840, 12 p., scale 1:24,000, 4 sheets.
- 1976g, Preliminary geologic maps showing Quaternary deposits of the Madera area, eastern San Joaquin Valley, Madera and Fresno Counties, California: U.S. Geological Survey Open-File Report 76-841, 12 p., scale 1:24,000, 8 sheets.
- 1977, The Cenozoic history of the San Joaquin Valley and the adjacent Sierra Nevada as inferred from the geology and soils of the eastern San Joaquin Valley, in Singer, M.H., ed., *Soil development, geomorphology, and Cenozoic of the northeastern San Joaquin Valley and adjacent areas, California*: Soil Science of America-Geological Society of America joint field session, 1977, guidebook, p. 39-50.
- Marchand, D.E., and Allwardt, Alan, 1981, Late Cenozoic stratigraphic units in northeastern San Joaquin Valley, California: U.S. Geological Survey Bulletin 170, 70 p.
- Marchand, D.E., and Harden, J.W., 1978, Preliminary geologic maps showing Quaternary deposits on the lower Tuolumne and Stanislaus alluvial fans and along the lower San Joaquin River, Stanislaus County, California: U.S. Geological Survey Open-File Report 78-656, 9 p., 4 sheets.
- Machette, M.N., 1983, Geologic map of the southwest quarter of the Beaver quadrangle, Beaver County, Utah: U.S. Geological Survey Miscellaneous Investigations Series Map I-1444, scale 1:24,000.
- Machette, M.N., and Steven, T.A., 1983, Geologic map of the northwest quarter of the Beaver quadrangle, Beaver County: U.S. Geological Survey Miscellaneous Investigations Series Map I-1445, scale 1:24,000.
- Machette, M.N., Steven, T.A., Cunningham, C.G., and Anderson, J.J., 1984, Geologic map of the Beaver

- quadrangle, Beaver and Piute Counties, Utah: U.S. Geological Survey Miscellaneous Investigations Series Map I-1520, scale 1:50,000.
- Matthes, F.E., 1960, Reconnaissance of the geomorphology and glacial geology of the San Joaquin Basin, Sierra Nevada, California: U.S. Geological Survey Professional Paper 329, 62 p.
- Merrill, G.P., 1906, A treatise on rocks, rock weathering and soils: New York, Macmillan, 400 p.
- Meixner, R.E., and Singer, M.J., 1981, Use of a field morphology rating system to evaluate soil formation and discontinuities: *Soil Science*, v. 131, no. 2, p. 114-123.
- Morrison, R.B., 1967, Principles in Quaternary soils, in Morrison, R.B., and Wright, H.E., Jr. eds., *Quaternary soils: International Association for Quaternary Research Congress, 7th, Reno, Nev., 1967, Proceedings*, v. 9, p.
- Nikiforoff, C.C., 1941, Hardpan and microrelief in certain soil complexes of California: U.S. Department of Agriculture Technical Bulletin 745, p. 45.
- Packer, R., McCleary, J.R., Chervan, V.O., and Blum, R.L., 1977, Paleomagnetic investigations of the Turlock Lake Formation at the type section, in Singer, M.J., ed., *Soil development, geomorphology, and Cenozoic history of the northeastern San Joaquin Valley and adjacent areas, California: Soil Science Society of America-Geological Society of America joint field session, 1977, guidebook*, p. 22-38.
- Page, W.D., Swan, F.H., III, Hanson, K.L., Muller, David, and Blum, Raymond, 1977, Prairie Mound (Mima Mound, Hog Wallows) in the Central Valley, in Singer, M.J., ed., *Soil development, geomorphology, and Cenozoic history of the northeastern San Joaquin Valley and adjacent areas, California: Soil Science Society of America-Geological Society of America joint field session, 1977, guidebook*, p. 267-276.
- Reheis, M.C., 1984, Chronologic and climatic control on soil development, northeastern Bighorn Basin, Wyoming and Montana: Boulder, University of Colorado, Ph.D. thesis, 293 p.
- Rogers, T.H., compiler, 1966, San Jose sheet of Geologic map of California: Sacramento, California Division of Mines and Geology, scale 1:250,000.
- Rosholt, J.N., 1978, Uranium-trend dating of alluvial deposits, in *Short papers of the Fourth International Conference, Geochronology, Cosmochronology, Isotope Geology: U.S. Geological Survey Open-File Report 78-701*, p. 360-362.
- 1980, Uranium-trend dating of Quaternary sediments: U.S. Geological Survey Open-File Report 80-1087, 41 p.
- Shackleton, N.J., and Opdyke, N D., 1976, Oxygen-isotope and paleomagnetic stratigraphy of Pacific core V28-239, late Pliocene to latest Pleistocene, in Cline, R.M., and Hays, J.D., eds., *Investigation of late Quaternary paleoclimatology and paleoclimatology: Geological Society of America Memoir 145*, p. 449-464.
- Shlemon, R.J., 1967, Quaternary geology of northern Sacramento County: Geological Society of Sacramento annual field trip, 1967, guidebook, 60 p.
- 1975, Soil taxonomy—a basic system of soil classification for making and interpreting soil surveys: U.S. Department of Agriculture Handbook 436, 754 p.
- Singer, M.J., and Janitsky, Peter, 1986, Field and laboratory procedures used in a soil chronosequence study: U.S. Geological Survey Bulletin 1648, 49 p.
- Soil Survey staff, 1962, Soil Survey manual: U.S. Department of Agriculture Agriculture Handbook 18, 503 p.
- 1975, Soil taxonomy: A basic system of soil classification for making and interpreting soil surveys: U.S. Department of Agriculture Agriculture Handbook 436, 754 p.
- Steidtmann, Edward, 1908, A graphic comparison of the alteration of rocks by weathering with their alteration by hot solutions: *Economic Geology*, v. 3, no. 5, p. 381-409.
- Sudom, M.D., and St. Arnaud, R.J., 1971, Use of quartz, zirconium and titanium as indices in pedological studies: *Canadian Journal of Soil Science*, v. 51, no. 3, p. 385-396.
- Tate, M.W., and Clelland, R.C., 1957, Nonparametric and shortcut statistics in the social, biological and medical sciences: Danvill, Il., Interstate, 171 p.
- Ulrich, R., and Stromberg, L.K., 1962, Soil survey of the Madera area, California: U.S. Department of Agriculture Soil Survey Series 1951, no. 11, 155 p.
- Wahrhaftig, Clyde, and Birman, J.H., 1965, The Quaternary of the Pacific mountain system in California, in Wright, H.E., Jr., and Frey, D.G., eds., 1965, *The Quaternary of the United States: Princeton, N.J., Princeton University Press*, 299-340.
- Wild, A., 1961, Loss of zirconium from 12 soils derived from granite: *Australian Journal of Agricultural Resources*, v. 12, p. 230-305.
- Williams, G.P., 1983, Improper use of regression equations in earth sciences: *Geology*, v. 11, no. 4, 195-197.
- Yaalon, D.H., 1975, Conceptual models in pedogenesis: Can soil-forming functions be solved? *Geoderma*, v. 14, no. 3, p. 189-205.
- Yount, J.C., Birkeland, P.W., and Burke, R.M., 1982, Holocene glaciation: Mono Creek, central Sierra Nevada, California [abs.]: *Geological Society of America Abstracts with Programs*, v. 14, no. 4, p. 246.

SUPPLEMENTARY TABLES

Supplementary Table 1. Field descriptions

EXPLANATION
(see fig. 13 for sample locations)

SOIL STRUCTURE

Grade	Size	Type
m, massive	vf, very fine (v thin)	gr, granular
sg, single grained	f, fine (thin)	pl, platy
1, weak	m, medium,	pr, prismatic
2, moderate	c, coarse (thick)	cpr, columnar
3, strong	vc, very coarse (v thick)	abk, angular blocky sbk, subangular blocky

If two structures-listed as primary and secondary

SOIL TEXTURE

co, coarse	S, sand	SCL, sandy-clay loam
f, fine	LS, loamy sand	CL, clay loam
vf, very fine	SL, sandy loam	SiCL, silty-clay loam
	L, Loam	SC, sandy clay
	SiL, silt loam	C, clay
	Si, silt	SiC, silty clay

SOIL CONSISTENCE

Dry	Moist	Wet	
lo, loose	lo, loose	so, nonsticky	po, nonplastic
so, soft	vfr, very friable	ss, slightly sticky	ps, slightly plastic
sh, slightly hard	fr, friable	s, sticky	p, plastic
h, hard	fi, firm	vs, very sticky	vp, very plastic
vh, very hard	vf, very firm		
eh, extremely hard	efi, extremely firm		

HORIZON BOUNDARIES

Distinctness	Topography
va, very abrupt	s, smooth
a, abrupt	w, wavy
c, clear	i, irregular
g, gradual	b, broken
d, diffuse	

ROOTS AND PORES

Size	Abundance	Pore Shape
vf, very fine	1 few	tub, tubular
f, fine	2 common	ir, irregular
m, medium	3 many	v, vesicular
co, coarse		

CLAY FILMS

Frequency	Thickness	Morphology
v1, very few	n, thin	pf, ped face coatings
1, few	mk, moderately thick	br, bridging grains
2, common		po, pore linings
3, many	k, thick	(w, occurs as waves or lamellae)
4, continuous		co, coats on clasts

Site	Geologic unit	Elev. (ft)	Present vegetation	Recent land use	Parent texture	Location (Mount Diablo Base meridian)
Modern river alluvium						
MRA1	---	40	Annual grass	---	SL	Chr. SMI/4 sec. 2, T. 7 S., R. 9 E.
MRA2	---	40	Annual grass	---	SL	NEI/4NEI/4 sec. 1, T. 7 S., R. 9 E.
MRA3	---	40	Annual grass	---	SL	NEI/4NEI/4 sec. 2, T. 7 S., R. 9 E.
MRA4	---	260	Annual grass	---	SL	NEI/4NEI/4 sec. 10, T. 5 S., R. 14 E.
Post-Mojave deposits						
PM5	111	65	Annual grass	None	SL	SEI/4SEI/4 sec. 24, T. 6 S., R. 10 E.
PM6	111	70	Annual grass	None	SL/SL	NEI/4NEI/4 sec. 1, T. 6 S., R. 10 E.
PM8	111	70	Annual grass	None	SL/SL	NEI/4NEI/4 sec. 2, T. 7 S., R. 10 E.
PM3	11	65	Annual grass	do	SL/SL	NEI/4NEI/4 sec. 2, T. 7 S., R. 9 E.
PM4	11	65	Annual grass	do	SL/SL	NEI/4NEI/4 sec. 2, T. 7 S., R. 9 E.
PM6	11	65	Annual grass	2-5-yr melons	SL	E1/2 sec. 3, 34, T. 7 S., R. 10 E.
PM8	11	265	Annual grass	Settlement	SL	Chr. SMI/4 sec. 3, T. 6 S., R. 14 E.
Mojave Formation						
M31	Upper member	70	Annual grass	None	SL/SL	NEI/4NEI/4 sec. 5, T. 7 S., R. 14 E.
M46	do	105	Irrigated pasture	Pre-1965 crops	SL	Chr. N1/2 sec. 28, T. 6 S., R. 11 E.
M12	Lower member	160	Annual grass	None	SL	NEI/4SEI/4 sec. 9, T. 6 S., R. 12 E.
Riverbank Formation						
R9	Upper unit	295	Irrigated Pasture	---	SL	SMI/4SEI/4 sec. 10, T. 5 S., R. 14 E.
R33	do	295	Annual grass	do	SL	NEI/4NEI/4 sec. 15, T. 5 S., R. 14 E.
R2	Middle unit	260	do	None	SL	SEI/4NEI/4 sec. 11, T. 5 S., R. 13 E.
R10	do	260	do	do	SL	SEI/4NEI/4 sec. 11, T. 5 S., R. 13 E.
R30	Lower	275	do	do	SL	Chr. N1/2 sec. 13, T. 5 S., R. 13 E.
Turlock Lake formation						
T2	Upper unit	435	Annual grass	None	SL	SEI/4NEI/4 sec. 31, T. 3 S., R. 14 E.
T6	do	305	do	do	SL	SMI/4SMI/4 sec. 31, T. 3 S., R. 13 E.
T11	do	355	do	Turkey farm	SL	NEI/4NEI/4 sec. 11, T. 4 S., R. 13 E.
Laguna Formation						
CH1	China Hat Gaeel Member	590	Annual grass	Pasture	SL/gps	NEI/4NEI/4 sec. 2, T. 6 S., R. 14 E.
CH2	do	720	do	do	SL/gps	SEI/4SMI/4 sec. 30, T. 5 S., R. 15 E.
CH3	do	730	do	do	SL/gps	NEI/4SEI/4 sec. 30, T. 5 S., R. 15 E.

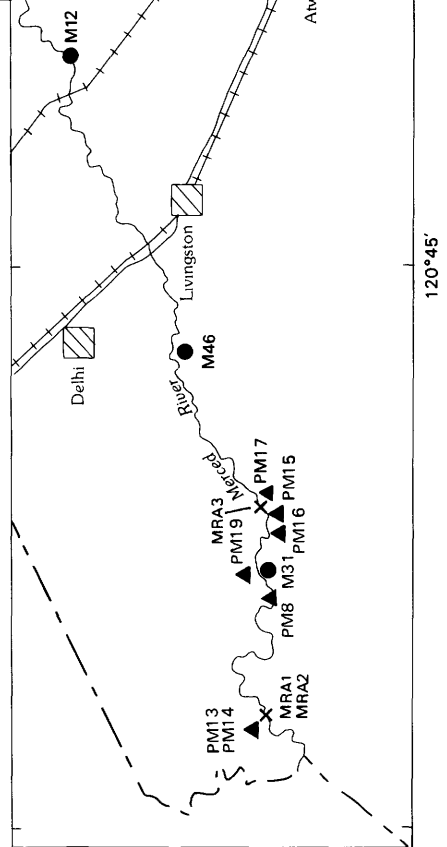
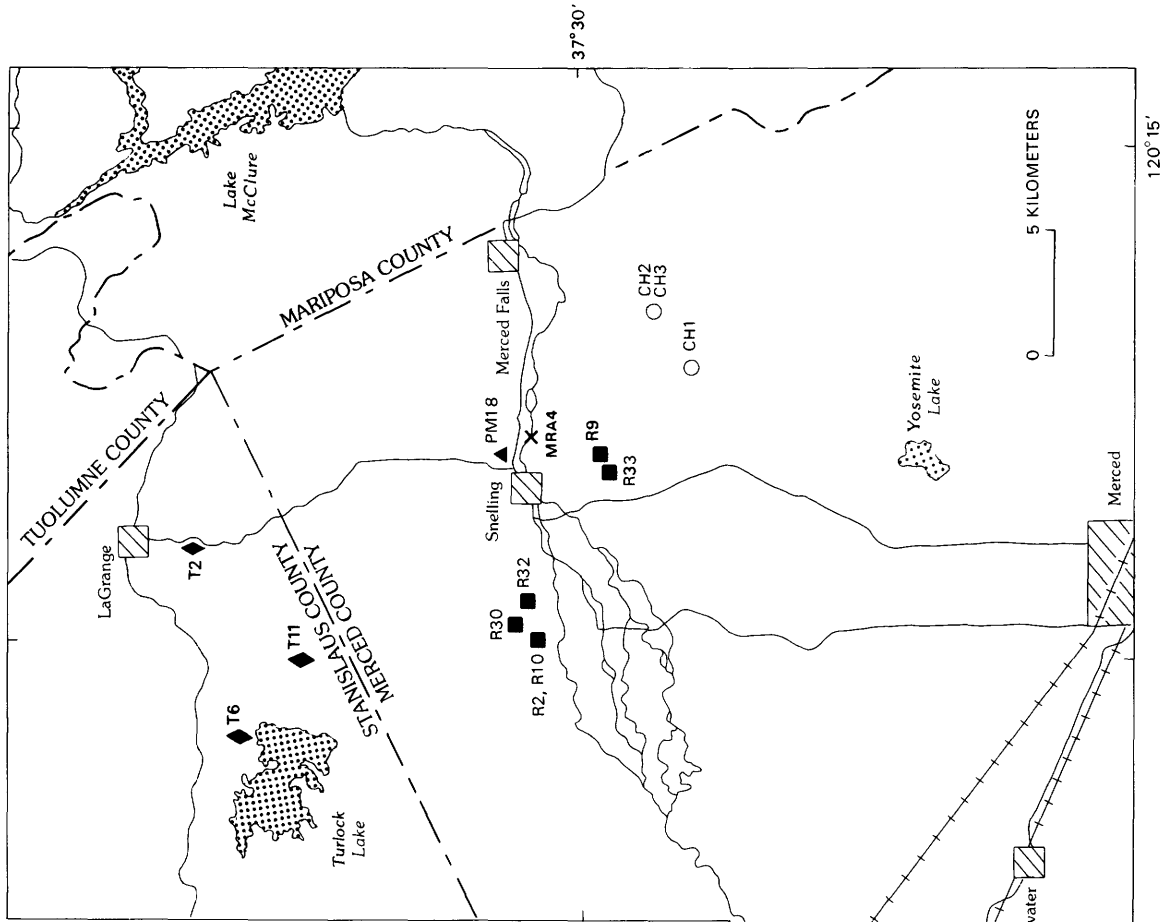


Figure 13. Study area in central California, showing locations of sampling sites.

Supplementary Table 1. Field descriptions--Continued

[Analyst: J.W. Harden U.S. Geological Survey]

No.	Sample	Horizon	Basal depth (cm)	Lower boundary	Moist color	Dry color	Texture	Structure	Consistence			Roots	Pores	Clay films	pH	Assumed Parent Material	
									Dry	Moist	Wet					Texture	Wet consistence
Modern River Alluvium																	
1	MRA1	--	--	--	--	--	--	--	--	--	--	--	--	--	--	--	--
2	MRA2	--	--	--	--	--	--	--	--	--	--	--	--	--	--	--	--
3	MRA3	--	--	--	--	--	--	--	--	--	--	--	--	--	--	--	--
4	MRA4	--	--	--	--	--	--	--	--	--	--	--	--	--	--	--	--
Post-Modesto Deposits, .2 Ka																	
5	PM15	A	0-4	a,w	10YR3/3	10YR5/3	S	l m gr	lo	lo	so,po	3vf	--	0	5.84	S	so,po
6		I1C1ox	4-19	a,w	10YR4/4	10YR5/4	LS	m	sh	fr	so,po	2vf,2f	1ftub	0	5.69	LS	so,po
7		I1C2ox	19-42	--,w	10YR4/3	10YR5/3	S	sg	lo	lo	so,po	2vf,1m	--	0	5.56	S	so,po
8		IVC3ox	42-47	a,l	10YR3/3,5	10YR6/4, 10YR5/6	LS	sg	lo	vf	so,po	2m	--	0	5.55	LS	so,po
9	VICn	VC4n	47-51	a,w	10YR4/2	10YR6,5/2	coS	sg	lo	lo	so,po	--	--	0	5.72	coS	so,po
10		VICn	51-	--	10YR4/3,5	10YR6/3	S	sg	lo	lo	so,po	1f	--	0	5.82	S	so,po
11	PM19	A11	0-7	c,w	10YR2/2	10YR6/3	SL	l m gr	sh	fr	so,po	3vf,3f	1fir	0	5.56	SL	so,po
12		I1A12	7-12	g,w	10YR3/2	10YR6/3	fSL	m, l m sbk	--	fr	so,po	2f	2f	0	6.25	fSL	so,po
13	I1C1ox	12-23	g,w	10YR3/3	10YR6/3	LS	m	--	fr	so,po	2f	1ftub	0	6.32	LS	so,po	
14		IVC2ox	23-43	a,w	10YR3/3	10YR5/3	L	m, l m sbk	--	fr	ss,po	1m,1f, lcs	2f, 1mtub	0	6.91	L	ss,po
15	VIC4ox	43-49	a,w	10YR3/3	10YR6/3	LS	sg	--	lo	so,po	1f	--	0	6.79	LS	so,po	
16		VIC4ox	49-55	a,w	10YR3/2	10YR6/3	vfSL	m	--	fr	so,po	1f	2ftub	0	6.98	vfSL	so,po
17	VIIC6	VIC5ox	55-66	a,w	10YR3/2	10YR6,5/3	S	sg	--	lo	so,po	--	--	0	6.54	S	so,po
18		VIIC6	66-80+	--	10YR3/2	10YR6/3	SiL	m	--	fr	ss,po	2vcs	2ftub	0	--	SiL	ss,po
Post-Modesto Deposits, 3 Ka																	
19	PM8	Ao	4-0	c,s	--	--	--	2 gr	--	--	--	3f,3m	--	0	--	--	--
20		A1	0-28	g,w	10YR3/3	10YR5/4	SiL	l m sbk	so	fr	ss,po	3f,3m	1ftub	0	6.33	SiL	ss,po
21		I1C1	28-51	c,w	10YR3/3	10YR5/3	vfSL	l co sbk	sh	fr	so,po	1f	1mtub	0	7.20	vfSL	so,po
22		I1C2	51-62	g,s	10YR4/3	10YR6/3	LS	m	sh	vf	so,po	--	--	0	7.33	LS	so,po
23	PM13	IVC3ox	62-76	--	--	--	FS	sg	--	lo	so,po	--	--	0	7.48	FS	so,po
24		A11	0-5	a,s	10YR3/2	10YR5/4	SiL	2 f gr	so	vf	ss,po	--	2m, 2fir	0	6.30	SiL	ss,po
25		A12	5-35	c,w	10YR3/3	10YR4/3	L	m, m sbk, f gr	so	vf	ss,po	2f	2f, 1mtub	0	7.71	L	ss,po
26		I1C1ox	35-86	g,w	10YR4/3	10YR5/3	SL	m, m sbk	--	vf	so,po	1m, lco	2vf tub	0	7.85	LS	so,po
27		I1C2ox	86-112	--	10YR4/3	10YR5/4	LS	m, m sbk	--	vf	so,po	1f	1vf tub	0	7.35	LS	so,po
28		VIC3ox	112-136	--	10YR4/3	10YR5/3	LS	sg	--	lo	so,po	--	--	0	--	LS	so,po
29			VC4ox	136-160+	--	10YR4/4, 3/6	10YR5/4	SiL	m	--	lo	so,po	--	--	0	--	SiL
30		PM14	A11	0-3	a,s	10YR3/3	10YR5/3	L	2 m gr	--	vf	ss,po	3f	3fir	0	6.42	L
31	I1A12		3-33	c,w	10YR3/3	10YR4/3	SiL	m, m sbk	--	vf	ss,po	2m,2f	2ftub	0	7.83	SiL	ss,po
32	I1C1ox		33-99	g,w	10YR4/3	10YR5/3	SL	m, m sbk	--	vf	so,po	2vf	1f tub	0	7.83	SL	so,po
33	IVC2ox		99-130	c,w	10YR4/3	10YR5/3	LS	m, l m sbk	--	vf	so,po	lco, lvc	1vf tub	0	6.88	LS	so,po
34	VC3ox		130-175	c,w	10YR3/3	10YR5/4	SL	m	--	vf	so,po	--	--	0	6.54	SL	so,po
35	VIC4ox		175-200	c,w	10YR3/3	10YR5/3	LS	m	--	vf	so,po	--	--	0	6.66	LS	so,po
36	VIIC5n	200-230+	--	10YR5/2	10YR7/2	S	sg	--	lo	so,po	--	--	0	6.92	S	so,po	
37	PM16	A	0-2	a,w	10YR3/4	10YR4/3	SL	l m gr	sh	fr	so,po	3vf	1mir	0	6.50	SL	so,po
38		C1ox	2-25	g,w	10YR3/4	10YR5/4	fSL	m, 2 m sbk	sh	fr	so,po	2vf	2vf tub	0	6.48	fSL	so,po
39		I1C2ox	25-35	g,w	10YR3/3	10YR5/3	fSL	m, 2 m sbk	sh	fr	ss,po	2vf	2vf tub	0	6.86	fSL	ss,po
40		I1C3ox	35-65	g,w	10YR4/4	10YR5/4	LS	m, l m sbk	so	vf	so,po	1f	1vf, 1ftub	0	7.29	LS	so,po
41		VIC4ox	65-90	g,w	10YR4/3	10YR6/2	S	sg	--	vf	so,po	1f	--	0	7.22	S	so,po
42			VC5ox	90-116+	g,w	10YR4/4	10YR5/4	LS	m	--	vf	so,po	1f	--	0	7.42	LS
43		VC6n	216-236	--	10YR3/4	10YR5/4	--	sg	--	--	--	--	--	0	--	--	--
44	PM17	A	0-6	a,w	10YR3,5/4	10YR5/4	LS	l co gr	sh	fr	so,po	3f	1ftub	0	6.61	LS	so,po
45		I1C1ox	6-45	g,w	10YR3/4	10YR5/3	fSL	m, l m sbk	sh	fr	so,po	2f	1ftub	0	6.99	fSL	so,po
46		I1C2ox	45-63	g,w	10YR3/4	10YR5/3	vfSL	m, l m sbk	sh	fr	so,po	2f	2ftub	0	7.18	vfSL	so,po
47		I1C3ox	63-74	g,w	10YR4/4	10YR5/4	vfSL	m, l m sbk	sh	fr	ss,po	2vf	2ftub	0	8.03	vfSL	ss,po
48	VIIC4n	74-120+	--	10YR4/3	10YR5/3	LS	sg	--	--	--	--	--	0	7.83	LS	--	
49	PM18	A	0-6	g,w	10YR3/2	10YR4/2	SL	2 m gr	sh	fr	so,po	3f	2fir	0	7.26	LS	so,po
50		I1C1ox	6-65	d,w	10YR3/4	10YR5/4	LS	m, l m sbk	sh	fr	so,po	2m,2f	1ftub	0	6.00	LS	so,po
51		I1C2ox	65-115	g,w	10YR4/4	10YR5/4	L	m, l m sbk	so	vf	so,po	3m,2co	1mtub	0	5.75	LS	so,po
52		I1C3ox	115-164	g,w	10YR4/4	10YR5/4	S	sg	--	lo	so,po	1m,lco	--	0	5.98	S	so,po
53		IVC4ox	164-175+	--	10YR4/4	10YR6/3	slgrS	sg	--	lo	so,po	--	--	0	6.20	slgrS	so,po

Supplementary Table 1. Field descriptions—Continued

No.	Sample	Horizon	Basal depth (cm)	Lower boundary	Moist color	Dry color	Texture	Structure	Consistence			Roots	Pores	Clay films	pH	Assumed parent Material	
									Dry	Moist	Wet					Texture	Wet consistence
Modesto Formation, upper member, 10 Ka																	
54	M31	A11	0-20	c,s	10YR3/2	10YR5/4	SL	2 m gr	so	vfr	ss,po	2f	1ftub	0	7.62	SL	ss,po
55		A12	20-63	g,w	10YR3/3	10YR6/4	fSL	m	so	fr	so,po	2m,1f	2mtub	0	9.64	fSL	so,po
56		AC	63-150	g,w	10YR3/3	10YR6/4	fSL	m	sh	--	so,po	--	3m, 3ftub	0	10.0	fSL	so,po
57		I1C1	150-200	c,w	10YR3/3	10YR5/4	fSL	m	h	--	so,po	--	2mtub	0	10.0	fSL	so,po
58		I1C2	200-254	a,s	--	--	LS	sg	lo	lo	so,po	--	--	0	9.64	LS	so,po
59	M46	A11p	0-5	c,w	10YR4/2	10YR6/3, 5/3	fSL	2 m+co gr	so	vfr	so,po	3m,2f, 2vf	2fir	0	6.29	fSL	so,po
60		A12p	5-14	c,w	10YR4/2, 4/6	10YR5/3	fSL	1 m pl	sh	fr	ss,po	2m, 1f	2f, 2vftub	0	6.76	fSL	so,po
61		I1A13p	14-32	c,s	10YR3/3	10YR5/3	fSL	m, 2 m sbk	sh	fi	so,po	2m, 2f	3f, 2vftub	0	6.77	fSL	so,po
62		I1IAC	32--66	g,w	10YR4/3	10YR5/3	fSL	m, 2 co sbk	h	fi	so,po	1m, 1f	1m, 2ftub	2npo, v1npo	7.01	fSL	so,po
63		I1Cox	66-250	c,s	10YR4/3	10YR5/4	fSL	sg	so	fr	so,po	1f, 1vf	--	7.04	fSL	so,po	
		I18b	250+	--	--	--	--	--	--	--	--	--	--	0	--	--	--
Modesto Formation, lower member, 40 Ka																	
64	M12	A11	0-15	c,w	10YR3/3	10YR5/3	fSL	1 m sbk	so	lo	so,po	--	--	0	--	fSL	so,po
65		A12	15-81	c,w	10YR3/2	10YR6/3	LS	1 m sbk	h	fr	so,po	--	3mtub	0	6.45	LS	so,po
66		I1B21t	81-102	g,w	10YR4/3	10YR5/4	LS	2 m sbk	h	fr	s,ps	--	3mtub	1npo, 1nbr	6.87	LS	so,po
67		I1B22t	102-170	c,w	10YR5/6	10YR5/6	SL+	2 m sbk	vh	fi	s,ps	--	2m, 1ftub	2mko, 2mko, v1npo	6.67	LS	so,po
68		I1B3	170-201	g,w	10YR5/4	10YR6/6	LS	2 m sbk	h	fr	ss,ps	--	--	1npo, 1nbr	6.98	LS	so,po
69		V1C1	201-231	d,w	10YR4/4	10YR6/4	S	1 m sbk	so	lo	ss,po	--	--	0	7.34	S	so,po
70		V1C2	230-413+	--	10YR6/2	10YR7/2	S	sg	so	lo	so,po	--	--	0	--	S	so,po
Riverbank Formation, upper member, 130 Ka																	
71	R9	A11p	0-30	g,s	10YR3/3	--	SL	--	--	fr	so,po	2m	2mtub	0	5.83	SL	so,po
72		A12p	30-60	g,w	10-7, 5YR, 4/3	--	SL	1 f sbk	--	fr	so,po	2m	2mtub	0	5.77	SL	so,po
73		B1	60-105	c,w	10YR4/3	--	SL+	1 m sbk	--	--	ss,ps	--	--	1npo, 1nbr	5.77	SL	so,po
74		I1B21	105-180	c,w	7.5YR5/4	--	SCL	1 m sbk	--	--	s,p	--	--	2mko, 2mko	6.13	SL	so,po
75		I1B22	180-235	g,w	7.5YR6/4	--	SL	sg	--	--	so,po	--	--	1npo, 1nbr	6.05	SL	so,po
76		I1B3	235-350	c,s	7.5YR4/4	--	SL+	sg	--	--	ss,ps	--	--	2mko, 2mko	6.15	SL	so,po
77		I1C	350-400+	--	7.5YR5.5/6	--	LS	sg	--	--	so,po	--	--	0	6.13	LS	so,po
78	R33	A11	0-4	c,s	--	--	SL	2 co gr	sh	fr	so,po	2f	2f,2mtub	0	6.26	SL	so,po
79		I1A12	4-19	c,w	--	--	SL	2 co sbk	sh	fr	so,po	2f, 2m	2co,2f, 2vftub	0	6.29	SL	so,po
80		I1IA3	19-39	g,w	--	--	SL	2 vco sbk	h	fr	so,po	1f	3vf,3f, 1mtub	v1npo	6.12	SL	so,po
81		I1I821t	39-62	g,w	--	--	coSCL-	2 co sbk	vh	fi	ss,ps	1f	2f,2m, 2vftub	3nbr, 1mko	5.94	SL	so,po
82		I1I822t	62-83	g,w	--	--	SCL	1 fi pr	vh	fi	ss,ps	--	2f,1m tub	3nbr, 2mko	6.21	SL	so,po
83		I1I823t	83-122	g,w	--	--	coSCL	1 fi pr	vh	vfi	s,p	--	2f,2m tub	1npo, 4nbr	--	SL	so,po
84		I1I831	122-151	g,w	--	--	coSCL-	2 vco sbk	vh	fi	ss,ps	--	2f,2m tub	4nbr, 2mko	--	SL	so,po
85		I1I832	151-210	c,w	--	--	vgrSL	m,vco sbk	--	fi	ss,ps	--	3f,2m tub	3nbr, 2mko	--	SL	so,po
86		I1B33	210-260	c,w	--	--	vgrSL	sg	--	vfr	ss,ps	--	3f,2m tub	2n-mk coats	--	LS	so,po
87		V1Cox	260-300+	--	--	--	S	sg	--	--	so,po	--	--	0	--	S	so,po
Riverbank Formation, middle member, 250 Ka																	
88	R2	Ap	0-25	c,s	10YR3/3	--	SL	2 f sbk	--	--	ss,po	--	--	0	--	--	--
89		B21	25-81	c,w	7.5YR4/4, 10YR3/3	--	SCL	3 co sbk	--	--	ss,ps	--	--	0	--	--	--
90		B22t	81-185	c,w	7.5YR4/4	--	SCL+	3 vco cpr	--	--	s,ps	--	--	0	--	--	--
91		B3	185-386	g,w	10YR4/4	--	SCL	2 co sbk	--	--	ss,po	--	--	0	--	--	--
92		C1	386-500	g,w	10YR5/4, 4/4	--	SL	m	--	--	so,po	--	--	0	--	--	--
93		C2n	500+	--	10YR5/3	--	S	sg	--	--	so,po	--	--	0	--	--	--

Supplementary Table 1. Field descriptions—Continued

No.	Sample	Horizon	Basal depth (cm)	Lower boundary	Moist color	Dry color	Texture	Structure	Consistence			Roots	Pores	Clay films	pH	Assumed Parent Material	
									Dry	Moist	Wet					Texture	Wet consistence
Riverbank Formation, middle member, 250 Ka																	
94	R10	A	0-46	c,s	10YR3/3	10YR6/3	SL	2 co sbk	sh	--	so,po	1m	3m,2co tub	0	6.20	SL	so,po
95		I1B1	46-70	c,w	7.5YR4/4	10YR6/4	SL+	2 co pr	vh	--	ss,ps	1m	2m,1co tub	3nbr	6.83	SL	so,po
96		I1B21t	70-140	g,l	7.5YR4/6, 5YR4/4	7.5YR6/6	SL+	3 v co sbk	eh	--	s,p	--	1co,3m tub	3mkbr, 3mkpo	7.17	SL	so,po
97		I1B22t	140-210	g,l	7.5YR4/6, 5YR4/4	7.5YR6/6	SL	3 v co sbk	eh	--	s,p	--	3m,1co tub	3mkbr, 1kpo, 2mkpf	7.47	SL	so,po
98		I1B3t	210-386	g,w	7.5YR4/4	10YR6/6, 7.5YR4/4	SL	3 v co sbk	eh	--	ss,po	--	--	2mkbr, 2mkpo	7.47	SL	so,po
99		I1Cox	386-500	g,w	10YR4/4	10YR5/4	SL	sg	vh	--	so,po	--	--	2mkbr, 2mkpo	--	SL	so,po
100	R32	A11	0-26	g,w	10YR3/2	10YR6/3	SL	m, 1 f sbk	sh	fr	so,ps	1f, 1vf	3fir,1vf tub	0	6.41	SL	so,po
101		A12	26-50	c,w	10YR3/3	10YR6/3	SL	m, 2 m sbk	sh	fr	ss,po	1f, 1vf	2m,2f, 3vftub	0	6.28	SL	so,po
102		A3	50-70	c,w	7.5YR3/4	10YR6/3, 7.5YR5/4	SL	m, 2 f sbk	h	fr	ss,po	1f	1m,2f, 3vftub	0	6.26	SL	so,po
103		B21t	70-105	g,w	7.5YR4/4	7.5YR5/4	SL+	1 m sbk	h	fi	s,ps	--	3vf,2f tub	1nbr	6.18	SL	so,po
104		B22t	105-150	g,w	7.5YR4/5	7.5YR5/4	SCL	1 co sbk	vh	fi	s,ps	--	2vf,1f tub	4nbr, 1kpf, 3mkbrw	6.56	SL	so,po
105		831t	150-220	d,w	7.5YR4/4	7.5YR5/4	SL+	m,1 co sbk	h	fi	s,ps	--	1f,1vf tub	3nbr, 1mkbrw	--	SL	so,po
106		I1B32	220-354	g,w	--	--	SL	sg	--	vfr	ss,po	--	2vftub	1nbrw, 1mkbrw	--	SL	so,po
107		I1Cox	354-360+	--	10YR5/4	--	S+	sg	--	lo	so,po	--	--	v1nbr	--	S	so,po
Riverbank Formation, lower member, 330 Ka																	
108	R30	Ap	49-65	a,w	7.5YR4/4	10YR6/3	SL	m	sh	vfr	so,po	--	3vf,2fir	0	6.45	SL	so,po
109		B1	65-78	c,w	5YR4/4	7.5YR5/6	SL+	m,1 co abk	h	fi	ss,ps	--	1vfir	2nbr	6.00	SL	so,po
110		B21t	78-127	g,w	5YR4/6	5YR5/6	SCL	2 co sbk	vh	fi	s,ps	--	2fir	3nbr, 2npf	5.75	SL	so,po
111		I1B22t	127-179	g,w	5YR5/6, 4/4	5YR5/6	SCL	2 co abk	vh	fi	s,p	--	2fir	1kpf, 4mkbr	5.90	SL	so,po
112		I1B3t	179-197	g,w	5YR5/6, 4/4	7.5YR7/6	SL	m	--	fr	ss,po	--	2fir	3nbr, 1kbr	6.45	SL	so,po
113		I1C1ox	197-220	c,w	7.5YR4/4	7.5YR6/6	SL+	m	sh	vfr	so,po	--	--	2nbr, 1mkbrw	6.95	SL	so,po
		I1Bb	220+	--	--	--	--	--	--	--	--	--	--	0	--	--	--
Turlock Lake Formation, 600 Ka																	
114	T2	A	0-31	g	5YR3/4	--	coSL	m sbk	--	vfi	--	--	--	0	6.58	SL	--
115		B21	31-173	i	2.5YR3/6	--	CL	co abk	--	vfi	--	--	--	0	5.82	SL	--
116		I1B22	173-386	i	7.5YR5/6, 2.5YR3/6	--	SL	m-co abk	--	vfi	--	--	--	0	6.52	SL	--
117		I1IC	386-417	--	2.5YR5/8, 5YR5/6	--	S	1 m sbk	--	--	--	--	--	0	6.48	S	--
118	T6	A11	0-20	g,w	10YR3/4	10YR4/4	LS	--	--	fr	so,po	3f	3mir	0	6.50	LS	so,po
119		A12	20-40	a,l	10YR3/4	10YR5/3	LS	--	sh	fr	so,po	2f	3m,3co tub	0	6.00	LS	so,po
120		I1B21t	40-90	g,w	5YR3/6	5YR4/8	LS	2 med pr	h	fi	s,ps	--	2 m	3mkpo, 3mkbr, 2mkpf	7.00	LS	so,po
121		I1B22t	90-190	g,w	2.5YR3/6	2.5YR3/4, 3/6	SCL	--	h	vfi	vs,p	--	2cotub	3mkpo, 3mkbr, 2mkpo	6.20	LS	so,po
122		I1IB+C	190-370	g,w	2.5-5YR, 3/4 and 30% 10YR5/4	2.5YR3/6, 4/6 10YR6/4	coSL	sg	sh	fi	ss,po	--	2co,1f tub	3mkbr, 2mkpo, 2mkbr	6.60	coSL	so,po
123	T11	A11p	0-5	--	10YR3/2	10YR5/2	SL	--	sh	fr	so,po	--	--	0	6.82	SL	so,po
124		I1A12p	5-11	a	10YR3/3	10YR5/3	SL	--	h	fr	so,po	--	2f,2vfr	0	6.95	SL	so,po
125		I1A+B	11-20	g	5YR4/4, 7.5YR4/4	7.5YR5/4, 10YR6/3	SCL	--	h	fi	ss,ps	--	--	0	6.85	SL	so,po
126		I1B1t	20-33	g	2.5YR3/6	5YR4/6	SCL	2 co abk	h	fi	s,p	--	2f,vf tub	4nbr	6.70	SL	so,po
127		I1B2t	33-80	g	2.5YR4/4, 3/6	5YR5/6, 4/6	SCL	2 m sbk	vh	vfi	vs,pv	--	3vfr	4mkbr, 3mkpo, 3kpow	6.60	SL	so,po
128		I1B31t	80-191	g	2.5YR4/4	5YR5/6	SCL	m	--	fi	s,p	--	3vf,3f ir	4mkbr, 3mkpf	6.90	SL	so po
129		1VB32t	191-256	g	5YR4/4, 2.5YR4/4	5YR6/6	SL+	m	--	fr	s,p	--	2fir	2mkpf, 4nbr	7.10	SL	so,po
130		VB+C	256-292	g	5YR4/4, 5YR5/6	5YR6/6	SL+	m	--	vfr	ss,ps	--	2fir	3nbr	6.95	SL	so,po
131		VC1ox	292-375	g	5YR4/6	7.5YR6/6	SL-	m	--	vfr	ss,ps	--	1ftub	3nbr	7.00	LS	so,po
132		VC2ox	375+	--	7.5YR4/6	--	LS	sg	--	--	so,po	--	--	0	7.15	LS	so,po

Supplementary Table 1. Field descriptions--Continued

No. Sample	Horizon	Basal depth (cm)	Lower boundary	Moist color	Dry color	Texture	Structure	Consistence			Roots	Pores	Clay films	Assumed Parent Material			
								Dry	Moist	Wet				pH	Texture	Wet consistence	
China Hat gravel member of Laguna Formation, 3,000 Ka																	
133	CH1	01	1-0	a,s	--	--	--	--	--	--	--	--	--	--	--	--	
134		A1	0-12	g,w	10YR5/4, 7.5YR4/4	7.5YR6/6, slgr L	1 f sbk	sh	--	ss,ps	2f, 2m	2m,2co tub	0	4.84	L	ss,ps	
135		AB	12-53	a,w	7.5YR4/4, kroto. 2.5YR4/4	7.5YR6/6, slgr SIL	1 f sbk	sh	--	ss,ps	2f, 2m	2m, 2co tub	2npo, 2nbr	4.93	L	ss,ps	
136		I1B21t	53-140	g,w	2.5YR4/4 2.5YR3/6, 4/6	5YR4/8, 2.5YR3/6, 4/8, skins1OR 3/6, 4/8	grC	2 m sbk	exh	--	vs,pv	1m	2mtub	3kpo, 3kbr, 3kpf	4.55	L	ss,ps
137		I1B22t	140-234	g,i	10YR4/7, cr.coats 2.5YR4/8, skins	2.5YR4/8, skins 1OR4/8, 1OR3/6	grC	2 m sbk	exh	--	vs,ps	--	2mtub	4kpo, 4kbr, 4kpf	4.40	L	so,po
138		I1B31t	234-310	g,i	1OR3/6, 1OR4/8, 5Y-5GY4/1	2.5YR4/8, gr.stains 1OR4/8	grco C	1 m sbk	--	--	vs,pv	--	1mtub	2mkbr, 2mkpo, 2mkco	4.00	L	so,po
139		I1B32t	310-350+	--	1OR3/6, 4/8	2.5YR3/6, 5YR6/8, stains 1OR4/8,gley 10YR8/2	grco C-	1 m sbk	--	--	vs,pv	--	--	1mkbr, 1mkco	4.06	L	so,po
140	CH2	A1	0-8	c,w	7.5YR4/4	10YR6/4	slgr L	2 f sbk	h	fr	ss,po	2f, 2vf	2co,3f tub	0	4.71	L	ss,po
141		A3	8-30	g,w	7.5YR4/6	10YR6/4	slgr L	2 f sbk	h	fr	s,po	2f	3m,3f, 2vftub	2n-mkpo	4.55	L	ss,po
142		A+B	30-50	a,s	5YR4/4	7.5YR6/4	slgr CL	1 f sbk	h	fr	s,ps	1f	2m,3f tub	2mkpo-br, 2npo-br	4.17	L	ss,po
143		I1B21t	50-110	g,w	2.5YR4/6, 2.5YR4/6	5YR5/6	grC	m	vh	fi	vs,p	--	2f,3vf tub	2mkbr, 3mkpo	4.36	L	ss,po
144		I1B22	110-170	c,w	2.5YR4/6, some10YR 8/8	2.5YR4/6	grC	m	eh	fi	vs,pv	--	1vftub	4kbr, 4kco	4.20	LS	ss,po
145		I1B23	170-200	g,w	2.5YR3/6, 2.5YR4/6	2.5YR4/6, 2.5YR4/8, 5Y8/2	grCL	m	eh	fi	vs,pv	--	1vftub	4kbr, 4kco	4.12	LS	ss,po
146		I1B24	200-290	g,w	2.5YR4/8, 1OR4/6	1OR4/6, 2.5YR4/8	grC	m	eh	fi	vs,pv	--	1vftub	4kbr, 4kco	4.14	LS	ss,po
147		I1B3	290-350	--	--	--	grC	m	eh	fi	vs,pv	--	--	4kbr, 4kco	4.14	LS	ss,po
		8+C or Cox	750-1000	d	7.5YR6/6, clay 2.5YR4/6	10YR7/6	grLS	sg	lo	lo	ss,po	-- 4kco	--	1nbr,	--	LS	so,po
148	CH3	Ao A1	1.5-0 0-9	-- c,w	-- 7.5YR4/4	-- 7.5YR6/4	-- slgr L	-- 2 m sbk	-- h	-- fr	-- ss,po	-- 3f, 1m 3f	-- 3f,1m tub	0	5.84	L	ss,po
149		A3	9-35	g,w	7.5YR3/4	7.5YR6/4	slgr L	2 m sbk	sh	fr	ss,po	3f	3f,2m, 2vftub	0	5.44	L	ss,po
150		A+B	35-68	a,w	5YR4/4	5YR6/4	slgr L	1 m sbk	h	fr	ss,ps	3f	2f,3m, 2vftub	2mkpo	5.01	L	ss,po
151		I1B2t	68-105	g,w	2.5YR4/6	5YR5/6	grC	m	h	fr	so,po	2f, 2vf	2f,3m, 2vftub	3mk-kpo, 3mkco	4.62	L	so,po
152		I11B22t	105-153	g,w	1OR3/6, 2.5YR5/8	2.5YR4/8	grC	m	h	fr	s,ps	2f	3f,3vf tub	4kbr, 4kco	4.48	SL	so,po
153		IVB23	153-173	c,w	2.5YR4/8, 5Y6/1	2.5YR4/8	grC	m	vh	fi	vs,pv	--	3vftub	4kbr, 4kco	4.06	SL	so,po
154		VB24	173-260	g,w	1OR4/8, 7.5YR6/6	10YR4/6, 7.5YR6/6	slgr L	m	eh	fi	vs,pv	--	--	4kbr, 4kco	4.33	SL	so,po
155		VI1B31	260-340	g,w	1OR3/6	1OR3/6	grSCL	m	eh	fr	s,ps	--	--	3mkbr	4.20	SL	so,po
156		VI32	340-750+	--	1OR3/6	1OR3/6	grCL	m	--	--	--	--	--	3mkbr	4.10	SL	so,po

Supplementary Table 2. Physical properties

[Analysts: A.J. Busacca, Peter Janitsky, and R. Meixner, University of California, Davis]

No.	Sample	Horizon	Basal depth (cm)	>2-mm	Percentage of <2-mm fraction							<2- μ clay	<1- μ clay	Bulk density (g/cm ³)
					Total sand	vco sand	co sand	m sand	fi+vfi sand	Silt				
Modern River Alluvium														
1	MRA1	--	--	--	--	--	--	--	--	--	--	--	--	
2	MRA2	--	--	--	--	--	--	--	--	--	--	--	--	
3	MRA3	--	--	--	--	--	--	--	--	--	--	--	--	
4	MRA4	--	--	--	--	--	--	--	--	--	--	--	--	
Post-Modesto deposits, .2 Ka														
5	PM15	A1	4	0	87.1	0.1	11.1	21.8	54.1	10.0	2.9	2.3	--	
6	PM15	2C1ox	19	0	80.5	0.4	2.6	7.4	70.3	15.4	4.1	3.4	1.43	
7	PM15	3C2ox	42	0	92.4	0.1	5.2	18.2	68.9	4.9	2.7	2.5	--	
8	PM15	4C3ox	47	0	87.3	0.0	3.0	7.7	76.5	9.1	3.6	2.3	1.41	
9	PM15	5C4ox	51	0	95.4	0.2	19.4	41.7	34.1	3.2	1.4	1.0	--	
10	PM15	6C5ox	51+	0	90.0	0.0	2.1	11.7	76.1	6.7	3.3	2.4	1.37	
11	PM19	A11	7	0	71.1	0.1	2.5	12.4	56.1	27.0	6.9	5.1	1.29	
12	PM19	2A12	12	0	68.6	0.1	2.3	11.9	54.3	71.3	7.0	5.4	1.47	
13	PM19	3C1ox	23	0	75.5	0.2	2.6	13.1	59.6	19.3	5.2	4.2	1.32	
14	PM19	4C2ox	43	0	46.3	0.3	1.9	4.8	39.3	43.9	9.8	7.2	1.42	
15	PM19	5C35C3ox	49	0	85.9	0.0	0.1	1.6	84.1	11.4	2.7	2.4	1.40	
16	PM19	6C4n	55	0	63.4	0.6	9.7	14.1	39.0	31.0	5.6	4.6	1.39	
17	PM19	7C5n	66	0	89.9	0.2	17.9	45.4	26.4	7.7	2.4	1.8	--	
18	PM19	8C6n	80+	0	30.4	0.0	0.4	1.7	28.3	59.9	9.7	6.7	1.36	
Post-Modesto deposits, 3 Ka														
19	PM8	A1	32	0	36.4	0.2	2.6	2.6	33.7	52.8	13.5	10.0	1.24	
20	PM8	2C1	55	0	55.4	0.0	0.2	1.2	50.4	41.1	5.9	3.8	1.21	
21	PM8	3C2	66	0	81.5	0.1	1.8	14.6	65.0	12.5	4.2	3.0	1.30	
22	PM8	4C3	76+	0	92.9	0.0	3.7	27.4	61.4	3.8	2.7	1.2	--	
23	PM13	A11	5	0	38.5	0.0	0.0	0.9	37.0	49.9	12.1	9.5	1.17	
24	PM13	A12	35	0	44.8	0.1	2.0	3.8	39.0	37.8	10.2	7.2	1.27	
25	PM13	2C1ox	86	0	72.9	0.1	2.3	6.2	64.2	23.2	3.9	2.2	1.39	
26	PM13	3C2ox	112	0	81.7	0.0	0.6	4.4	76.6	15.6	2.8	2.0	1.31	
27	PM13	4C3ox	136	0	--	--	--	--	--	--	--	--	--	
28	PM13	5C4ox	200	0	--	--	--	--	--	--	--	--	--	
29	PM13	6C5n	720	0	--	--	--	--	--	--	--	--	--	
30	PM14	A11	3	0	50.1	0.0	0.9	1.8	47.4	39.1	10.8	7.2	--	
31	PM14	2A12	33	0	39.1	0.1	1.3	2.3	35.4	49.7	11.2	7.8	1.28	
32	PM14	3C1ox	99	0	71.1	0.0	4.2	7.3	59.2	23.4	5.5	3.9	1.39	
33	PM14	4C2ox	130	0	80.3	0.1	2.3	5.7	72.2	15.4	4.3	3.0	1.41	
34	PM14	5C3ox	175	0	71.7	0.4	3.2	2.9	65.3	22.6	5.7	3.9	1.40	
35	PM14	6C4ox	200	0	85.7	0.4	6.0	9.0	70.3	10.6	3.7	2.8	1.38	
36	PM14	7C5n	230+	0	96.5	4.5	58.6	24.3	9.1	2.8	0.7	0.6	--	
37	PM16	A	2	0	73.7	0.1	0.2	4.7	68.3	19.9	6.4	4.8	--	
38	PM16	C1ox	25	0	74.9	0.0	0.3	3.7	70.9	18.9	6.2	4.5	1.38	
39	PM16	2C2ox	35	0	75.1	0.0	0.2	3.7	71.1	19.5	5.4	4.6	1.40	
40	PM16	3C3ox	65	0	83.3	0.0	0.5	6.6	76.1	12.4	4.3	3.8	1.35	
41	PM16	4C4ox	90	0	92.5	0.0	1.7	21.8	69.1	5.6	1.9	1.8	--	
42	PM16	5C5ox	116	0	82.9	0.0	0.2	4.3	78.5	13.9	3.2	2.3	1.37	
43	PM16	5C6n	236	0	--	--	--	--	--	--	--	--	--	
44	PM17	A	6	0	74.6	0.2	2.3	7.0	65.0	22.5	2.9	1.2	--	
45	PM17	2C1ox	45	0	74.1	0.1	1.7	6.6	65.8	21.0	5.0	3.9	1.34	
46	PM17	2C2ox	63	0	73.0	0.0	0.4	1.3	71.3	21.3	5.7	4.4	1.24	
47	PM17	2C3ox	74	0	64.2	0.0	0.1	1.5	62.5	28.9	6.9	4.8	1.22	
48	PM17	3C4n	120+	0	85.9	0.0	0.3	6.0	79.6	10.9	3.2	2.6	1.34	
49	PM18	A	6	0	70.1	0.5	5.1	13.7	50.9	21.3	8.6	6.8	--	
50	PM18	2C1ox	65	0	77.7	1.0	6.5	13.4	57.0	18.2	4.1	2.9	1.53	
51	PM18	2C2ox	115	0	83.0	1.3	8.5	18.5	54.5	13.3	3.7	2.6	1.53	
52	PM18	3C3ox	164	0	90.4	1.1	11.4	28.1	49.8	7.0	2.6	2.3	1.52	
53	PM18	4C4ox	175+	10	88.7	0.7	9.6	31.1	47.3	9.0	2.3	1.7	--	

Supplementary Table 2. Physical properties—Continued

No.	Sample	Horizon	Basal depth (cm)	Percentage of <2-mm fraction									Bulk density (g/cm ³)
				>2-mm	Total sand	vco sand	co sand	m sand	fi+vf _i sand	Silt	<2-μ clay	<1-μ clay	
Modesto Formation, upper member, 10 Ka													
54	M31	A11	20	0.0	53.6	0.0	0.7	4.0	48.5	36.8	8.8	6.1	1.26
55	M31	A12	63	0.0	61.5	0.1	0.6	4.1	54.8	31.9	4.8	2.2	1.28
56	M31	AC	150	0.0	67.7	--	--	--	--	28.1	4.2	1.7	1.43
57	M31	2C1	200	0.0	62.2	0.0	0.4	2.5	55.7	27.7	6.5	4.1	1.52
58	M31	3C2	254	0.0	83.0	0.0	1.3	10.1	68.7	11.6	3.6	2.1	1.42
59	M46	A11p	5	0	68.6	0.8	9.7	13.4	44.7	25.8	5.6	4.4	--
60	M46	A12p	14	0	63.7	0.9	10.9	13.5	38.3	30.0	6.9	4.7	1.61
61	M46	2A13p	32	0	65.3	0.7	10.4	13.9	40.4	28.9	5.8	4.6	1.66
62	M46	3AC	66	0	58.2	0.5	7.0	12.4	38.7	33.6	8.2	6.0	1.65
63	M46	4Cox	250	0	60.1	0.1	4.5	12.8	42.7	31.2	8.7	6.4	1.62
Modesto Formation, lower member, 40 Ka													
64	M12	A11	15	0	--	--	--	--	--	--	--	--	--
65	M12	A12	81	0	80.5	2.3	24.4	17.2	36.6	13.5	6.0	3.3	1.68
66	M12	2B21t	102	0	87.4	1.1	21.3	15.7	34.9	1.4	11.2	7.6	1.68
67	M12	3B22t	170	0	78.9	2.7	22.7	15.5	31.3	4.0	16.8	15.8	1.89
68	M12	4B3	201	0	85.9	2.6	27.0	17.6	33.5	7.8	6.3	4.2	1.85
69	M12	5C1	231	0	90.6	3.9	39.2	19.0	27.0	6.1	3.3	1.6	--
70	M12	6C2	413+	0	97.0	--	--	--	--	2.2	0.8	0.4	--
Riverbank Formation, upper member, 130 Ka													
71	R9	A11p	30	0	73.2	2.8	24.5	16.0	17.6	19.6	7.2	4.5	1.75
72	R9	A12p	60	0	71.4	2.4	24.0	16.4	26.7	21.3	7.3	4.3	1.75
73	R9	B1	105	0	68.0	2.2	22.5	16.4	26.7	19.4	12.6	10.0	1.84
74	R9	2B21	180	0	64.0	1.8	18.8	15.9	26.9	15.2	20.8	18.2	1.93
75	R9	2B22	235	0	73.5	4.3	29.8	17.4	20.7	12.8	13.7	11.8	1.84
76	R9	3B3	350	0	72.8	6.4	36.4	17.7	15.6	14.2	13.0	11.6	1.88
77	R9	4C	400+	20	87.9	16.5	32.6	18.6	19.6	5.8	6.8	6.2	1.42
78	R33	A11	4	0	70.3	4.4	24.3	14.6	51.7	23.2	6.5	4.4	1.57
79	R33	2A12	19	0	58.2	3.4	18.5	11.8	--	36.1	5.7	3.5	1.73
80	R33	3A3	39	0	67.8	4.6	22.5	13.7	--	23.0	9.2	6.8	1.77
81	R33	3B21t	62	0	60.4	3.1	19.1	12.3	--	21.9	17.7	14.8	2.03
82	R33	3B22t	83	0	57.0	2.9	17.7	11.8	--	18.0	25.0	21.9	2.04
83	R33	3B23t	122	0	59.2	2.7	18.0	12.6	--	15.6	25.2	22.4	2.01
84	R33	3B31	151	0	69.8	3.5	22.7	16.3	--	12.3	17.9	16.0	1.89
85	R33	3B32	210	--	71.9	4.3	24.1	16.0	--	15.6	12.5	11.0	1.97
86	R33	4B33	260	--	79.4	19.5	31.5	13.1	--	7.5	13.1	12.6	1.94
87	R33	5Cox	300+	0	90.7	8.9	40.7	20.7	--	2.1	7.2	6.6	--
Riverbank Formation, middle member, 250 Ka													
88	R2	Ap	25	0	--	--	--	--	--	--	--	--	1.43
89	R2	B21	81	0	--	--	--	--	--	--	--	--	1.57
90	R2	B22t	185	0	--	--	--	--	--	--	--	--	2.01
91	R2	B3	386	0	--	--	--	--	--	--	--	--	1.86
92	R2	C1	500	0	--	--	--	--	--	--	--	--	1.72
93	R2	C2	500+	0	--	--	--	--	--	--	--	--	--
94	R10	A	46	0	73.4	3.8	24.1	14.4	32.3	19.3	7.3	5.2	1.80
95	R10	2B1	70	0	68.1	5.7	30.4	12.4	22.9	18.8	13.1	11.5	1.86
96	R10	2B21t	140	0	68.4	5.6	30.0	12.9	22.5	18.0	13.6	11.1	1.92
97	R10	2B22t	210	0	72.9	6.1	33.3	13.7	22.9	14.9	12.2	10.2	1.93
98	R10	3B3t	386	0	77.6	10.2	39.8	7.9	19.4	9.8	11.6	9.8	1.85
99	R10	3Cox	500	0	--	--	--	--	--	--	--	--	--
100	R32	A11	26	0	72.4	2.6	19.0	16.1	34.7	20.6	7.0	4.4	1.67
101	R32	A12	50	0	73.0	2.4	19.7	16.0	35.0	19.2	7.8	5.2	1.63
102	R32	A3	70	0	69.4	2.2	18.2	15.2	43.8	19.9	10.7	7.6	1.86
103	R32	B21t	105	0	64.7	2.1	16.7	14.5	31.3	19.2	16.1	13.2	2.05
104	R32	B22t	150	0	63.7	1.8	17.0	14.8	30.2	16.7	19.6	16.7	2.06
105	R32	B31t	220	0	69.1	1.7	17.9	16.4	33.1	13.7	17.2	14.7	1.96
106	R32	2B32	354	0	76.7	2.1	24.1	20.4	30.1	8.5	14.8	14.5	1.82
107	R32	3Cox	360+	0	88.0	7.9	42.8	17.7	19.6	4.2	8.0	7.6	--

Supplementary Table 2. Physical properties--Continued

No.	Sample	Horizon	Basal depth (cm)	>2-mm	Percentage of <2-mm fraction							Bulk density (g/cm ³)	
					Total sand	vco sand	co sand	m sand	fi+vfi sand	Silt	<2- μ clay		<1- μ clay
Riverbank Formation, lower member, 330 Ka													
108	R30	Ap	65	0	75.0	2.0	21.4	18.7	32.9	19.0	8.0	6.6	1.71
109	R30	B10	78	0	66.7	1.4	19.9	16.0	29.4	14.2	19.1	17.0	1.97
110	R30	B21t	127	0	63.5	1.4	17.7	15.2	29.2	11.1	25.4	24.6	1.95
111	R30	2B22t	179	0	69.8	5.7	29.8	15.2	19.1	5.0	25.2	25.1	1.93
112	R30	3B3t	197	0	78.2	5.9	37.6	18.5	16.2	3.3	18.5	18.4	1.85
113	R30	3C10x	220	0	77.5	4.6	34.1	19.9	18.9	2.5	20.0	18.8	--
Turlock Lake Formation, 600 Ka													
114	T2	A	31	0	67.9	4.1	21.4	13.4	25.9	26.6	5.5	2.4	--
115	T2	B21	173	0	44.1	2.8	15.3	8.7	16.1	18.2	37.7	35.0	--
116	T2	2B22	386	0	70.6	4.0	14.1	6.7	42.1	17.0	12.4	11.1	1.90
117	T2	3C	417	0	89.3	20.2	42.3	10.5	14.2	4.5	6.2	5.6	--
118	T6	A11	20	0	85.6	19.1	31.7	17.5	17.3	10.1	4.3	3.4	--
119	T6	A12	40	0	83.3	15.2	29.2	18.1	20.8	11.5	5.3	4.3	--
120	T6	2B21t	90	0	83.3	29.6	37.6	10.9	5.2	7.4	9.3	7.2	--
121	T6	2B22t	190	0	68.1	19.8	33.1	8.8	6.4	4.8	27.1	27.1	--
122	T6	3B+C	370	0	79.9	12.3	43.6	16.0	8.0	7.9	12.2	2.2	--
123	T11	Allp	5	0	79.1	6.6	26.4	18.6	27.5	14.1	5.4	3.5	1.49
124	T11	2A12p	11	0	74.4	10.2	25.0	14.5	24.7	16.4	7.1	4.4	1.85
125	T11	2A+B	20	0	63.1	8.0	19.7	13.2	22.2	15.1	20.9	17.3	1.91
126	T11	2B1t	33	0	58.0	6.9	19.1	11.3	20.7	12.0	28.9	24.5	1.88
127	T11	2B2t	80	0	64.3	7.4	21.8	13.8	21.3	8.6	26.0	23.8	1.95
128	T11	3B31t	191	0	76.0	13.2	22.3	17.8	22.7	3.0	20.0	18.3	1.81
129	T11	4B32t	256	0	79.2	5.6	19.1	24.8	29.7	2.5	18.3	18.0	1.81
130	T11	5B+C	292	0	84.5	10.5	38.9	19.7	15.4	1.0	13.9	12.6	1.76
131	T11	5C10x	375	0	84.2	9.2	33.6	21.9	19.5	0.8	14.2	13.5	--
132	T11	6C20x	375+	0	86.4	15.7	41.7	18.3	10.7	1.7	11.8	11.2	--
China Hat gravel member of Laguna Formation, 3,000 Ka													
133	CH1	A1	12	20	37.7	9.8	7.4	3.3	17.4	46.0	16.5	13.6	1.64
134	CH1	2AB	53	20	34.1	5.2	6.3	3.5	19.1	43.3	22.7	19.0	1.60
135	CH1	2B21t	88	30	24.9	4.5	3.5	2.0	14.5	31.8	43.3	39.7	1.49
136	CH1	2B22t	140	20	24.9	4.5	3.5	2.0	14.5	20.4	55.8	52.8	1.65
137	CH1	2B31	234	--	30.7	9.2	6.0	3.2	14.8	26.4	42.9	36.7	1.84
138	CH1	2B32	310	--	24.2	6.0	4.3	2.6	11.6	20.6	55.2	49.7	1.92
139	CH1	3B33	350	--	41.0	12.6	15.4	3.0	7.6	18.4	40.6	34.3	1.54
140	CH2	A1	8	20	48.9	6.2	8.1	4.3	30.3	38.8	12.5	8.6	1.68
141	CH2	A3	30	10	40.3	5.6	6.6	3.8	24.3	35.6	24.0	20.0	--
142	CH2	2A+B	50	10	35.6	3.1	6.0	3.7	22.8	33.7	30.7	26.7	1.67
143	CH2	2B21t	110	30	25.6	3.4	4.2	2.4	15.7	21.5	52.9	49.8	1.66
144	CH2	2B22	170	20	34.2	6.2	8.7	3.9	15.3	18.6	46.9	43.3	1.74
145	CH2	2B23	200	10	37.8	5.9	10.2	4.6	17.0	23.0	39.2	35.1	1.82
146	CH2	3B24	290	20	29.3	6.5	10.3	3.0	9.4	24.8	45.9	40.9	1.75
147	CH2	3B3	350	30	30.9	7.0	10.2	3.8	9.8	24.3	44.8	40.0	--
148	CH3	A1	9	20	44.0	6.2	7.8	5.1	24.8	41.7	14.3	10.4	1.53
149	CH3	A3	35	10	41.9	4.5	7.5	5.1	24.9	38.0	20.0	15.7	1.67
150	CH3	A+B	68	10	39.1	3.5	7.5	4.8	23.3	35.6	25.2	20.1	1.72
151	CH3	B2t	105	50	26.4	3.0	4.5	3.1	15.8	26.2	47.5	43.0	1.67
152	CH3	B22t	153	40	21.4	2.8	4.6	3.0	10.9	16.1	62.6	60.2	1.73
153	CH3	2B23	173	20	30.3	1.9	5.0	10.0	13.2	12.0	57.7	54.7	1.84
154	CH3	3B24	260	10	47.5	10.5	15.6	6.1	15.2	29.0	23.5	20.5	1.81
155	CH3	4B31	340	30	60.8	5.9	18.0	16.8	20.2	10.1	29.1	24.6	1.75
156	CH3	5B32	750+	30	29.9	7.2	9.2	3.7	9.8	30.5	39.6	32.5	1.82
157	CH4	2B31	750	--	50.5	8.0	25.4	5.6	11.6	23.0	26.5	21.3	1.71
158	CH4	4C10x	1000	--	63.1	2.9	25.0	17.3	17.9	18.0	18.9	14.8	1.61

Supplementary Table 3, Part 1. Extractive chemical analyses

[CEC, cation-exchange capacity; m, with magnetic minerals; w, without magnetic minerals. Analysts: A. L. Walker, U.S. Geological Survey, and A.J. Busacca, Peter Janitsky, and R. Meixner, University of California, Davis]

No.	Sample	Horizon	Basal depth (cm)	Percentage of <2-mm		mg/100 g soil					CEC	pH 1:1H ₂ O	pH 1:1KCl	pH Saturated
				Total N	Organic C	Exchange Na	Exchange K	Exchange Ca	Exchange Mg	Exchange N				
Modern River Alluvium														
1	MRA1	--	--	--	--	--	--	--	--	--	--	--	--	--
2	MRA2	--	--	--	--	--	--	--	--	--	--	--	--	--
3	MRA3	--	--	--	--	--	--	--	--	--	--	--	--	--
4	MRA4	--	--	--	--	--	--	--	--	--	--	--	--	--
Post-Modesto Deposits, .2 Ka														
5	PM15	A1	4	0.0371	0.54	0.39	0.23	3.84	2.93	1.29	4.83	5.84	5.25	--
6	PM15	2C1ox	19	0.0428	0.44	0.41	0.14	4.04	3.23	1.69	6.66	5.69	4.68	--
7	PM15	3C2ox	42	0.0255	0.14	0.41	0.09	3.13	1.92	1.33	3.25	5.56	4.37	--
8	PM15	4C3ox	47	0.0226	0.20	0.42	0.11	4.54	2.63	1.08	5.99	5.55	4.75	--
9	PM15	5C4ox	51	0.0097	0.08	0.39	0.05	2.83	1.82	0.64	1.66	5.72	5.01	--
10	PM15	6C5ox	51+	0.0205	0.14	0.41	0.07	4.34	3.03	1.04	4.91	5.82	5.03	--
11	PM19	A11	7	0.2790	3.81	--	--	--	--	4.99	--	5.56	5.12	--
12	PM19	2A12	12	0.1443	1.62	--	--	--	--	2.57	--	6.25	5.85	--
13	PM19	3C1ox	23	0.0983	1.10	--	--	--	--	1.85	--	6.32	5.87	--
14	PM19	4C2ox	43	0.0635	0.60	--	--	--	--	1.53	--	6.91	6.30	--
15	PM19	5C3ox	49	0.0185	0.52	--	--	--	--	0.72	--	6.79	6.33	--
16	PM19	6C4n	55	0.0322	0.31	--	--	--	--	1.33	--	6.98	6.36	--
17	PM19	7C5n	66	0.0121	0.08	--	--	--	--	0.64	--	6.54	6.22	--
18	PM19	8C6n	80+	--	--	--	--	--	--	1.41	--	--	--	--
Post-Modesto Deposits, 3 Ka														
19	PM8	A1	32	0.199	2.26	0.18	1.76	15.30	2.53	4.66	22.73	6.33	5.72	--
20	PM8	2C1	55	0.049	0.66	0.13	0.17	11.01	2.52	1.25	13.82	7.20	6.36	--
21	PM8	3C2	66	0.038	0.41	0.22	0.22	5.25	3.13	0.76	7.08	7.33	7.13	--
22	PM8	4C3	76+	0.018	0.13	0.04	0.15	3.84	1.61	0.84	3.66	7.48	6.72	--
23	PM13	A11	5	0.2609	3.26	--	--	--	--	4.10	--	6.30	5.89	--
24	PM13	A12	35	0.0877	0.99	--	--	--	--	1.04	--	7.71	6.93	--
25	PM13	2C1ox	86	0.0278	0.32	--	--	--	--	0.84	--	7.85	6.67	--
26	PM13	3C2ox	112	0.0187	0.30	--	--	--	--	1.45	--	7.35	5.90	--
27	PM13	4C3ox	136	--	--	--	--	--	--	--	--	--	--	--
28	PM13	5C4ox	200	--	--	--	--	--	--	--	--	--	--	--
29	PM13	6C5n	720	--	--	--	--	--	--	--	--	--	--	--
30	PM14	A11	3	0.2429	2.91	--	--	--	--	2.65	--	6.42	5.99	--
31	PM14	2A12	33	0.0942	1.21	--	--	--	--	0.32	--	7.83	7.12	--
32	PM14	3C1ox	99	0.0301	1.00	--	--	--	--	0.48	--	7.83	6.62	--
33	PM14	4C2ox	130	0.0153	0.30	--	--	--	--	1.21	--	6.88	5.42	--
34	PM14	5C3ox	175	0.0242	0.25	--	--	--	--	1.45	--	6.54	5.11	--
35	PM14	6C4ox	200	0.0146	0.11	--	--	--	--	1.13	--	6.66	5.32	--
36	PM14	7C5n	239+	0.0077	0.04	--	--	--	--	0.24	--	6.92	5.52	--
37	PM16	A	2	0.2215	2.64	0.49	0.88	8.79	2.94	2.29	12.57	6.50	6.00	--
38	PM16	C1ox	25	0.0670	0.58	0.53	0.63	6.26	3.13	1.53	9.07	6.48	5.68	--
39	PM16	2C2ox	35	0.0404	0.48	0.53	0.14	7.58	3.03	0.96	9.41	6.86	6.33	--
40	PM16	3C3ox	65	0.0273	0.34	0.53	0.14	6.46	3.12	0.48	7.57	7.29	6.70	--
41	PM16	4C4ox	90	0.0124	0.12	0.49	0.07	4.14	2.83	0.32	3.50	7.29	6.89	--
42	PM16	5C5ox	116	0.0169	0.16	0.23	0.07	6.06	5.56	1.45	5.83	7.22	6.95	--
43	PM16	5C6n	236	--	--	0.79	0.07	6.87	6.26	0.64	8.91	7.42	--	--
44	PM17	A	6	0.2098	2.14	--	--	--	--	2.05	--	6.61	6.25	--
45	PM17	2C2ox	45	0.0594	0.62	--	--	--	--	1.04	--	6.99	6.32	--
46	PM17	2C2ox	63	0.0378	0.44	--	--	--	--	0.36	--	7.18	6.65	--
47	PM17	2C3ox	74	0.0439	0.50	--	--	--	--	0.36	--	8.03	7.42	--
48	PM17	3C4n	120+	0.0175	0.18	--	--	--	--	0.16	--	7.83	7.36	--
49	PM18	A	6	0.3966	3.69	--	--	--	--	2.21	--	7.26	6.92	--
50	PM18	2C1ox	65	0.0358	0.37	--	--	--	--	1.29	--	5.69	5.54	--
51	PM18	2C2ox	115	0.0245	0.25	--	--	--	--	1.57	--	5.75	4.64	--
52	PM18	3C3ox	164	0.0260	0.10	--	--	--	--	1.04	--	5.98	4.77	--
53	PM18	4C4ox	175+	0.0145	0.12	--	--	--	--	0.84	--	6.18	5.10	--

Supplementary Table 3, Part 1. Extractive chemical analyses--Continued

No.	Sample	Horizon	Basal depth (cm)	Percentage of <2-mm		mg/100 g soil					CEC	pH 1:1H ₂ O	pH 1:1KCl	pH Saturated
				Total N	Organic C	Exchange Na	Exchange K	Exchange Ca	Exchange Mg	Exchange N				
Modesto Formation, upper member, 10 Ka														
54	M31	A11	20	0.101	1.23	0.32	1.83	11.82	1.81	1.37	15.23	7.62	6.83	--
55	M31	A12	63	0.041	0.45	7.42	1.13	5.45	1.32	0.04	9.32	9.64	7.88	--
56	M31	AC	150	0.022	0.21	8.38	0.97	2.42	0.51	0.00	6.83	10.00	8.78	--
57	M31	2C1	200	0.018	0.13	8.68	0.22	1.62	0.80	0.68	7.24	10.01	8.36	--
58	M31	3C2	254	0.011	0.06	2.99	0.10	1.92	1.11	0.80	3.58	9.64	7.45	--
59	M46	A11p	5	0.1881	2.24	0.53	0.76	7.37	2.22	2.01	10.57	6.29	5.87	--
60	M46	A12p	14	0.0959	1.00	0.44	0.53	5.86	1.31	1.37	8.74	6.76	6.06	--
61	M46	2A13p	32	0.0544	0.52	0.25	0.48	4.65	1.11	1.00	6.65	6.80	6.23	--
62	M46	3AC	66	0.0331	0.26	0.26	0.54	4.95	1.41	0.92	7.33	7.01	6.23	--
63	M46	4Cox	250	0.0206	0.11	0.26	0.28	6.16	1.52	0.76	8.41	7.04	5.80	--
Modesto Formation, lower member, 40 Ka														
64	M12	A11	15	--	--	--	--	--	--	--	--	--	--	--
65	M12	A12	81	0.025	0.23	0.13	0.24	3.43	0.11	1.42	2.91	6.45	5.59	--
66	M12	2B21t	102	0.019	0.16	0.28	0.13	3.74	1.21	2.11	4.33	6.87	5.48	--
67	M12	3B22t	170	0.020	0.10	0.19	0.10	6.67	2.12	2.35	7.99	6.67	5.32	--
68	M12	4B3	201	0.012	0.40	0.14	0.08	4.95	2.37	1.26	5.83	6.98	5.40	--
69	M12	5C1	231	0.006	0.40	0.65	0.06	3.74	1.21	1.22	3.91	7.34	5.22	--
70	M12	6C2	413+	--	0.02	--	--	--	--	--	--	--	--	--
Riverbank Formation, upper member, 130 Ka														
71	R9	A11p	30	0.044	0.36	0.13	0.22	2.73	0.40	2.73	3.83	5.83	4.87	--
72	R9	A12p	60	0.040	0.29	0.09	0.11	3.23	0.00	2.45	4.24	5.77	4.88	--
73	R9	B1	105	--	0.15	0.11	0.08	3.84	0.26	2.49	4.66	5.77	4.70	--
74	R9	2B21	180	--	0.08	0.04	0.09	4.44	1.82	4.66	6.83	6.13	4.56	--
75	R9	2B22	235	--	0.04	0.09	0.09	4.34	1.11	4.58	4.49	6.05	4.38	--
76	R9	3B3	350	--	0.03	0.13	0.10	5.35	1.72	2.10	7.08	6.15	4.44	--
77	R9	4C	400+	--	0.03	0.13	0.08	5.25	1.01	1.87	6.08	6.13	4.28	--
78	R33	A11	4	0.1261	1.53	--	--	--	--	1.85	--	6.26	5.69	--
79	R33	2A12	19	0.0492	0.47	--	--	--	--	1.33	--	6.11	5.54	--
80	R33	3A3	39	0.0248	0.16	--	--	--	--	1.29	--	5.56	5.11	--
81	R33	3B21t	62	0.0229	0.06	--	--	--	--	1.61	--	5.94	4.60	--
82	R33	3B22t	83	0.0240	0.06	--	--	--	--	1.61	--	6.21	4.86	--
83	R33	3B23t	122	--	--	--	--	--	--	2.81	--	--	--	--
84	R33	3B31	151	--	--	--	--	--	--	1.22	--	--	--	--
85	R33	3B32	210	--	--	--	--	--	--	1.10	--	--	--	--
86	R33	4B33	260	--	--	--	--	--	--	1.08	--	--	--	--
87	R33	5Cox	300+	--	--	--	--	--	--	0.64	--	--	--	--
Riverbank Formation, middle member, 250 Ka														
88	R2	Ap	25	--	--	--	--	--	--	--	--	--	--	--
89	R2	B21	81	--	--	--	--	--	--	--	--	--	--	--
90	R2	B22t	185	--	--	--	--	--	--	--	--	--	--	--
91	R2	B3	386	--	--	--	--	--	--	--	--	--	--	--
92	R2	C1	500	--	--	--	--	--	--	--	--	--	--	--
93	R2	C2n	500+	--	--	--	--	--	--	--	--	--	--	--
94	R10	A	46	0.023	0.16	0.13	0.22	3.53	0.01	1.74	3.00	6.20	5.12	--
95	R10	2B1	70	--	0.07	0.06	0.23	3.43	0.81	1.71	4.33	6.82	5.08	--
96	R10	2B21t	140	--	0.03	0.19	0.10	4.65	2.11	2.47	6.49	7.17	4.98	--
97	R10	2B22t	210	--	0.03	0.15	0.08	3.64	2.72	1.46	5.91	7.47	4.98	--
98	R10	3B3t	386	--	0.03	0.19	0.08	4.75	1.82	1.10	5.58	7.47	5.32	--
99	R10	3Cox	500	--	--	--	--	--	--	--	--	--	--	--
100	R32	A11	26	0.0351	0.31	0.17	0.32	3.54	0.50	1.29	4.83	6.41	5.57	--
101	R32	A12	50	0.0278	0.15	0.26	0.23	3.03	0.61	1.00	3.83	6.28	5.41	--
102	R32	A3	70	0.0195	0.10	0.25	0.22	3.23	0.71	1.13	3.91	6.26	4.99	--
103	R32	B21t	105	0.0200	0.08	0.22	0.24	3.33	1.32	1.53	4.74	6.18	4.77	--
104	R32	B22t	150	0.0180	0.04	0.25	0.23	4.54	1.01	1.93	6.08	6.56	4.85	--
105	R32	B31t	220	--	--	0.25	0.20	3.94	1.41	1.21	4.99	--	--	--
106	R32	2B32	354	--	--	0.31	0.22	4.34	1.52	0.48	5.49	--	--	--
107	R32	3Cox	360+	--	--	0.36	0.14	3.84	1.51	0.48	3.66	--	--	--
Riverbank Formation, lower member, 330 Ka														
108	R30	Ap	65	0.019	0.18	0.09	0.18	2.52	0.00	1.10	2.75	6.45	4.73	6.6
109	R30	B10	78	--	--	0.15	0.23	4.34	0.61	2.23	6.49	6.00	4.49	6.1
110	R30	B21t	127	--	--	0.19	0.18	4.95	1.92	2.47	8.24	5.75	4.21	5.8
111	R30	2B22t	179	--	--	0.63	0.26	8.69	2.72	2.63	12.90	5.90	4.11	6.0
112	R30	3B3t	197	--	--	0.28	0.14	9.90	2.93	1.58	12.90	6.45	4.62	6.8
113	R30	3C1ox	220	--	--	0.19	0.16	9.09	2.42	1.46	11.41	6.95	4.90	7.0

Supplementary Table 3, Part 1. Extractive chemical analyses—Continued

No.	Sample	Horizon	Basal depth (cm)	Percentage of <2-mm		mg/100 g soil					CEC	pH 1:1H ₂ O	pH 1:1KCl	pH Saturated
				Total N	Organic C	Exchange Na	Exchange K	Exchange Ca	Exchange Mg	Exchange N				
Turlock Lake Formation, 600 Ka														
114	T2	A	31	0.037	0.38	0.08	0.27	2.73	0.50	1.87	3.50	6.58	5.20	--
115	T2	B21	173	--	0.17	0.11	0.26	4.65	1.81	4.16	8.91	5.82	4.30	--
116	T2	B22	386	--	0.05	0.26	0.11	5.96	2.12	1.74	8.41	6.52	4.65	--
117	T2	3C	417	--	0.04	0.06	0.07	3.28	0.20	0.86	3.17	6.48	4.46	--
118	T6	A11	20	0.0364	--	0.27	0.28	3.33	0.00	--	3.08	6.50	--	--
119	T6	A12	40	0.0214	--	0.25	0.31	3.33	0.21	--	2.66	6.00	--	--
120	T6	2B21t	90	0.0091	--	0.29	0.42	8.69	1.71	--	8.99	7.00	--	--
121	T6	2B22t	190	--	--	0.26	0.35	8.08	1.62	--	10.41	6.20	--	--
122	T6	3B+C	370	--	--	0.36	0.17	5.05	1.41	--	7.41	6.60	--	--
123	T11	A11p	5	--	--	0.09	0.81	8.58	0.41	1.95	11.07	6.82	6.44	6.9
124	T11	2A12p	11	0.032	0.64	0.04	0.34	3.94	0.00	1.18	4.00	6.95	5.99	7.1
125	T11	2A+B	20	--	--	0.06	0.34	4.65	0.60	1.91	6.66	6.85	5.51	6.8
126	T11	2B1t	33	--	--	0.17	0.27	5.35	2.22	2.87	9.65	6.70	4.96	6.5
127	T11	2B2t	80	--	--	0.18	0.11	5.66	2.12	2.59	9.57	6.60	4.61	6.4
128	T11	831t	191	--	--	0.21	0.12	7.27	2.51	1.58	8.99	6.90	5.21	6.6
129	T11	4B32t	256	--	--	0.23	0.12	5.81	1.41	1.50	7.41	7.10	5.03	6.5
130	T11	5B+C	292	--	--	0.21	0.13	5.05	0.51	1.38	7.16	6.95	4.90	6.4
131	T11	5C1ox	375	--	--	0.19	0.14	5.35	1.21	1.26	6.91	7.00	4.88	6.5
132	T11	61C2ox	375+	--	--	0.19	0.19	5.86	1.31	1.22	6.91	7.15	4.96	6.5
China Hat gravel member of Laguna Formation, 3,000 Ka														
133	CH1	A1	12	0.053	0.34	0.11	0.26	1.92	0.60	4.80	6.58	4.84	3.66	--
134	CH1	2A8	53	0.046	0.28	0.11	0.27	2.52	0.36	5.16	7.08	4.93	3.56	--
135	CH1	2B21t	88	--	0.12	0.19	0.22	2.83	0.30	9.15	11.57	4.55	3.19	--
135	CH1	2B22t	140	--	0.26	0.15	0.06	4.44	0.21	8.98	12.15	4.40	3.05	--
137	CH1	2B31	234	--	0.21	0.24	0.05	5.65	0.71	6.81	11.90	4.00	2.84	--
138	CH1	2B32	310	--	0.22	0.39	0.10	6.56	2.73	7.66	15.73	3.96	2.77	--
139	CH1	31B33	350	--	0.21	0.37	0.09	5.85	2.94	6.61	15.32	4.06	2.94	--
140	CH2	A1	8	--	0.80	1.06	0.33	2.83	0.71	5.79	7.76	4.71	--	--
141	CH2	A3	30	--	0.29	1.50	0.32	1.62	0.45	7.52	7.82	4.55	--	--
142	CH2	2A+B	50	--	0.23	1.62	0.26	1.48	0.36	8.20	8.66	4.17	--	--
143	CH2	2B21t	110	--	0.12	1.42	0.24	2.91	0.71	11.26	11.87	4.36	--	--
144	CH2	2B22	170	--	0.08	1.34	0.20	4.12	1.41	11.78	12.32	4.20	--	--
145	CH2	2B23	200	--	0.06	0.83	0.10	5.02	2.08	11.42	14.23	4.12	--	--
146	CH2	3B24	290	--	0.05	0.98	0.17	7.60	3.10	12.63	16.76	4.14	--	--
147	CH2	311B3	350+	--	0.04	1.34	0.19	6.28	3.71	12.71	18.28	4.14	--	--
148	CH3	A1	9	--	2.01	0.88	0.50	10.21	1.13	4.83	11.19	5.84	--	--
149	CH3	A3	35	--	0.34	1.62	0.43	4.25	1.03	4.50	7.87	5.44	--	--
150	CH3	A+B	68	--	0.26	0.67	0.40	3.19	0.81	5.71	8.04	5.01	--	--
151	CH3	B2t	105	--	0.11	0.70	0.31	4.28	0.96	9.49	11.25	4.62	--	--
152	CH3	B22t	153	--	0.11	1.52	0.27	5.38	1.32	10.06	12.15	4.48	--	--
153	CH3	2B23	173	--	0.09	1.24	0.24	6.11	2.45	10.86	14.74	4.06	--	--
154	CH3	311B24	260	--	0.03	1.06	0.17	6.87	3.64	11.02	15.30	4.33	--	--
155	CH3	4VB31	340	--	0.03	0.88	0.15	6.07	3.74	11.26	15.86	4.20	--	--
156	CH3	5B32	750+	--	0.03	1.26	0.24	6.92	4.81	12.63	21.09	4.10	--	--
157	CH4	2B31	750	--	0.02	1.16	0.18	2.96	3.25	6.52	10.57	3.92	--	--
158	CH4	4C1ox	1000	--	0.02	1.68	0.31	3.78	4.60	3.38	10.29	4.41	--	--

Supplementary Table 3, Part 2. Extractive chemical analyses

[CEC, cation-exchange capacity; m, with magnetic minerals; w, without magnetic minerals. Analysts: A. L. Walker, U.S. Geological Survey, and A. J. Busacca, Peter Janitsky, and R. Meixner, University of California, Davis]

No.	Sample	Horizon	Basal depth (cm)	percentage of <2-mm					Fe _o	Al _o
				Fe _d (m)	Fe _d (w)	Al _d (w)	mags			
Modern River Alluvium										
1	MRA1	--	--	--	--	--	--	--	--	
2	MRA2	--	--	--	--	--	--	--	--	
3	MRA3	--	--	--	--	--	--	--	--	
4	MRA4	--	--	--	--	--	--	--	--	
Post-Modesto Deposits, .2 Ka										
5	PM15	A1	4	1.18	0.52	0.05	0.72	0.22	0.04	
6	PM15	2C1ox	19	0.65	0.59	0.06	0.99	0.22	0.04	
7	PM15	3C2ox	42	0.98	0.53	0.03	0.58	0.19	0.04	
8	PM15	4C3ox	47	1.19	0.71	0.08	0.34	0.24	0.04	
9	PM15	5C4ox	51	1.09	0.41	0.05	1.03	0.13	0.03	
10	PM15	6C5ox	51+	0.68	0.65	0.05	0.39	0.20	0.03	
11	PM19	A11	7	1.15	0.70	0.08	0.21	0.23	0.05	
12	PM19	2A12	12	0.81	0.76	0.08	0.43	0.24	0.05	
13	PM19	3C1ox	23	1.25	0.73	0.06	0.23	0.24	0.05	
14	PM19	4C2ox	43	1.10	1.07	0.11	0.25	0.34	0.07	
15	PM19	5C3ox	49	0.95	0.67	0.07	0.27	0.22	0.04	
16	PM19	6C4n	55	1.22	0.82	0.09	0.07	0.25	0.06	
17	PM19	7C5n	66	1.20	1.22	0.12	0.19	0.42	0.09	
18	PM19	8C6n	80+	--	0.56	0.06	--	0.18	0.04	
Post-Modesto Deposits, 3 Ka										
19	PM8	A1	32	1.13	--	--	--	--	--	
20	PM8	2C1	55	0.97	--	--	--	--	--	
21	PM8	3C2	66	0.68	--	--	--	--	--	
22	PM8	4C3	76+	0.53	--	--	--	--	--	
23	PM13	A11	5	1.14	1.09	0.12	0.09	0.25	0.06	
24	PM13	A12	35	1.18	1.03	0.11	0.03	0.26	0.06	
25	PM13	2C1ox	86	0.99	0.78	0.07	0.16	0.28	0.05	
26	PM13	3C2ox	112	0.83	0.83	0.05	0.07	0.31	0.05	
27	PM13	4C3ox	136	--	--	--	--	--	--	
28	PM13	5C4ox	200	--	--	--	--	--	--	
29	PM13	6C5n	720	--	--	--	--	--	--	
30	PM14	A11	3	--	0.94	0.11	0.02	0.31	0.06	
31	PM14	2A12	33	0.93	1.12	0.12	0.05	0.32	0.08	
32	PM14	3C1ox	99	0.71	0.78	0.08	0.24	0.28	0.05	
33	PM14	4C2ox	130	0.96	0.79	0.07	0.13	0.29	0.04	
34	PM14	5C3ox	175	1.03	0.87	0.09	0.03	0.36	0.05	
35	PM14	6C4ox	200	0.56	0.60	0.06	0.15	0.24	0.04	
36	PM14	7C5n	239+	0.08	0.26	0.05	0.20	0.09	0.03	
37	PM16	A	2	1.15	0.76	0.07	0.19	0.18	0.04	
38	PM16	C1ox	25	1.30	0.85	0.07	0.18	0.23	0.05	
39	PM16	2C2ox	35	1.37	0.84	0.09	0.18	0.24	0.05	
40	PM16	3C3ox	65	1.19	0.73	0.05	0.27	0.19	0.04	
41	PM16	4C4ox	90	0.99	0.56	0.04	0.40	0.15	0.04	
42	PM16	5C5ox	116	1.06	0.73	0.07	0.37	0.19	0.04	
43	PM16	5C6n	236	1.00	0.86	0.08	--	0.20	0.05	
44	PM17	A	6	0.80	0.70	0.06	0.34	0.18	0.04	
45	PM17	2C2ox	45	1.20	0.80	0.07	0.27	0.20	0.04	
46	PM17	2C2ox	63	1.47	0.88	0.08	0.18	0.22	0.05	
47	PM17	2C3ox	74	1.47	0.94	0.08	0.16	0.23	0.04	
48	PM17	3C4n	120+	1.31	0.66	0.08	0.49	0.19	0.05	
49	PM18	A	6	0.91	0.79	0.09	0.31	0.26	0.06	
50	PM18	2C1ox	65	0.97	0.85	0.09	0.37	0.16	0.06	
51	PM18	2C2ox	115	1.33	0.78	0.09	0.21	0.16	0.05	
52	PM18	3C3ox	164	1.06	0.68	0.08	0.28	0.14	0.05	
53	PM18	4C4ox	175+	0.73	0.65	0.08	0.32	0.13	0.04	
Modesto Formation, upper member, 10 Ka										
54	M31	A11	20	0.92	0.96	0.10	--	0.27	0.07	
55	M31	A12	63	0.81	0.87	0.09	--	0.20	0.07	
56	M31	AC	150	0.76	0.81	0.08	--	0.20	0.07	
57	M31	2C1	200	0.78	0.82	0.10	--	0.18	0.07	
58	M31	3C2	254	0.46	0.56	0.07	--	0.15	0.04	
59	M46	A11p	5	0.78	0.44	0.06	0.46	0.10	0.03	
60	M46	A12p	14	0.53	0.51	0.06	0.74	0.12	0.03	
61	M46	2A13p	32	0.96	0.54	0.06	0.52	0.10	0.03	
62	M46	3AC	66	0.67	0.60	0.07	0.69	0.11	0.03	
63	M46	4Cox	250	0.70	0.60	0.07	0.60	0.07	0.04	

Supplementary Table 3, Part 2. Extractive chemical analyses--Continued

No.	Sample	Horizon	Basal depth (cm)	percentage of <2-mm					
				Fe _d (m)	Fe _d (w)	Al _d (w)	mags	Fe _o	Al _o
Modesto Formation, lower member, 40 Ka									
64	M12	A11	15	--	--	--	--	--	--
65	M12	A12	81	0.34	0.27	0.03	--	0.06	0.04
66	M12	2821t	102	0.44	0.34	0.05	--	0.06	0.04
67	M12	3822t	170	0.49	0.45	0.06	--	0.06	0.06
68	M12	483	201	0.40	0.33	0.08	--	0.03	0.05
69	M12	5C1	231	0.42	--	--	--	--	--
70	M12	6C2	413+	--	0.24	0.05	3.77	0.03	0.04
Riverbank Formation, upper member, 130 Ka									
71	R9	A11p	30	0.48	0.40	0.05	--	0.13	0.04
72	R9	A12p	60	0.50	0.38	0.06	--	0.09	0.04
73	R9	B1	105	0.59	0.49	0.08	--	0.10	0.04
74	R9	2821	180	0.70	0.57	0.09	--	0.09	0.07
75	R9	2822	235	0.46	0.36	0.06	--	0.03	0.04
76	R9	383	350	0.48	0.45	0.08	--	0.03	0.05
77	R9	4C	400+	0.42	0.34	0.06	--	0.05	0.05
78	R33	A11	4	0.46	0.37	0.05	0.92	0.06	0.04
79	R33	2A12	19	1.07	0.40	0.05	0.04	0.07	0.04
80	R33	3A3	39	0.87	0.49	0.05	0.47	0.09	0.04
81	R33	3821t	62	1.32	0.62	0.08	0.10	0.12	0.06
82	R33	3822t	83	1.38	0.71	0.10	0.14	0.13	0.06
83	R33	3823t	122	--	0.65	0.09	--	0.10	0.06
84	R33	3831	151	1.19	0.47	0.08	0.22	0.07	0.05
85	R33	3832	210	1.05	0.50	0.06	0.21	0.05	0.04
86	R33	4833	260	1.29	0.57	0.08	--	0.05	0.07
87	R33	5Cox	300+	--	0.31	0.06	--	0.04	0.05
Riverbank Formation, middle member, 250 Ka									
88	R2	Ap	25	--	--	--	--	--	--
89	R2	B21	81	--	--	--	--	--	--
90	R2	B22t	185	--	--	--	--	--	--
91	R2	B3	386	--	--	--	--	--	--
92	R2	C1	500	--	--	--	--	--	--
93	R2	C2n	500+	--	--	--	--	--	--
94	R10	A	46	0.45	0.33	0.06	--	0.06	0.04
95	R10	281	70	0.56	0.42	0.06	--	0.07	0.05
96	R10	2821t	140	0.60	0.51	0.08	--	0.04	0.03
97	R10	2822t	210	0.57	0.43	0.08	--	0.04	0.04
98	R10	383t	386	0.50	0.37	0.06	--	0.03	0.04
99	R10	3Cox	500	--	--	--	--	--	--
100	R32	A11	26	0.52	0.38	0.05	1.49	0.07	0.03
101	R32	A12	50	0.97	0.45	0.06	0.10	0.06	0.03
102	R32	A3	70	1.07	0.46	0.06	0.21	0.07	0.04
103	R32	B21t	105	1.20	0.54	0.09	0.31	0.09	0.05
104	R32	B22t	150	0.70	0.60	0.09	1.36	0.09	0.05
105	R32	B31t	220	1.22	0.57	0.09	0.19	0.09	0.05
106	R32	2832	354	1.25	0.40	0.07	0.39	0.05	0.05
107	R32	3Cox	360+	--	0.40	0.07	--	0.07	0.05
Riverbank Formation, upper member, 330 Ka									
108	R30	Ap	65	0.60	0.37	0.06	--	0.12	0.03
109	R30	B10	78	0.84	0.59	0.09	--	0.06	0.06
110	R30	B21t	127	0.82	0.68	0.09	--	0.07	0.06
111	R30	2822t	179	0.75	0.58	0.10	--	0.05	0.06
112	R30	383t	197	0.70	0.53	0.09	--	0.04	0.07
113	R30	3C1ox	220	0.64	0.51	0.08	--	0.05	0.06
Turlock Lake Formation, 600 Ka									
114	T2	A	31	1.03	0.74	0.05	--	0.04	0.04
115	T2	B21	173	2.19	1.70	0.13	--	0.11	0.09
116	T2	2822	386	1.11	1.04	0.07	--	0.03	0.04
117	T2	3C	417	0.62	0.44	0.05	--	0.02	0.04
118	T6	A11	20	0.39	0.26	0.02	--	0.04	0.03
119	T6	A12	40	--	0.28	0.04	--	0.04	0.03
120	T6	2821t	90	0.49	0.48	0.08	--	0.04	0.06
121	T6	2822t	190	--	0.64	0.10	--	0.05	0.06
122	T6	38+C	370	0.23	0.36	0.07	--	0.03	0.05
123	T11	A11p	5	0.42	0.30	0.04	--	0.04	0.03
124	T11	2A12p	11	0.64	0.46	0.02	--	0.03	0.03
125	T11	2A+B	20	1.08	0.82	0.07	--	0.04	0.06
126	T11	2B1t	33	1.06	0.98	0.08	--	0.07	0.08
127	T11	282t	80	0.90	0.74	0.08	--	0.04	0.06
128	T11	3831t	191	0.82	0.43	0.08	--	0.03	0.06
129	T11	4832t	256	0.85	0.55	0.08	--	0.03	0.06
130	T11	58+C	292	0.53	0.42	0.08	--	0.03	0.06
131	T11	5C1ox	375	0.53	0.37	0.08	--	0.05	0.05
132	T11	61C2ox	375+	0.58	0.40	0.07	--	0.03	0.05

Supplementary Table 3, Part 2. Extractive chemical analyses--Continued

No.	Sample	Horizon	Basal depth (cm)	percentage of <2-mm					
				Fe _d (m)	Fe _d (w)	Al _d (w)	mags	Fe _o	Al _o
China Hat gravel member of Laguna Formation, 3,000 Ka									
133	CH1	A1	12	1.41	1.42	0.13	--	0.10	0.05
134	CH1	2A8	53	1.63	1.66	0.14	--	0.10	0.06
135	CH1	2B21t	88	2.41	2.43	0.21	--	0.16	0.11
135	CH1	2B22t	140	3.31	3.33	0.22	--	0.13	0.08
137	CH1	2B31	234	3.31	3.35	0.13	--	0.06	0.06
138	CH1	2B32	310	2.06	2.27	0.13	--	0.03	0.06
139	CH1	31B33	350	2.61	2.35	0.14	--	0.06	0.06
140	CH2	A1	8	--	--	--	--	--	--
141	CH2	A3	30	--	--	--	--	--	--
142	CH2	2A+8	50	--	--	--	--	--	--
143	CH2	2B21t	110	--	--	--	--	--	--
144	CH2	2B22	170	--	--	--	--	--	--
145	CH2	2B23	200	--	--	--	--	--	--
146	CH2	3B24	290	--	--	--	--	--	--
147	CH2	311B3	350+	--	--	--	--	--	--
148	CH3	A1	9	--	--	--	--	--	--
149	CH3	A3	35	--	--	--	--	--	--
150	CH3	A+8	68	--	--	--	--	--	--
151	CH3	B2t	105	--	--	--	--	--	--
152	CH3	B22t	153	--	--	--	--	--	--
153	CH3	2B23	173	--	--	--	--	--	--
154	CH3	311B24	260	--	--	--	--	--	--
155	CH3	4VB31	340	--	--	--	--	--	--
156	CH3	5B32	750+	--	--	--	--	--	--
157	CH4	2B31	750	--	--	--	--	--	--
158	CH4	4C1ox	1000	--	--	--	--	--	--

Supplementary Table 4, Part 1. Mineralogy

[Percentages of very fine sand are based on approximately 200 grain counts per slide of each heavy (sp gr. greater than 3.08) and medium (sp gr. 2.50-3.09) mineral isolate. Etching scales, which range from 0 to 5, express average degree of etching of all grains observed in grain counts (after Gillam and others, 1977). Analyst, J.W. Harden]

No.	Soil age (Ka)	Profile	Horizon	Percentages of very fine sand for selected heavy-mineral groups							Etching scales for selected heavy-mineral groups in the very fine sand fraction						
				Horn-blende	Ortho-pyroxene	Clino-pyroxene	Zircon	Epidote sphene	Apatite	Opaque minerals	Unknown	Horn-blende	Ortho-pyroxene	Clino-pyroxene	Zircon	Epidote	Sphene
1	.2	PM15	A1	3.05	0.05	0.05	0.29	5.78	2.20	2.97	9.89	2.2	3.0	3.0	1.3	2.5	--
2	.2	PM15	11C1ox	6.26	0.76	1.22	0.92	5.01	0.65	4.54	13.35	2.1	2.0	3.9	1.0	2.9	--
3	.2	PM15	11C5ox	3.63	0.36	0.70	0.18	8.79	0.24	2.52	6.65	2.9	4.0	3.5	1.7	3.0	2.1
4	3	PM17	A	3.81	0.21	0.31	0.18	5.25	0.23	2.42	1.76	2.6	3.6	2.5	1.6	2.8	2.0
5	3	PM17	11C2ox	4.91	0.35	0.72	0.42	4.12	0.20	1.71	2.06	2.5	2.9	2.8	1.0	2.5	2.3
6	3	PM17	11C4n	5.41	0.86	1.85	0.30	8.98	0.05	2.11	5.14	1.8	--	3.0	--	2.5	--
7	10	M31	A12	5.26	0.02	0.15	0.07	9.77	0.0	1.35	6.90	1.9	3.0	3.1	1.6	3.1	2.4
8	10	M31	11C2	5.68	0.33	0.70	0.16	5.06	0.34	1.58	2.80	3.0	3.3	2.7	1.6	3.4	3.7
9	10	M46	A12	3.82	0.001	0.30	0.22	2.13	0.18	2.16	2.53	2.3	--	2.6	1.4	2.6	1.8
10	10	M46	AC	4.14	0.18	0.20	0.11	1.35	0.47	2.75	1.80	2.4	3.2	3.3	1.2	2.9	2.3
11	10	M46	11Cdx	5.06	0.17	0.46	0.18	1.67	0.10	2.19	1.63	2.1	2.8	2.8	1.2	2.8	1.6
12	40	M12	VC1	4.62	0.08	0.05	0.15	1.2	0.04	1.76	1.94	3.3	--	3.0	2.0	3.1	3.1
13	130	R9	111B3	--	--	--	--	--	--	--	--	3.1	3.8	3.6	1.3	2.9	3.3
14	130	R9	11C	5.08	0.17	0.41	0.12	3.04	0.0	2.82	2.46	2.9	3.3	4.0	2.0	2.9	2.7
15	130	R33	11A12	3.26	0.06	0.34	0.06	1.54	0.09	2.30	1.56	2.7	3.0	3.0	1.6	3.0	2.6
16	130	R33	111B23t	2.44	0.11	0.11	0.20	1.49	0.0	1.38	0.34	3.0	3.6	3.3	1.3	3.0	2.5
17	130	R33	11Cox	6.00	0.19	0.04	0.15	1.03	0.16	7.85	1.64	3.4	3.0	--	1.8	3.2	2.8
18	250	R10	A	3.52	0.15	0.15	0.23	1.15	0.0	2.30	0.23	2.9	3.5	3.0	1.8	3.0	3.0
19	600	T11	11A12p	0.55	0.04	0.07	0.15	0.62	0.0	2.09	0.50	3.3	4.0	3.8	1.9	3.0	3.1
20	600	T11	11B2t	0.35	0.04	0.0	0.14	0.43	0.0	4.54	0.25	3.3	4.5	--	2.0	3.1	3.4
21	600	T11	11C1ox	--	--	--	--	--	--	--	--	3.7	4.5	--	--	3.6	3.3

Supplementary Table 4, Part 2. Mineralogy

[Analysts: A.J. Busacca, University of California, Davis, and A.L. Waller, U.S. Geological Survey]

No.	Sample	Horizon	Basal depth (cm)	Kaolinite	Chlorite	Chloritized Vermiculite	Vermiculite	Mica Vermiculite	Mica	Mica chloritized	Smectite	Quartz	Feldspar
Modern River Alluvium													
1	MRA1	--	--	--	--	--	--	--	--	--	--	--	--
2	MRA2	--	--	--	--	--	--	--	--	--	--	--	--
3	MRA3	--	--	--	--	--	--	--	--	--	--	--	--
4	MRA4	--	--	--	--	--	--	--	--	--	--	--	--
Post-Modesto Deposits, .2 Ka													
5	PM15	A1	4	--	--	--	--	--	--	--	--	--	--
6	PM15	2C1ox	19	--	--	--	--	--	--	--	--	--	--
7	PM15	3C2ox	42	--	--	--	--	--	--	--	--	--	--
8	PM15	4C3ox	47	--	--	--	--	--	--	--	--	--	--
9	PM15	5C4ox	51	--	--	--	--	--	--	--	--	--	--
10	PM15	6C5ox	51+	--	--	--	--	--	--	--	--	--	--
11	PM19	A11	7	--	--	--	--	--	--	--	--	--	--
12	PM19	2A12	12	--	--	--	--	--	--	--	--	--	--
13	PM19	3C1ox	23	--	--	--	--	--	--	--	--	--	--
14	PM19	4C2ox	43	--	--	--	--	--	--	--	--	--	--
15	PM19	5C3ox	49	--	--	--	--	--	--	--	--	--	--
16	PM19	6C4n	55	--	--	--	--	--	--	--	--	--	--
17	PM19	7C5n	66	--	--	--	--	--	--	--	--	--	--
18	PM19	8C6n	80+	--	--	--	--	--	--	--	--	--	--
Post-Modesto Deposits, 3 Ka													
19	PM8	A1	32	+++	+	+	++	--	+++	--	++	X	X
20	PM8	2C1	55	--	--	--	--	--	--	--	--	--	--
21	PM8	3C2	86	--	--	--	--	--	--	--	--	--	--
22	PM8	4C3	76+	++	--	--	++	--	+	--	--	X	XX
23	PM13	A11	5	--	--	--	--	--	--	--	--	--	--
24	PM13	A12	35	--	--	--	--	--	--	--	--	--	--
25	PM13	2C1ox	86	--	--	--	--	--	--	--	--	--	--
26	PM13	3C2ox	112	--	--	--	--	--	--	--	--	--	--
27	PM13	4C3ox	136	--	--	--	--	--	--	--	--	--	--
28	PM13	5C4ox	200	--	--	--	--	--	--	--	--	--	--
29	PM13	6C5n	720	--	--	--	--	--	--	--	--	--	--
30	PM14	A11	3	--	--	--	--	--	--	--	--	--	--
31	PM14	2A12	33	--	--	--	--	--	--	--	--	--	--
32	PM14	3C1ox	99	--	--	--	--	--	--	--	--	--	--
33	PM14	4C2ox	130	--	--	--	--	--	--	--	--	--	--
34	PM14	5C3ox	175	--	--	--	--	--	--	--	--	--	--
35	PM14	6C4ox	200	--	--	--	--	--	--	--	--	--	--
36	PM14	7C5n	230+	--	--	--	--	--	--	--	--	--	--
37	PM16	A	2	--	--	--	--	--	--	--	--	--	--
38	PM16	C1ox	25	--	--	--	--	--	--	--	--	--	--
39	PM16	2C2ox	35	--	--	--	--	--	--	--	--	--	--
40	PM16	3C3ox	65	--	--	--	--	--	--	--	--	--	--
41	PM16	4C4ox	90	--	--	--	--	--	--	--	--	--	--
42	PM16	5C5ox	116	--	--	--	--	--	--	--	--	--	--
43	PM16	5C6n	236	--	--	--	--	--	--	--	--	--	--
44	PM17	A	6	--	--	--	--	--	--	--	--	--	--
45	PM17	2C2ox	45	--	--	--	--	--	--	--	--	--	--
46	PM17	2C3ox	63	--	--	--	--	--	--	--	--	--	--
47	PM17	2C3ox	74	--	--	--	--	--	--	--	--	--	--
48	PM17	3C4n	120+	--	--	--	--	--	--	--	--	--	--
49	PM18	A	6	--	--	--	--	--	--	--	--	--	--
50	PM18	2C1ox	65	--	--	--	--	--	--	--	--	--	--
51	PM18	2C2ox	115	--	--	--	--	--	--	--	--	--	--
52	PM18	3C3ox	164	--	--	--	--	--	--	--	--	--	--
53	PM18	4C4ox	175+	--	--	--	--	--	--	--	--	--	--
Modesto Formation, upper member, 10 Ka													
54	M31	A11	20	+++	+	--	++	--	+++	--	+	X	X
55	M31	A12	63	--	--	--	--	--	--	--	--	--	--
56	M31	AC	150	+++	+	--	+	--	+++	--	++	X	X
57	M31	2C1	200	+++	+	--	++	--	+++	--	++	X	X
58	M31	3C2	254	--	--	--	--	--	--	--	--	--	--
59	M46	A11p	5	--	--	--	--	--	--	--	--	--	--
60	M46	A12p	14	--	--	--	--	--	--	--	--	--	--
61	M46	2A13p	32	--	--	--	--	--	--	--	--	--	--
62	M46	3AC	66	--	--	--	--	--	--	--	--	--	--
63	M46	4Cox	250	--	--	--	--	--	--	--	--	--	--

Supplementary Table 4, Part 2. Mineralogy--Continued

No.	Sample	Horizon	Basal depth (cm)	Kaolinite	Chlorite	Chloritized Vermiculite	Vermiculite	Mica Vermiculite	Mica	Mica chloritized	Smectite	Quartz	Feldspar
Modesto Formation, lower member, 40 Ka													
64	M12	A11	85	--	--	--	--	--	--	--	--	--	--
65	M12	A12	81	+++	--	--	--	--	++++	--	--	XX	X
66	M12	2B21t	102	--	--	--	--	--	--	--	--	--	--
67	M12	3B22t	170	+++	--	+	+++	+	++	--	--	X	X
68	M12	4B3	201	--	--	--	--	--	--	--	--	--	--
69	M12	5C1	231	++	--	--	+++	+	+	--	--	X	X
70	M12	6C2	413+	--	--	--	--	--	--	--	--	--	--
Riverbank Formation, upper member, 130 Ka													
71	R9	A11p	30	+++	--	--	--	--	++	--	--	XX	XX
72	R9	A12p	60	--	--	--	--	--	--	--	--	--	--
73	R9	B1	105	--	--	--	--	--	--	--	--	--	--
74	R9	2B21	180	--	--	--	--	--	--	--	--	--	--
75	R9	2B22	235	+++	--	--	++	--	+	+	--	X	X
76	R9	3B3	350	--	--	--	--	--	--	--	--	--	--
77	R9	4C	400+	+++	--	--	++	+	+	--	--	X	XX
78	R33	A11	4	--	--	--	--	--	--	--	--	--	--
79	R33	2A12	19	--	--	--	--	--	--	--	--	--	--
80	R33	3A3	39	--	--	--	--	--	--	--	--	--	--
81	R33	3B21t	62	--	--	--	--	--	--	--	--	--	--
82	R33	3B22t	83	--	--	--	--	--	--	--	--	--	--
83	R33	3B23t	122	--	--	--	--	--	--	--	--	--	--
84	R33	3B31	151	--	--	--	--	--	--	--	--	--	--
85	R33	3B32	210	--	--	--	--	--	--	--	--	--	--
86	R33	4B33	260	--	--	--	--	--	--	--	--	--	--
87	R33	5Cox	300+	--	--	--	--	--	--	--	--	--	--
Riverbank Formation, middle member, 250 Ka													
88	R2	Ap	25	--	--	--	--	--	--	--	--	--	--
89	R2	B21	81	--	--	--	--	--	--	--	--	--	--
90	R2	B22t	185	--	--	--	--	--	--	--	--	--	--
91	R2	B3	386	--	--	--	--	--	--	--	--	--	--
92	R2	C1	500	--	--	--	--	--	--	--	--	--	--
93	R2	C2n	500+	--	--	--	--	--	--	--	--	--	--
94	R10	A	46	+++	--	--	--	--	+++	+	--	X	X
95	R10	2B10	70	--	--	--	--	--	--	--	--	--	--
96	R10	2B21t	140	--	--	--	--	--	--	--	--	--	--
97	R10	2B22t	210	++++	--	--	++	--	+	--	--	X	X
98	R10	3B3t	386	--	--	--	--	--	--	--	--	--	--
99	R10	3Cox	500	--	--	--	--	--	--	--	--	--	--
100	R32	A11	26	--	--	--	--	--	--	--	--	--	--
101	R32	A12	50	--	--	--	--	--	--	--	--	--	--
102	R32	A3	70	--	--	--	--	--	--	--	--	--	--
103	R32	B21t	105	--	--	--	--	--	--	--	--	--	--
104	R32	B22t	150	--	--	--	--	--	--	--	--	--	--
105	R32	B31t	220	--	--	--	--	--	--	--	--	--	--
106	R32	2B32	354	--	--	--	--	--	--	--	--	--	--
107	R32	3Cox	360+	--	--	--	--	--	--	--	--	--	--
Riverbank Formation, lower member, 330 Ka													
108	R30	Ap	65	+	+++	--	--	--	--	++	--	--	XXX
109	R30	B10	78	--	--	--	--	--	--	--	--	--	--
110	R30	B21t	127	--	--	--	--	--	--	--	--	--	--
111	R30	2B22t	179	+++	--	--	++	--	+	--	--	X	X
112	R30	3B3t	197	--	--	--	--	--	--	--	--	--	--
113	R30	3C1ox	220	++	--	--	+	--	++	--	--	X	--
Turlock Lake Formation, 600 Ka													
114	T2	A	31	+++	--	--	--	--	++	--	--	XX	X
115	T2	B21	173	--	--	--	--	--	--	--	--	--	--
116	T2	2B22	386	++++	+	--	+	+	+	--	--	X	X
117	T2	3C	417	+++	+	--	++	--	+	+	--	X	X
118	T6	A11	20	--	--	--	--	--	--	--	--	--	--
119	T6	A12	40	--	--	--	--	--	--	--	--	--	--
120	T6	2B21t	90	--	--	--	--	--	--	--	--	--	--
121	T6	2B22t	190	--	--	--	--	--	--	--	--	--	--
122	T6	3B+C	370	--	--	--	--	--	--	--	--	--	--
123	T11	A11p	5	--	--	--	--	--	--	--	--	--	--
124	T11	2A12p	11	+++	+	--	++	--	++	+	+	X	X
125	T11	2A+B	20	--	--	--	--	--	--	--	--	--	--
126	T11	2B1t	33	--	--	--	--	--	--	--	--	--	--
127	T11	2B2t	80	++++	--	--	++	--	++	+	--	X	X
128	T11	3B31t	191	--	--	--	--	--	--	--	--	--	--
129	T11	4B32t	256	--	--	--	--	--	--	--	--	--	--
130	T11	5B+C	292	--	--	--	--	--	--	--	--	--	--
131	T11	5C1ox	375	--	--	--	--	--	--	--	--	--	--
132	T11	6C2ox	375+	++++	--	--	++	--	++	--	--	X	X

Supplementary Table 4, Part 2. Mineralogy--Continued

No.	Sample	Horizon	Basal depth (cm)	Kaolinite	Chlorite	Chloritized Vermiculite	Vermiculite	Mica Vermiculite	Mica	Mica chloritized	Smectite	Quartz	Feldspar
China Hat gravel member of Laguna Formation, 3,000 Ka													
133	CH1	A1	12	++++	--	--	+	--	+	--	+	XX	X
134	CH1	2AB	53	--	--	--	--	--	--	--	--	--	--
135	CH1	2B21t	88	--	--	--	--	--	--	--	--	--	--
136	CH1	2B22t	140	++++	--	--	+	--	+	--	++	X	X
137	CH1	2B31	234	--	--	--	--	--	--	--	--	--	--
138	CH1	2B32	310	++++	--	--	--	--	--	--	++++	X	X
139	CH1	3B33	350	--	--	--	--	--	--	--	--	--	--
140	CH2	A1	8	--	--	--	--	--	--	--	--	--	--
141	CH2	A3	30	--	--	--	--	--	--	--	--	--	--
142	CH2	2A+B	50	--	--	--	--	--	--	--	--	--	--
143	CH2	2B21t	110	--	--	--	--	--	--	--	--	--	--
144	CH2	2B22	170	--	--	--	--	--	--	--	--	--	--
145	CH2	2B23	200	--	--	--	--	--	--	--	--	--	--
146	CH2	3B24	290	--	--	--	--	--	--	--	--	--	--
147	CH2	3B3	350	--	--	--	--	--	--	--	--	--	--
148	CH3	A1	9	--	--	--	--	--	--	--	--	--	--
149	CH3	A3	35	--	--	--	--	--	--	--	--	--	--
150	CH3	A+B	68	--	--	--	--	--	--	--	--	--	--
151	CH3	B2t	105	--	--	--	--	--	--	--	--	--	--
152	CH3	B22t	153	--	--	--	--	--	--	--	--	--	--
153	CH3	2B23	173	--	--	--	--	--	--	--	--	--	--
154	CH3	3B24	260	--	--	--	--	--	--	--	--	--	--
155	CH3	4B31	340	--	--	--	--	--	--	--	--	--	--
156	CH3	5B32	750+	--	--	--	--	--	--	--	--	--	--
157	CH4	2B31	750	--	--	--	--	--	--	--	--	--	--
158	CH4	4C1ox	1000	--	--	--	--	--	--	--	--	--	--

+ Trace
 ++ Moderate amount present
 +++ Large amount present
 ++++ Dominant

Supplementary Table 5. Total chemical analyses of the fine (less than 47 μm) fraction by X-ray fluorescence

[All analyses in weight percent. Analysts: J. Baker, A. Bartel, J. Carr, D. Hopping, V.G. Mossotti, J. Taggart, and J.S. Wahlberg]

No.	Sample	Horizon	Basal Depth (cm)	SiO ₂	Al ₂ O ₃	Fe ₂ O ₃	MgO	CaO	Na ₂ O	K ₂ O	TiO ₂	P ₂ O ₅	MnO	ZrO ₂
Modern River Alluvium														
1	MRA1	--	--	60.4	14.3	7.83	2.1	2.49	1.6	1.82	0.86	0.3	0.14	--
2	MRA2	--	--	61.4	14.6	6.59	2.1	2.47	1.7	1.86	0.77	0.2	0.16	--
3	MRA3	--	--	58.6	14.3	7.31	1.9	2.33	2.2	1.86	0.74	0.3	0.38	--
4	MRA4	--	--	58.7	16.0	6.54	2.4	2.30	1.4	1.41	0.77	0.3	0.24	--

Supplementary Table 5. Total chemical analyses of the fine (less than 47 μm) fraction by X-ray fluorescence—Continued

No.	Sample	Horizon	Basal Depth (cm)	SiO ₂	Al ₂ O ₃	Fe ₂ O ₃	MgO	CaO	Na ₂ O	K ₂ O	TiO ₂	P ₂ O ₅	MnO	ZrO ₂
Post-Modesto Deposits, .2 Ka														
5	PM15	A1	4	67.30	12.82	5.53	1.72	3.31	2.07	1.74	0.86	0.17	0.123	0.104
6	PM15	2C1ox	19	66.69	13.11	5.88	1.80	3.14	1.99	1.72	0.88	0.17	0.109	0.1
7	PM15	3C2ox	42	--	--	--	--	--	--	--	--	--	--	--
8	PM15	4C3ox	47	--	--	--	--	--	--	--	--	--	--	--
9	PM15	5C4ox	51	--	--	--	--	--	--	--	--	--	--	--
10	PM15	6C5ox	51+	65.37	13.39	6.29	1.85	3.13	1.95	1.76	0.89	0.18	0.154	0.1
11	PM19	A11	7	--	--	--	--	--	--	--	--	--	--	--
12	PM19	2A12	12	61.82	13.63	6.05	1.80	2.63	1.75	2.14	0.77	0.28	0.119	0.04
13	PM19	3C1ox	23	--	--	--	--	--	--	--	--	--	--	--
14	PM19	4C2ox	43	63.50	14.45	6.45	1.95	2.47	1.84	2.20	0.79	0.20	0.124	0.036
15	PM19	5C3ox	49	--	--	--	--	--	--	--	--	--	--	--
16	PM19	6C4n	55	--	--	--	--	--	--	--	--	--	--	--
17	PM19	7C5n	66	--	--	--	--	--	--	--	--	--	--	--
18	PM19	8C6n	80+	63.56	14.28	6.34	1.82	2.51	1.62	2.02	0.77	0.15	0.112	0.03
Post-Modesto Deposits, 3 Ka														
19	PM8	A1	32	62.20	14.65	6.17	1.82	2.52	1.67	2.08	0.77	0.27	0.124	0.033
20	PM8	2C1	55	64.65	14.24	6.26	2.15	2.81	1.42	1.79	0.81	0.12	0.104	0.037
21	PM8	3C2	66	--	--	--	--	--	--	--	--	--	--	--
22	PM8	4C3	76+	65.41	13.31	6.05	2.03	3.05	1.45	1.77	0.88	0.15	0.120	0.081
23	PM13	A11	5	--	--	--	--	--	--	--	--	--	--	--
24	PM13	A12	35	--	--	--	--	--	--	--	--	--	--	--
25	PM13	2C1ox	86	--	--	--	--	--	--	--	--	--	--	--
26	PM13	3C2ox	112	--	--	--	--	--	--	--	--	--	--	--
27	PM13	4C3ox	136	--	--	--	--	--	--	--	--	--	--	--
28	PM13	5C4ox	200	--	--	--	--	--	--	--	--	--	--	--
29	PM13	6C5n	720	--	--	--	--	--	--	--	--	--	--	--
30	PM14	A11	3	--	--	--	--	--	--	--	--	--	--	--
31	PM14	2A12	33	61.35	14.40	6.43	1.96	2.68	1.65	2.00	0.78	0.16	0.125	0.031
32	PM14	3C1ox	99	65.32	13.52	5.80	1.82	2.85	2.03	1.80	0.80	0.14	0.107	0.053
33	PM14	4C2ox	130	--	--	--	--	--	--	--	--	--	--	--
34	PM14	5C3ox	175	--	--	--	--	--	--	--	--	--	--	--
35	PM14	6C4ox	200	66.90	13.47	5.68	1.72	2.92	1.86	1.75	0.82	0.15	0.107	0.072
36	PM14	7C5n	230+	--	--	--	--	--	--	--	--	--	--	--
37	PM16	A	2	--	--	--	--	--	--	--	--	--	--	--
38	PM16	C1ox	25	--	--	--	--	--	--	--	--	--	--	--
39	PM16	2C2ox	35	--	--	--	--	--	--	--	--	--	--	--
40	PM16	3C3ox	65	--	--	--	--	--	--	--	--	--	--	--
41	PM16	4C4ox	90	--	--	--	--	--	--	--	--	--	--	--
42	PM16	5C5ox	116	--	--	--	--	--	--	--	--	--	--	--
43	PM16	5C6n	236	--	--	--	--	--	--	--	--	--	--	--
44	PM17	A	6	--	--	--	--	--	--	--	--	--	--	--
45	PM17	2C2ox	45	--	--	--	--	--	--	--	--	--	--	--
46	PM17	2C2ox	63	--	--	--	--	--	--	--	--	--	--	--
47	PM17	2C3ox	74	--	--	--	--	--	--	--	--	--	--	--
48	PM17	3C4n	120+	--	--	--	--	--	--	--	--	--	--	--
49	PM18	A	6	53.14	11.67	6.16	2.06	3.38	1.47	2.18	0.79	0.29	0.137	0.039
50	PM18	2C1ox	65	66.02	13.08	6.31	1.88	2.82	1.52	1.75	0.87	0.16	0.112	0.055
51	PM18	2C2ox	115	--	--	--	--	--	--	--	--	--	--	--
52	PM18	3C3ox	164	--	--	--	--	--	--	--	--	--	--	--
53	PM18	4C4ox	175+	64.84	13.55	6.30	1.93	2.81	1.66	1.83	0.85	0.17	0.109	0.053

Supplementary Table 5. Total chemical analyses of the fine (less than 47 μm) fraction by X-ray fluorescence--
Continued

No.	Sample	Horizon	Basal Depth (cm)	SiO ₂	Al ₂ O ₃	Fe ₂ O ₃	MgO	CaO	Na ₂ O	K ₂ O	TiO ₂	P ₂ O ₅	MnO	ZrO ₂
Modesto Formation, upper member, 10 Ka														
54	M31	A11	20	62.55	14.01	6.04	1.85	2.79	1.72	2.13	0.77	0.25	0.12	.037
55	M31	A12	63	--	--	--	--	--	--	--	--	--	--	--
56	M31	AC	150	--	--	--	--	--	--	--	--	--	--	--
57	M31	2C1	200	64.39	14.74	6.24	1.89	2.42	2.02	2.11	0.81	0.18	0.103	0.045
58	M31	3C2	254	65.80	14.06	5.87	1.90	2.70	2.04	2.05	0.85	0.17	0.099	0.062
59	M46	A11p	5	57.8	14.6	6.09	2.00	2.60	2.05	2.51	0.75	0.28	0.09	0.0317
60	M46	A12p	14	63.32	14.66	5.21	1.61	2.86	2.56	2.62	0.73	0.20	0.097	0.042
61	M46	2A13p	32	60.5	15.6	6.29	2.02	2.65	2.21	2.63	0.79	0.26	0.13	0.0350
62	M46	3AC	66	63.43	15.93	5.90	1.56	2.68	2.12	2.61	0.79	0.19	0.118	0.04
63	M46	4Cox	250	64.12	14.93	5.57	1.73	2.83	2.37	2.43	0.76	0.17	0.100	0.04
Modesto Formation, lower member, 40 Ka														
64	M12	A11	15	57.10	15.80	7.78	1.90	1.32	1.30	1.38	0.76	0.10	0.13	--
65	M12	A12	81	65.13	15.74	4.77	1.17	2.90	2.95	2.57	0.80	0.14	0.098	0.053
66	M12	2B21t	102	--	--	--	--	--	--	--	--	--	--	--
67	M12	3B22t	170	56.31	19.81	6.74	1.52	2.37	2.12	1.88	0.80	0.14	0.097	0.037
68	M12	4B3	201	--	--	--	--	--	--	--	--	--	--	--
69	M12	5C1	231	63.38	15.99	5.32	1.51	3.17	2.59	2.17	0.81	0.13	0.092	0.055
70	M12	6C2	413+	59.30	16.20	7.66	1.70	1.48	1.40	1.23	0.81	0.10	0.13	--
Riverbank Formation, upper member, 130 Ka														
71	R9	A11p	30	65.80	16.31	4.46	0.84	2.30	2.64	2.43	0.84	0.11	0.134	0.046
72	R9	A12p	60	61.9	17.1	4.92	1.11	2.11	2.33	2.39	0.80	0.12	0.16	0.0346
73	R9	B1	105	59.1	19.5	5.65	1.21	1.76	2.06	2.35	0.85	0.14	0.13	0.0335
74	R9	2B21	180	54.0	22.9	6.16	1.22	1.38	1.57	1.78	0.81	0.14	0.14	0.0265
75	R9	2B22	235	56.59	22.48	6.19	1.02	1.42	1.58	1.93	0.86	0.13	0.115	0.028
76	R9	3B3	350	55.8	20.0	6.82	1.96	1.77	1.63	2.32	0.83	0.12	0.1	0.0213
77	R9	4C	400+	57.71	18.94	6.51	1.88	2.79	1.97	2.19	1.08	0.18	0.092	0.044
78	R33	A11	4	63.30	15.69	4.33	1.00	2.27	2.66	2.53	0.81	0.15	0.163	0.05
79	R33	2A12	19	--	--	--	--	--	--	--	--	--	--	--
80	R33	3A3	39	--	--	--	--	--	--	--	--	--	--	--
81	R33	3B21t	62	--	--	--	--	--	--	--	--	--	--	--
82	R33	3B22t	83	--	--	--	--	--	--	--	--	--	--	--
83	R33	3B23t	122	55.53	21.22	6.28	0.87	1.31	1.55	1.96	0.87	0.16	0.092	0.029
84	R33	3B31	151	--	--	--	--	--	--	--	--	--	--	--
85	R33	3B32	210	--	--	--	--	--	--	--	--	--	--	--
86	R33	4B33	260	--	--	--	--	--	--	--	--	--	--	--
87	R33	5Cox	300+	51.30	20.60	7.70	1.63	1.90	1.05	1.68	0.85	0.23	0.078	0.035

Supplementary Table 5. Total chemical analyses of the fine (less than 47 μm) fraction by X-ray fluorescence--
Continued

No.	Sample	Horizon	Basal Depth (cm)	SiO ₂	Al ₂ O ₃	Fe ₂ O ₃	MgO	CaO	Na ₂ O	K ₂ O	TiO ₂	P ₂ O ₅	MnO	ZrO ₂
Riverbank Formation, middle member, 250 Ka														
88	R2	Ap	25	65.01	15.57	4.08	0.74	2.85	3.12	2.55	0.79	0.13	0.108	0.069
89	R2	B21	81	6.10	18.3	5.20	1.18	1.96	2.30	2.62	0.84	0.16	0.12	0.0416
90	R2	B22t	185	58.45	21.30	6.29	1.06	1.51	1.68	2.28	0.86	0.20	0.123	0.032
91	R2	B3	386	52.4	22.2	7.24	1.85	1.64	1.54	2.01	0.83	0.16	0.11	0.0263
92	R2	C1	500	49.4	21.7	9.13	2.81	1.65	1.36	2.34	0.93	0.19	0.16	0.0240
93	R2	C2n	500+	55.01	18.30	6.04	1.59	2.77	2.04	2.70	0.69	0.30	0.186	0.047
94	R10	A	46	65.98	15.93	4.36	1.04	2.36	2.75	2.66	0.83	0.12	0.085	0.062
95	R10	2B10	70	59.5	19.3	5.58	1.12	1.76	2.13	2.42	0.84	0.15	0.11	0.0396
96	R10	2B21t	140	60.07	18.92	5.65	0.85	1.84	2.04	2.11	0.87	0.12	0.093	0.04
97	R10	2B22t	210	55.6	21.6	6.18	1.33	1.68	1.79	1.78	1.78	0.13	0.10	0.0297
98	R10	3B3t	386	55.99	19.61	6.45	1.32	2.14	2.03	1.96	0.85	0.13	0.073	0.038
99	R10	3Cox	500	--	--	--	--	--	--	--	--	--	--	--
100	R32	A11	26	64.32	15.95	4.54	0.98	2.50	2.73	2.61	0.84	0.13	0.102	0.05
101	R32	A12	50	--	--	--	--	--	--	--	--	--	--	--
102	R32	A3	70	--	--	--	--	--	--	--	--	--	--	--
103	R32	B21t	105	--	--	--	--	--	--	--	--	--	--	--
104	R32	B22t	150	58.02	20.29	6.03	0.95	1.66	1.95	2.19	0.85	0.15	0.088	0.035
105	R32	B31t	220	--	--	--	--	--	--	--	--	--	--	--
106	R32	2B32	354	--	--	--	--	--	--	--	--	--	--	--
107	R32	3Cox	360+	54.45	18.84	8.08	1.70	2.35	1.59	2.17	1.01	0.15	0.051	0.051
Riverbank Formation, lower member, 330 Ka														
108	R30	Ap	65	65.88	16.27	4.45	0.99	2.19	2.71	2.74	0.86	0.08	0.072	0.062
109	R30	B10	78	--	--	--	--	--	--	--	--	--	--	--
110	R30	B21t	127	53.87	21.75	6.86	0.89	1.39	1.60	1.89	0.96	0.11	0.077	0.03
111	R30	2B22t	179	--	--	--	--	--	--	--	--	--	--	--
112	R30	3B3t	197	--	--	--	--	--	--	--	--	--	--	--
113	R30	3C1ox	220	49.05	20.93	8.98	1.18	1.32	0.77	1.41	0.95	0.14	0.070	0.014
Turlock Lake Formation, 600 Ka														
114	T2	A	31	69.07	14.20	4.70	0.38	0.82	1.56	3.02	1.02	0.10	0.151	0.067
115	T2	B21	173	53.89	22.40	7.01	0.32	0.27	0.61	2.03	1.01	0.12	0.037	0.035
116	T2	2B22	386	57.72	21.52	6.23	0.77	1.66	1.95	1.70	0.89	0.09	0.049	0.055
117	T2	3C	417	61.93	18.10	6.41	0.90	1.38	1.59	1.96	0.89	0.10	0.055	0.051
118	T6	A11	20	61.17	16.75	5.07	1.36	2.77	2.92	2.51	0.90	0.15	0.173	0.062
119	T6	A12	40	56.5	18.1	7.00	1.70	2.29	2.18	2.75	1.04	0.16	0.15	0.0402
120	T6	2B21t	90	47.7	23.0	8.80	2.08	1.17	0.37	1.64	0.90	0.11	0.06	0.0150
121	T6	2B22t	190	47.61	23.06	8.83	1.12	1.14	0.86	1.84	1.08	0.13	0.080	0.02
122	T6	3B+C	370	54.45	18.60	7.50	2.15	4.35	2.37	1.95	1.16	0.11	0.280	0.061
123	T11	A11p	5	--	--	--	--	--	--	--	--	--	--	--
124	T11	2A12p	11	66.62	15.59	4.20	0.47	1.64	2.47	3.04	0.81	0.12	0.079	0.051
125	T11	2A+B	20	--	--	--	--	--	--	--	--	--	--	--
126	T11	2B1t	33	56.35	20.88	6.13	0.49	0.88	1.33	2.29	0.92	0.12	0.043	0.035
127	T11	2B2t	80	--	--	--	--	--	--	--	--	--	--	--
128	T11	3B31t	191	--	--	--	--	--	--	--	--	--	--	--
129	T11	4B32t	256	--	--	--	--	--	--	--	--	--	--	--
130	T11	5B+C	292	--	--	--	--	--	--	--	--	--	--	--
131	T11	5C1ox	375	--	--	--	--	--	--	--	--	--	--	--
132	T11	6C2ox	375+	50.32	21.19	8.35	0.90	1.32	0.88	1.51	0.87	0.17	0.038	0.019

Supplementary Table 5. Total chemical analyses of the fine (less than 47 μ m) fraction by X-ray fluorescence--
Continued

No.	Sample	Horizon	Basal depth (cm)	SiO ₂	Al ₂ O ₃	Fe ₂ O ₃	MgO	CaO	Na ₂ O	K ₂ O	TiO ₂	MnO	P ₂ O ₅	ZrO ₂
China Hat gravel member of Laguna Formation, 3,000 Ka														
133	CH1	A1	12	73.93	12.55	4.52	0.29	0.41	1.17	2.17	0.94	0.11	0.058	0.067
134	CH1	2A8	53	--	--	--	--	--	--	--	--	--	--	--
135	CH1	2B21t	88	62.50	20.57	6.81	0.36	0.28	0.99	1.55	0.99	0.15	0.080	0.044
136	CH1	2B22t	140	--	--	--	--	--	--	--	--	--	--	--
137	CH1	2B31	234	--	--	--	--	--	--	--	--	--	--	--
138	CH1	2B32	310	--	--	--	--	--	--	--	--	--	--	--
139	CH1	3B33	350	53.54	23.81	10.34	0.47	0.17	0.51	1.25	0.92	0.15	0.024	0.024
140	CH2	A1	8	71.8	12.5	4.94	0.61	0.18	0.5	2.11	0.98	0.1	0.05	--
141	CH2	A3	30	64.2	16.4	6.54	0.65	0.12	0.46	1.83	1.02	0.17	0.03	0.0513
142	CH2	2A+B	50	61.2	18.5	7.18	0.68	0.08	0.41	1.68	1.05	0.18	0.03	0.0470
143	CH2	2B21t	110	53.1	23.6	8.56	0.55	0.05	0.28	1.03	1.02	0.20	0.08	0.0350
144	CH2	2B22	170	49.5	25.6	10.0	0.49	0.07	0.22	0.41	0.93	0.14	0.02	0.0261
145	CH2	2B23	200	51.3	25.3	8.58	0.55	0.07	0.2	0.66	0.86	0.1	0.02	--
146	CH2	3B24	290	48.7	24.5	11.3	0.75	0.11	0.21	0.57	0.98	0.1	0.02	0.0192
147	CH2	3B3	350	48.6	25.2	10.4	0.80	0.1	0.2	0.55	0.83	0.1	0.02	--
148	CH3	A1	9	69.8	13.2	4.95	0.61	0.38	0.7	2.17	1.00	0.1	0.1	--
149	CH3	A3	35	--	--	--	--	--	--	--	--	--	--	--
150	CH3	A+B	68	--	--	--	--	--	--	--	--	--	--	--
151	CH3	B2t	105	--	--	--	--	--	--	--	--	--	--	--
152	CH3	B22t	153	--	--	--	--	--	--	--	--	--	--	--
153	CH3	2B23	173	48.0	27.2	8.31	0.55	0.12	0.2	0.58	0.84	0.1	0.02	--
154	CH3	3B24	260	--	--	--	--	--	--	--	--	--	--	--
155	CH3	4B31	340	--	--	--	--	--	--	--	--	--	--	--
156	CH3	5B32	750+	49.3	23.9	9.91	0.98	0.11	0.2	0.66	0.87	0.1	0.02	--
157	CH4	2B31	750	52.3	24.6	8.09	0.98	0.05	0.4	1.32	0.70	0.1	0.02	--
158	CH4	4C1ox	1000	50.9	26.4	6.24	1.1	0.11	0.4	1.16	0.71	0.1	0.02	--

Supplementary Table 6. Total chemical analyses of the less-than-2-mm fraction by X-ray fluorescence

[All analyses in weight percent. Analysts: J. Baker, A. Bartel, J. Lindsay, V.G. Mossotti, S. Ramage, B. Scott, J. Taggart, J.S. Wahlberg, and K. Wong]

No.	Sample	Horizon	Basal depth (cm)	SiO ₂	Al ₂ O ₃	Fe ₂ O ₃	MgO	CaO	Na ₂ O	K ₂ O	TiO ₂	MnO	P ₂ O ₅	ZrO ₂
Modern River Alluvium														
1	MRA1	--	--	--	--	--	--	--	--	--	--	--	--	--
2	MRA2	--	--	--	--	--	--	--	--	--	--	--	--	--
3	MRA3	--	--	--	--	--	--	--	--	--	--	--	--	--
4	MRA4	--	--	--	--	--	--	--	--	--	--	--	--	--

Supplementary Table 6. Total chemical analyses of the less-than-2-mm fraction by X-ray fluorescence--
Continued

No.	Sample	Horizon	Basal depth (cm)	SiO ₂	Al ₂ O ₃	Fe ₂ O ₃	MgO	CaO	Na ₂ O	K ₂ O	TiO ₂	MnO	P ₂ O ₅	ZrO ₂
Post-Modesto Deposits, .2 Ka														
5	PM15	A1	4	70.65	12.85	4.32	1.37	3.21	2.47	2.30	0.58	0.082	0.09	0.035
6	PM15	2C1ox	19	68.52	13.33	5.14	1.59	3.43	2.63	2.09	0.71	0.107	0.11	0.028
7	PM15	3C2ox	42	--	--	--	--	--	--	--	--	--	--	--
8	PM15	4C3ox	47	--	--	--	--	--	--	--	--	--	--	--
9	PM15	5C4ox	51	--	--	--	--	--	--	--	--	--	--	--
10	PM15	6C5ox	51+	70.16	13.67	4.29	1.49	3.33	2.58	2.27	0.57	0.090	0.09	0.033
11	PM19	A11	7	--	--	--	--	--	--	--	--	--	--	--
12	PM19	2A12	12	--	--	--	--	--	--	--	--	--	--	--
13	PM19	3C1ox	23	--	--	--	--	--	--	--	--	--	--	--
14	PM19	4C2ox	43	--	--	--	--	--	--	--	--	--	--	--
15	PM19	5C3ox	49	--	--	--	--	--	--	--	--	--	--	--
16	PM19	6C4n	55	--	--	--	--	--	--	--	--	--	--	--
17	PM19	7C5n	66	--	--	--	--	--	--	--	--	--	--	--
18	PM19	8C6n	80+	--	--	--	--	--	--	--	--	--	--	--
Post-Modesto Deposits, 3 Ka														
19	PM8	A1	32	61.32	14.41	5.91	2.01	2.87	1.88	2.13	0.71	0.139	0.19	0.033
20	PM8	2C1	55	64.48	14.38	5.60	2.00	3.09	2.20	1.98	0.71	0.114	0.09	0.035
21	PM8	3C2	66	--	--	--	--	--	--	--	--	--	--	--
22	PM8	4C3	76+	70.27	13.45	3.52	1.27	2.91	2.82	2.46	0.42	0.080	0.04	0.017
23	PM13	A11	5	--	--	--	--	--	--	--	--	--	--	--
24	PM13	A12	35	--	--	--	--	--	--	--	--	--	--	--
25	PM13	2C1ox	86	--	--	--	--	--	--	--	--	--	--	--
26	PM13	3C2ox	112	--	--	--	--	--	--	--	--	--	--	--
27	PM13	4C3ox	136	--	--	--	--	--	--	--	--	--	--	--
28	PM13	5C4ox	200	--	--	--	--	--	--	--	--	--	--	--
29	PM13	6C5n	720	--	--	--	--	--	--	--	--	--	--	--
30	PM14	A11	3	--	--	--	--	--	--	--	--	--	--	--
31	PM14	2A12	33	--	--	--	--	--	--	--	--	--	--	--
32	PM14	3C1ox	99	--	--	--	--	--	--	--	--	--	--	--
33	PM14	4C2ox	130	--	--	--	--	--	--	--	--	--	--	--
34	PM14	5C3ox	175	--	--	--	--	--	--	--	--	--	--	--
35	PM14	6C4ox	200	--	--	--	--	--	--	--	--	--	--	--
36	PM14	7C5n	239+	--	--	--	--	--	--	--	--	--	--	--
37	PM16	A	2	--	--	--	--	--	--	--	--	--	--	--
38	PM16	C1ox	25	--	--	--	--	--	--	--	--	--	--	--
39	PM16	2C2ox	35	--	--	--	--	--	--	--	--	--	--	--
40	PM16	3C3ox	65	--	--	--	--	--	--	--	--	--	--	--
41	PM16	4C4ox	90	--	--	--	--	--	--	--	--	--	--	--
42	PM16	5C5ox	116	--	--	--	--	--	--	--	--	--	--	--
43	PM16	5C6n	236	--	--	--	--	--	--	--	--	--	--	--
44	PM17	A	6	--	--	--	--	--	--	--	--	--	--	--
45	PM17	2C2ox	45	--	--	--	--	--	--	--	--	--	--	--
46	PM17	2C2ox	63	--	--	--	--	--	--	--	--	--	--	--
47	PM17	2C3ox	74	--	--	--	--	--	--	--	--	--	--	--
48	PM17	3C4n	120+	--	--	--	--	--	--	--	--	--	--	--
49	PM18	A	6	--	--	--	--	--	--	--	--	--	--	--
50	PM18	2C1ox	65	--	--	--	--	--	--	--	--	--	--	--
51	PM18	2C2ox	115	--	--	--	--	--	--	--	--	--	--	--
52	PM18	3C3ox	164	--	--	--	--	--	--	--	--	--	--	--
53	PM18	4C4ox	175+	--	--	--	--	--	--	--	--	--	--	--

Supplementary Table 6. Total chemical analyses of the less-than-2-mm fraction by X-ray fluorescence--
Continued

No.	Sample	Horizon	Basal depth (cm)	SiO ₂	Al ₂ O ₃	Fe ₂ O ₃	MgO	CaO	Na ₂ O	K ₂ O	TiO ₂	MnO	P ₂ O ₅	ZrO ₂
Modesto Formation, upper member, 10 Ka														
54	M31	A11	20	65.56	14.00	5.23	1.69	3.10	2.21	2.32	0.66	0.108	0.19	0.029
55	M31	A12	63	--	--	--	--	--	--	--	--	--	--	--
56	M31	AC	150	--	--	--	--	--	--	--	--	--	--	--
57	M31	2C1	200	66.81	14.14	5.00	1.64	3.16	2.69	2.26	0.65	0.094	0.12	0.036
58	M31	3C2	254	70.10	13.57	4.09	1.45	3.20	2.86	2.38	0.57	0.077	0.09	0.033
59	M46	A11p	5	66.3	13.4	3.21	0.98	2.72	2.68	2.72	0.41	0.04	0.14	0.0185
60	M46	A12p	14	68.5	14.0	3.51	1.07	2.75	2.69	2.83	0.46	0.05	0.14	0.0199
61	M46	2A13p	32	69.6	14.0	3.45	0.99	2.75	2.63	2.84	0.45	0.06	0.12	0.0186
62	M46	3AC	66	68.2	14.4	4.00	1.25	2.73	2.49	2.81	0.50	0.07	0.13	0.0195
63	M46	4Cox	250	68.2	14.4	4.01	1.26	2.82	2.46	2.68	0.49	0.07	0.12	0.0211
Modesto Formation, lower member, 40 Ka														
64	M12	A11	15	--	--	--	--	--	--	--	--	--	--	--
65	M12	A12	81	70.91	13.86	2.79	0.48	2.57	2.98	2.96	0.38	0.080	0.03	0.020
66	M12	2B21t	102	--	--	--	--	--	--	--	--	--	--	--
67	M12	3B22t	170	67.69	16.00	4.08	0.77	2.65	2.77	2.51	0.44	0.080	0.04	0.021
68	M12	4B3	201	--	--	--	--	--	--	--	--	--	--	--
69	M12	5C1	231	69.58	14.96	3.22	0.66	3.02	3.39	2.69	0.36	0.080	0.03	0.017
70	M12	6C2	413+	--	--	--	--	--	--	--	--	--	--	--
Riverbank Formation, upper member, 130 Ka														
71	R9	A11p	30	71.71	13.43	3.14	0.38	2.19	2.95	2.50	0.45	0.080	0.01	0.023
72	R9	A12p	60	72.7	13.3	2.80	0.55	2.10	2.96	2.42	0.40	0.060	0.05	0.0199
73	R9	B1	105	71.7	14.0	3.12	0.60	1.98	2.97	2.25	0.44	0.050	0.06	0.0171
74	R9	2B21	180	68.9	15.4	3.45	0.61	1.75	2.77	1.86	0.44	0.060	0.06	0.0167
75	R9	2B22	235	68.96	15.45	3.67	0.45	1.78	2.75	1.91	0.48	0.082	0.02	0.019
76	R9	3B3	350	67.5	16.0	3.20	0.94	2.53	2.67	2.71	0.41	0.040	0.05	0.0136
77	R9	4C	400+	64.74	16.52	3.82	1.25	3.58	2.63	3.04	0.52	0.080	0.06	0.017
78	R33	A11	4	71.2	13.1	2.73	0.53	2.04	3.00	2.35	0.41	0.05	0.07	0.0227
79	R33	2A12	19	--	--	--	--	--	--	--	--	--	--	--
80	R33	3A3	39	--	--	--	--	--	--	--	--	--	--	--
81	R33	3B21t	62	--	--	--	--	--	--	--	--	--	--	--
82	R33	3B22t	83	--	--	--	--	--	--	--	--	--	--	--
83	R33	3B23t	122	68.0	15.9	3.57	0.65	1.53	2.83	1.90	0.43	0.07	0.08	0.0172
84	R33	3B31	151	--	--	--	--	--	--	--	--	--	--	--
85	R33	3B32	210	--	--	--	--	--	--	--	--	--	--	--
86	R33	4B33	260	--	--	--	--	--	--	--	--	--	--	--
87	R33	5Cox	300+	72.3	14.0	2.43	0.53	2.33	3.06	2.68	0.25	0.02	0.06	0.0082

Supplementary Table 6. Total chemical analyses of the less-than-2-mm fraction by X-ray fluorescence--
Continued

No.	Sample	Horizon	Basal depth (cm)	SiO ₂	Al ₂ O ₃	Fe ₂ O ₃	MgO	CaO	Na ₂ O	K ₂ O	TiO ₂	MnO	P ₂ O ₅	ZrO ₂
Riverbank Formation, middle member, 250 Ka														
88	R2	Ap	25	74.39	12.36	2.61	0.40	2.13	3.14	2.26	0.38	0.08	0.02	0.025
89	R2	B21	81	72.6	13.3	3.03	0.52	1.92	3.21	2.37	0.45	0.05	0.06	0.0193
90	R2	B22t	185	69.68	14.86	4.09	0.42	1.69	3.03	1.94	0.52	0.08	0.04	0.022
91	R2	B3	386	69.0	15.2	3.41	0.68	2.31	2.78	2.67	0.38	0.03	0.05	0.0132
92	R2	C1	500	72.0	14.3	2.02	0.54	2.34	3.28	3.21	0.25	0.02	0.05	0.0104
93	R2	C2n	500+	72.89	14.76	1.29	0.31	2.20	4.01	3.23	0.16	0.08	0.02	0.008
94	R10	A	46	74.77	12.68	2.68	0.31	1.81	3.27	2.34	0.41	0.067	0.06	0.025
95	R10	2B1	70	72.2	13.5	2.91	0.51	1.68	3.23	1.85	0.43	0.04	0.05	0.0201
96	R10	2B21t	140	71.48	14.29	3.42	0.43	1.74	3.09	2.29	0.45	0.066	0.06	0.020
97	R10	2B22t	210	71.4	14.1	3.05	0.55	1.82	2.99	2.28	0.38	0.04	0.05	0.0167
98	R10	3B3t	386	70.09	15.04	3.53	0.68	2.37	2.74	2.74	0.41	0.04	0.05	0.018
99	R10	3Cox	500	--	--	--	--	--	--	--	--	--	--	--
100	R32	A11	26	72.4	13.5	3.39	0.59	2.21	3.01	2.52	0.47	0.05	0.05	0.0251
101	R32	A12	50	--	--	--	--	--	--	--	--	--	--	--
102	R32	A3	70	--	--	--	--	--	--	--	--	--	--	--
103	R32	B21t	105	--	--	--	--	--	--	--	--	--	--	--
104	R32	B22t	150	68.6	15.0	4.15	0.66	1.87	2.84	2.18	0.50	0.06	0.07	0.0234
105	R32	B31t	220	--	--	--	--	--	--	--	--	--	--	--
106	R32	2B32	354	--	--	--	--	--	--	--	--	--	--	--
107	R32	3Cox	360+	68.0	15.4	3.87	0.81	3.10	2.61	3.09	0.41	0.04	0.05	0.0136
Riverbank Formation, lower member, 330 Ka														
108	R30	Ap	65	74.69	12.38	3.58	0.29	1.68	3.29	2.23	0.44	0.06	0.04	0.031
109	R30	B10	78	--	--	--	--	--	--	--	--	--	--	--
110	R30	B21t	127	69.43	15.11	4.55	0.41	1.55	2.89	2.00	0.52	0.051	0.05	0.023
111	R30	2B22t	179	--	--	--	--	--	--	--	--	--	--	--
112	R30	3B3t	197	--	--	--	--	--	--	--	--	--	--	--
113	R30	3C1ox	220	67.94	14.71	4.63	0.58	2.31	2.85	2.37	0.54	0.043	0.05	0.014
Turlock Lake Formation, 600 Ka														
114	T2	A	31	77.66	10.18	3.18	0.02	0.64	3.70	1.03	0.48	0.08	0.02	0.040
115	T2	B21	173	66.96	16.26	5.17	0.08	0.23	3.02	0.51	0.44	0.028	0.08	0.028
116	T2	2B22	386	66.39	16.29	4.13	0.33	2.01	2.30	2.42	0.50	0.08	0.01	0.035
117	T2	3C	417	72.03	13.64	3.08	0.27	1.72	3.24	2.67	0.34	0.08	0.01	0.016
118	T6	A11	20	74.1	12.6	2.35	0.46	2.10	3.17	2.48	0.31	0.03	0.05	0.0166
119	T6	A12	40	73.4	12.9	2.72	0.53	2.14	3.18	2.47	0.36	0.04	0.05	0.0199
120	T6	2B21t	90	69.4	14.4	3.57	0.77	2.11	2.68	2.11	0.39	0.03	0.05	0.0104
121	T6	2B22t	190	66.9	16.0	3.85	0.80	1.70	2.90	1.91	0.42	0.04	0.05	0.0103
122	T6	3B+C	370	74.8	12.7	1.64	0.57	2.07	3.20	2.51	0.22	0.03	0.05	0.0095
123	T11	A11p	5	--	--	--	--	--	--	--	--	--	--	--
124	T11	2A12p	11	74.8	12.2	2.38	0.27	1.30	3.59	2.13	0.35	0.03	0.05	0.0224
125	T11	2A+B	20	--	--	--	--	--	--	--	--	--	--	--
126	T11	2B1t	33	69.2	15.2	3.46	0.42	0.90	3.30	1.60	0.46	0.02	0.06	0.0194
127	T11	2B2t	80	--	--	--	--	--	--	--	--	--	--	--
128	T11	3B31t	191	--	--	--	--	--	--	--	--	--	--	--
129	T11	4B32t	256	--	--	--	--	--	--	--	--	--	--	--
130	T11	5B+C	292	--	--	--	--	--	--	--	--	--	--	--
131	T11	5C1ox	375	--	--	--	--	--	--	--	--	--	--	--
132	T11	61C2ox	375+	70.5	14.2	3.52	0.53	1.97	2.69	2.53	0.35	0.02	0.06	0.0112

Supplementary Table 6. Total chemical analyses of the less-than-2-mm fraction by X-ray fluorescence—Continued

No.	Sample	Horizon	Basal depth (cm)	SiO ₂	Al ₂ O ₃	Fe ₂ O ₃	MgO	CaO	Na ₂ O	K ₂ O	TiO ₂	MnO	P ₂ O ₅	ZrO ₂
China Hat gravel member of Laguna Formation, 3,000 Ka														
133	CH1	A1	12	78.82	10.02	3.92	0.10	0.34	0.56	1.75	0.74	0.04	0.1	0.049
134	CH1	2AB	53	--	--	--	--	--	--	--	--	--	--	--
135	CH1	2B21t	88	66.93	16.75	6.06	0.17	0.26	0.47	1.35	0.84	0.08	0.08	0.040
135	CH1	2B22t	140	--	--	--	--	--	--	--	--	--	--	--
137	CH1	2B31	234	--	--	--	--	--	--	--	--	--	--	--
138	CH1	2B32	310	--	--	--	--	--	--	--	--	--	--	--
139	CH1	31B33	350	64.39	17.11	7.59	0.23	0.20	0.06	1.36	0.67	0.08	0.05	0.020
140	CH2	A1	8	77.8	8.89	3.80	0.41	0.15	0.39	1.62	0.74	0.02	0.12	0.0436
141	CH2	A3	30	74.4	11.4	4.76	0.44	0.10	0.37	1.52	0.77	0.02	0.13	0.0394
142	CH2	2A+B	50	70.4	13.6	5.45	0.49	0.07	0.33	1.48	0.82	0.07	0.16	0.0448
143	CH2	2B21t	110	60.8	19.3	7.13	0.46	0.04	0.21	0.99	0.87	0.02	0.12	0.0319
144	CH2	2B22	170	56.7	21.4	8.77	0.40	0.05	0.17	0.36	0.79	--	--	0.0208
145	CH2	2B23	200	58.6	19.8	8.80	0.46	0.07	0.15	0.55	0.75	0.02	0.08	0.0221
146	CH2	2B24	290	57.0	19.5	9.46	0.60	0.08	0.17	0.66	0.85	0.02	0.08	0.0178
147	CH2	311B3	350	59.0	18.5	9.25	0.64	0.09	0.16	0.76	0.82	0.02	0.09	0.0155
148	CH3	A1	9	75.4	8.88	3.61	0.43	0.34	0.47	1.62	0.71	0.09	0.09	0.0436
149	CH3	A3	35	--	--	--	--	--	--	--	--	--	--	--
150	CH3	A+B	68	--	--	--	--	--	--	--	--	--	--	--
151	CH3	B2t	105	--	--	--	--	--	--	--	--	--	--	--
152	CH3	B22t	153	--	--	--	--	--	--	--	--	--	--	--
153	CH3	2B23	173	60.6	19.9	6.62	0.44	0.08	0.15	0.65	0.72	0.02	0.09	0.0199
154	CH3	311B24	260	--	--	--	--	--	--	--	--	--	--	--
155	CH3	4VB31	340	65.3	16.0	6.53	0.59	0.08	0.19	1.14	0.57	0.02	0.06	0.0167
156	CH3	5B32	750+	--	--	--	--	--	--	--	--	--	--	--
157	CH4	2B31	750	--	--	--	--	--	--	--	--	--	--	--
158	CH4	4C10x	1000	--	--	--	--	--	--	--	--	--	--	--

Supplementary Table 7, Part 1. Total chemical analyses of the fine (less than 47 μm) fraction by instrumental neutron activation

[Fe and K values in weight percent; all others in parts per million. Analysts: J. Budahn, R. Knight, and D. McKown]

No.	Sample	Horizon	Basal depth (cm)	Ba	Ce	Co	Cr	Cs	Dy	Eu	Fe	Gd	Hf	K	La	Lu	Mn
Modern River Alluvium																	
1	MRA1	--	--	916	54.6	16.5	104	4.32	4.90	1.15	5.41	4.2	16.0	1.65	32.0	0.462	1090
2	MRA2	--	--	970	51.5	16.3	96.7	4.47	4.72	1.10	4.53	4.12	6.76	1.68	29.7	0.391	1250
3	MRA3	--	--	1180	52.7	18.8	90.7	4.55	4.36	1.10	5.09	3.97	7.35	1.61	30.3	0.350	2780
4	MRA4	--	--	1040	64.5	18.9	67.0	4.84	4.51	1.30	4.57	5.42	5.84	1.22	39.3	0.345	1850

Supplementary Table 7, Part 1. Total chemical analyses of the fine (less than 47 μm) fraction by instrumental neutron activation--Continued

No. Sample	Horizon	Basal depth (cm)	Ba	Ce	Co	Cr	Cs	Dy	Eu	Fe	Gd	Hf	K	La	Lu	Mn	
Post-Modesto Deposits, .2 Ka																	
5	PM15	A1	4	824	59.9	16.7	99.2	4.01	4.56	1.13	4.37	4.61	14.1	1.66	31.5	0.453	1040
6	PM15	2C1ox	19	891	63.5	19.3	110	4.62	5.22	1.23	4.92	5.3	12.1	1.56	32.9	0.458	1080
7	PM15	3C2ox	42	--	--	--	--	--	--	--	--	--	--	--	--	--	--
8	PM15	4C3ox	47	--	--	--	--	--	--	--	--	--	--	--	--	--	--
9	PM15	5C4ox	51	--	--	--	--	--	--	--	--	--	--	--	--	--	--
10	PM15	6C5ox	51+	908	63.2	21.3	106	4.54	5.11	1.23	4.93	5.34	12.3	1.74	33.7	0.462	1510
11	PM19	A11	7	--	--	--	--	--	--	--	--	--	--	--	--	--	--
12	PM19	2A12	12	952	50.8	16.0	98.0	4.98	--	1.02	4.67	3.92	6.02	2.06	26.9	0.369	979
13	PM1s	3C1ox	23	--	--	--	--	--	--	--	--	--	--	--	--	--	--
14	PM19	4C2ox	43	908	55.8	16.6	93.0	3.82	4.40	1.08	4.18	4.69	7.01	1.79	27.8	0.399	907
15	PM19	5C3ox	49	--	--	--	--	--	--	--	--	--	--	--	--	--	--
16	PM19	6C4n	55	--	--	--	--	--	--	--	--	--	--	--	--	--	--
17	PM19	7C5n	66	--	--	--	--	--	--	--	--	--	--	--	--	--	--
18	PM19	58C6n	80+	926	55.1	16.7	94.6	4.18	4.55	1.11	4.30	4.42	5.15	1.77	29.3	0.368	880
Post-Modesto Deposits, 3 Ka																	
19	PM8	A1	32	1080	55.0	15.9	115	4.15	4.78	1.05	3.88	--	6.43	1.81	30.2	0.459	896
20	PM8	2C1	55	1010	60.5	15.0	108	3.68	4.43	1.12	3.75	6.2	7.24	1.44	31.1	0.475	753
21	PM8	3C2	66	--	--	--	--	--	--	--	--	--	--	--	--	--	--
22	PM8	4C3	76+	1110	64.2	14.9	119	3.44	4.89	1.13	3.75	--	17.8	1.33	31.0	0.572	856
23	PM13	A11	5	--	--	--	--	--	--	--	--	--	--	--	--	--	--
24	PM13	A12	35	--	--	--	--	--	--	--	--	--	--	--	--	--	--
25	PM13	2C1ox	86	--	--	--	--	--	--	--	--	--	--	--	--	--	--
26	PM13	3C2ox	112	--	--	--	--	--	--	--	--	--	--	--	--	--	--
27	PM13	4C3ox	136	--	--	--	--	--	--	--	--	--	--	--	--	--	--
28	PM13	5C4ox	200	--	--	--	--	--	--	--	--	--	--	--	--	--	--
29	PM13	6C5n	720	--	--	--	--	--	--	--	--	--	--	--	--	--	--
30	PM14	A11	3	--	--	--	--	--	--	--	--	--	--	--	--	--	--
31	PM14	2A12	33	991	54.5	17.9	98.3	4.74	4.25	1.08	4.66	4.02	4.84	1.83	28.7	0.377	1010
32	PM14	3C1ox	99	972	65.0	18.9	102	4.75	4.72	1.15	4.84	4.93	8.26	1.56	32.2	0.398	1010
33	PM14	4C2ox	130	--	--	--	--	--	--	--	--	--	--	--	--	--	--
34	PM14	5C3ox	175	--	--	--	--	--	--	--	--	--	--	--	--	--	--
35	PM14	6C4ox	200	939	67.2	20.4	107	4.70	5.27	1.25	5.07	5.18	10.6	1.62	34.0	0.414	1130
36	PM14	7C5n	230+	--	--	--	--	--	--	--	--	--	--	--	--	--	--
37	PM16	A	2	--	--	--	--	--	--	--	--	--	--	--	--	--	--
38	PM16	C1ox	25	--	--	--	--	--	--	--	--	--	--	--	--	--	--
39	PM16	2C2ox	35	--	--	--	--	--	--	--	--	--	--	--	--	--	--
40	PM16	3C3ox	65	--	--	--	--	--	--	--	--	--	--	--	--	--	--
41	PM16	4C4ox	90	--	--	--	--	--	--	--	--	--	--	--	--	--	--
42	PM16	5C5ox	116	--	--	--	--	--	--	--	--	--	--	--	--	--	--
43	PM16	5C6n	236	--	--	--	--	--	--	--	--	--	--	--	--	--	--
44	PM17	A	6	--	--	--	--	--	--	--	--	--	--	--	--	--	--
45	PM17	2C2ox	45	--	--	--	--	--	--	--	--	--	--	--	--	--	--
46	PM17	2C2ox	63	--	--	--	--	--	--	--	--	--	--	--	--	--	--
47	PM17	2C3ox	74	--	--	--	--	--	--	--	--	--	--	--	--	--	--
48	PM17	3C4n	120+	--	--	--	--	--	--	--	--	--	--	--	--	--	--
49	PM18	A	6	936	43.4	16.4	94.3	4.53	--	0.912	4.40	3.67	6.16	2.05	23.5	0.336	1100
50	PM18	2C1ox	65	982	54.0	17.3	105	4.11	5.33	1.18	4.63	5.15	8.42	1.51	30.1	0.411	989
51	PM18	2C2ox	115	--	--	--	--	--	--	--	--	--	--	--	--	--	--
52	PM18	3C3ox	164	--	--	--	--	--	--	--	--	--	--	--	--	--	--
53	PM18	4C4ox	175+	1190	57.3	20.5	122	5.23	5.24	1.19	5.56	5.36	8.47	1.71	30.2	0.461	1010
Modesto Formation, upper member, 10 Ka																	
54	M31	A11	20	1050	53.4	18.1	99.2	4.90	4.73	1.14	4.66	4.44	5.33	2.04	29.1	0.388	1070
55	M31	A12	63	--	--	--	--	--	--	--	--	--	--	--	--	--	--
56	M31	AC	150	--	--	--	--	--	--	--	--	--	--	--	--	--	--
57	M31	2C1	200	986	52.8	16.0	92.6	4.66	4.23	1.01	4.47	3.58	5.99	1.75	27.1	0.346	845
58	M31	3C2	254	1010	56.5	17.4	98.6	5.14	4.36	1.02	4.63	4.48	8.19	1.85	27.6	0.351	904
59	M46	A11p	5	--	--	--	--	--	--	--	--	--	--	--	--	--	--
60	M46	A12p	14	1160	75.5	21.6	109	6.54	4.62	1.31	5.58	6.38	7.83	2.06	38.7	0.491	1010
61	M46	2A13p	32	--	--	--	--	--	--	--	--	--	--	--	--	--	--
62	M46	3AC	66	982	63.8	16.1	70.6	5.34	4.03	1.07	4.30	4.72	7.08	2.11	30.5	0.356	1040
63	M46	4Cox	250	958	62.9	16.0	72.0	5.19	4.14	0.999	4.25	4.83	6.46	2.12	28.5	0.325	990

Supplementary Table 7, Part 1. Total chemical analyses of the fine (less than 47 μm) fraction by instrumental neutron activation--Continued

No. Sample	Horizon	Basal depth (cm)	Ba	Ce	Co	Cr	Cs	Dy	Eu	Fe	Gd	Hf	K	La	Lu	Mn	
Modesto Formation, lower member, 40 Ka																	
64	M12	A11	85	--	--	--	--	--	--	--	--	--	--	--	--	--	
65	M12	A12	81	821	69.0	10.6	73.8	4.17	4.38	1.24	3.23	5.39	11.7	2.07	35.1	0.374	673
66	M12	2B21t	102	--	--	--	--	--	--	--	--	--	--	--	--	--	
67	M12	3B22t	170	741	89.9	14.7	84.5	4.85	5.52	1.36	4.70	--	8.20	1.50	49.0	0.372	671
68	M12	4B3	201	--	--	--	--	--	--	--	--	--	--	--	--	--	
69	M12	5C1	231	681	74.3	11.5	58.6	3.72	4.98	1.12	3.57	--	11.9	1.69	36.1	0.345	617
70	M12	6C2	413+	1680	129	31.1	47.0	9.43	5.83	1.24	5.80	0.00	8.54	2.17	61.2	0.420	1930
Riverbank Formation, upper member, 130 Ka																	
71	R9	A11p	30	928	69.1	13.2	86.3	4.00	4.51	1.28	3.00	5.06	9.69	2.08	35.5	0.390	888
72	R9	A12p	60	--	--	--	--	--	--	--	--	--	--	--	--	--	
73	R9	B1	105	--	--	--	--	--	--	--	--	--	--	--	--	--	
74	R9	2B21	180	--	--	--	--	--	--	--	--	--	--	--	--	--	
75	R9	2B22	235	660	85.3	15.0	88.6	4.90	4.37	1.38	4.19	5.31	6.25	1.54	43.7	0.349	823
76	R9	3B3	350	--	--	--	--	--	--	--	--	--	--	--	--	--	
77	R9	4C	400+	971	110	15.1	46.6	6.38	6.26	1.65	4.70	--	10.0	1.84	52.3	0.466	659
78	R33	A11	4	1070	73.4	13.6	81.7	5.21	3.95	1.29	3.66	4.95	9.49	2.12	38.6	0.437	1110
79	R33	2A12	19	--	--	--	--	--	--	--	--	--	--	--	--	--	
80	R33	3A3	39	--	--	--	--	--	--	--	--	--	--	--	--	--	
81	R33	3B21t	62	--	--	--	--	--	--	--	--	--	--	--	--	--	
82	R33	3B22t	83	--	--	--	--	--	--	--	--	--	--	--	--	--	
83	R33	3B23t	122	618	83.0	13.6	67.8	5.43	4.59	1.50	4.57	5.51	5.06	1.68	47.8	0.316	813
84	R33	3B31	151	--	--	--	--	--	--	--	--	--	--	--	--	--	
85	R33	3B32	210	--	--	--	--	--	--	--	--	--	--	--	--	--	
86	R33	4B33	260	--	--	--	--	--	--	--	--	--	--	--	--	--	
87	R33	5Cox	300+	665	167	14.0	55.2	6.31	5.50	1.54	6.07	8.18	2.60	1.24	85.0	0.352	758
Riverbank Formation, middle member, 250 Ka																	
88	R2	Ap	25	827	64.2	10.3	77.0	3.10	4.23	1.24	2.80	5.32	15.6	1.99	31.9	0.409	716
89	R2	B21	81	--	--	--	--	--	--	--	--	--	--	--	--	--	
90	R2	B22t	185	746	80.5	15.6	97.1	5.46	5.15	1.37	4.31	6.38	6.80	1.90	42.2	0.357	880
91	R2	B3	386	--	--	--	--	--	--	--	--	--	--	--	--	--	
92	R2	C1	500	--	--	--	--	--	--	--	--	--	--	--	--	--	
93	R2	C2n	500+	--	--	--	--	--	--	--	--	--	--	--	--	--	
94	R10	A	46	812	64.9	9.73	68.4	4.58	4.31	1.16	3.15	5.37	6.98	2.34	33.2	0.344	786
95	R10	2B1	70	--	--	--	--	--	--	--	--	--	--	--	--	--	
96	R10	2B21t	140	691	82.7	12.9	87.7	6.11	4.24	1.43	4.69	6.82	6.15	1.77	50.3	0.427	680
97	R10	2B22t	210	--	--	--	--	--	--	--	--	--	--	--	--	--	
98	R10	3B3t	386	590	107	13.1	57.0	6.21	4.32	1.27	4.87	6.25	4.38	1.54	62.6	0.362	689
99	R10	3Cox	500	--	--	--	--	--	--	--	--	--	--	--	--	--	
100	R32	A11	26	843	63.7	10.1	65.8	4.33	4.01	1.09	3.04	4.81	7.88	2.20	34.3	0.359	831
101	R32	A12	50	--	--	--	--	--	--	--	--	--	--	--	--	--	
102	R32	A3	70	--	--	--	--	--	--	--	--	--	--	--	--	--	
103	R32	B21t	105	--	--	--	--	--	--	--	--	--	--	--	--	--	
104	R32	B22t	150	649	77.6	12.4	71.5	4.94	4.36	1.27	4.11	4.73	6.32	2.07	42.2	0.322	809
105	R32	B31t	220	--	--	--	--	--	--	--	--	--	--	--	--	--	
106	R32	2B32	354	--	--	--	--	--	--	--	--	--	--	--	--	--	
107	R32	3Cox	360+	624	149	18.3	61.9	7.16	4.79	1.34	6.37	5.90	3.99	1.74	76.1	0.372	845
Riverbank Formation, lower member, 330 Ka																	
108	R30	Ap	65	863	77.0	11.7	72.1	5.80	4.51	1.33	3.74	5.33	8.58	2.52	40.0	0.375	667
109	R30	B10	78	--	--	--	--	--	--	--	--	--	--	--	--	--	
110	R30	B21t	127	503	95.1	14.5	59.4	5.72	3.82	1.19	4.51	5.03	4.65	1.56	43.5	0.291	725
111	R30	2B22t	179	--	--	--	--	--	--	--	--	--	--	--	--	--	
112	R30	3B3t	197	--	--	--	--	--	--	--	--	--	--	--	--	--	
113	R30	3C1ox	220	404	112	12.4	56.8	6.09	6.10	1.46	6.26	7.58	2.34	1.08	73.5	0.479	534

Supplementary Table 7, Part 1. Total chemical analyses of the fine (less than 47 μm) fraction by instrumental neutron activation--Continued

No. Sample	Horizon	Basal depth (cm)	Ba	Ce	Co	Cr	Cs	Dy	Eu	Fe	Gd	Hf	K	La	Lu	Mn	
Turlock Lake Formation, 600 Ka																	
114	T2	A	31	1080	77.2	18.4	114	4.28	4.45	1.09	3.00	5.52	13.1	2.72	33.0	0.447	1070
115	T2	B21	173	--	--	--	--	--	--	--	--	--	--	--	--	--	--
116	T2	2B22	386	697	124	13.2	60.2	3.33	6.92	1.73	4.11	--	12.6	1.57	52.6	0.571	363
117	T2	3C	417	667	114	12.6	74.5	4.58	7.69	2.17	4.26	--	10.9	1.80	57.5	0.556	416
118	T6	A11	20	1020	110	19.7	74.8	5.15	5.63	1.63	4.62	7.58	10.2	2.33	57.1	0.521	975
119	T6	A12	40	--	--	--	--	--	--	--	--	--	--	--	--	--	--
120	T6	2B21t	90	--	--	--	--	--	--	--	--	--	--	--	--	--	--
121	T6	2B22t	190	474	76.9	12.5	66.6	6.28	5.57	1.40	6.17	6.46	2.87	1.45	55.9	0.380	569
122	T6	3B+C	370	707	193	30.1	56.2	6.04	6.77	2.09	7.07	10.5	6.36	1.43	90.2	0.642	2230
123	T11	A11p	5	--	--	--	--	--	--	--	--	--	--	--	--	--	--
124	T11	2A12p	11	964	78.1	16.1	70.6	5.13	4.01	1.14	3.32	4.64	10.4	2.52	38.0	0.387	641
125	T11	2A+B	20	--	--	--	--	--	--	--	--	--	--	--	--	--	--
126	T11	2B1t	33	625	65.5	12.9	67.5	6.04	2.97	0.904	4.52	4.31	6.81	1.70	30.2	0.288	368
127	T11	2B2t	80	--	--	--	--	--	--	--	--	--	--	--	--	--	--
128	T11	3B31t	191	--	--	--	--	--	--	--	--	--	--	--	--	--	--
129	T11	4B32t	256	--	--	--	--	--	--	--	--	--	--	--	--	--	--
130	T11	5B+C	292	--	--	--	--	--	--	--	--	--	--	--	--	--	--
131	T11	5C1ox	375	--	--	--	--	--	--	--	--	--	--	--	--	--	--
132	T11	6C2ox	375+	333	152	12.8	68.2	5.86	6.69	1.62	6.90	9.80	2.61	1.09	91.0	0.529	360
China Hat gravel member of Laguna Formation, 3,000 Ka																	
133	CH1	A1	12	828	58.3	8.04	114	4.08	4.45	1.03	2.77	6.05	13.2	1.75	28.3	0.469	401
134	CH1	2A8	53	--	--	--	--	--	--	--	--	--	--	--	--	--	--
135	CH1	2B21t	88	644	76.1	15.8	111	4.43	3.47	1.00	4.28	--	8.85	1.30	31.1	0.408	597
136	CH1	2B22t	140	--	--	--	--	--	--	--	--	--	--	--	--	--	--
137	CH1	2B31	234	--	--	--	--	--	--	--	--	--	--	--	--	--	--
138	CH1	2B32	310	--	--	--	--	--	--	--	--	--	--	--	--	--	--
139	CH1	3B33	350	749	32	8.19	122	2.77	2.86	0.735	6.71	--	3.88	1.10	21.1	0.364	168
140	CH2	A1	8	755	44.5	6.99	103	4.66	3.40	0.637	3.24	3.37	9.54	1.86	23.8	0.330	449
141	CH2	A3	30	--	--	--	--	--	--	--	--	--	--	--	--	--	--
142	CH2	2A+B	50	--	--	--	--	--	--	--	--	--	--	--	--	--	--
143	CH2	2B21t	110	--	--	--	--	--	--	--	--	--	--	--	--	--	--
144	CH2	2B22	170	--	--	--	--	--	--	--	--	--	--	--	--	--	--
145	CH2	2B23	200	540	26.1	5.25	77.8	2.88	2.56	0.506	5.40	2.40	4.03	0.560	17.4	0.272	192
146	CH2	3B24	290	--	--	--	--	--	--	--	--	--	--	--	--	--	--
147	CH2	3B3	350	383	37.8	8.80	84.2	2.58	3.90	0.962	6.51	4.58	2.52	0.50	26.1	0.295	215
148	CH3	A1	9	926	48.6	9.27	99.1	4.86	3.72	0.756	2.98	3.71	8.72	1.80	27.3	0.337	776
149	CH3	A3	35	--	--	--	--	--	--	--	--	--	--	--	--	--	--
150	CH3	A+B	68	--	--	--	--	--	--	--	--	--	--	--	--	--	--
151	CH3	B2t	105	--	--	--	--	--	--	--	--	--	--	--	--	--	--
152	CH3	B22t	153	--	--	--	--	--	--	--	--	--	--	--	--	--	--
153	CH3	2B23	173	339	25.8	6.25	90.0	4.46	2.24	0.514	5.47	0.00	3.09	0.523	17.9	0.236	152
154	CH3	3B24	260	--	--	--	--	--	--	--	--	--	--	--	--	--	--
155	CH3	4B31	340	--	--	--	--	--	--	--	--	--	--	--	--	--	--
156	CH3	5B32	750+	522	58.9	9.67	101	2.63	4.22	1.31	6.27	5.3	2.49	0.530	33.9	0.341	187
157	CH4	2B31	750	656	--	8.61	70.9	3.48	5.02	1.41	5.32	5.95	3.31	1.12	32.1	10.422	170
158	CH4	4C1ox	1000	641	114	10.9	57.2	4.23	7.84	2.31	4.64	8.43	3.42	0.987	39.4	0.671	163

Supplementary Table 7, Part 2. Total chemical analyses of the fine (less than 47 μm) fraction by instrumental neutron activation

[Na values in weight percent; all others in parts per million. Analysts: J. Budahn, R. Knight, and D. McKown]

No.	Sample	Horizon	Basal depth (cm)	Na	Nd	Rb	Sb	Sc	Sm	Sr	Ta	Tb	Th	Tm	U	Yb	Zr
Modern River Alluvium																	
1	MRA1	--	--	1.24	29.2	81.1	1.07	18.0	5.63	168	0.947	0.760	15.5	0.520	12.8	2.99	582
2	MRA2	--	--	1.18	26.1	76.8	1.01	17.9	5.37	178	0.830	0.745	12.4	0.430	10.6	2.57	225
3	MRA3	--	--	1.60	29.4	81.5	1.04	16.5	5.48	206	0.813	0.692	13.4	0.390	16.4	2.48	230
4	MRA4	--	--	0.981	38.2	58.9	0.931	15.3	6.45	160	0.881	0.730	16.4	0.400	7.35	2.33	194
Post-Modesto Deposits, .2 Ka																	
5	PM15	A1	4	1.15	27.1	69.8	0.915	17.5	5.49	195	0.970	0.735	13.6	0.460	8.82	2.83	479
6	PM15	2C1ox	19	1.18	28.6	79.3	1.11	19.1	5.89	190	1.01	0.768	14.2	--	9.56	3.01	418
7	PM15	3C2ox	42	--	--	--	--	--	--	--	--	--	--	--	--	--	--
8	PM15	4C3ox	47	--	--	--	--	--	--	--	--	--	--	--	--	--	--
9	PM15	5C4ox	51	--	--	--	--	--	--	--	--	--	--	--	--	--	--
10	PM15	6C5ox	51+	1.10	27.2	79.3	1.08	18.8	5.91	189	0.989	0.799	14.5	--	11.1	3.02	420
11	PM19	A11	7	--	--	--	--	--	--	--	--	--	--	--	--	--	--
12	PM19	2A12	12	1.10	21.7	116	0.926	17.8	4.76	152	0.873	0.616	11.4	--	6.39	2.39	222
13	PM19	3C1ox	23	--	--	--	--	--	--	--	--	--	--	--	--	--	--
14	PM19	4C2ox	43	1.22	23.3	77.8	1.14	17.9	5.02	182	0.868	0.686	10.5	--	5.66	2.48	254
15	PM19	5C3ox	49	--	--	--	--	--	--	--	--	--	--	--	--	--	--
16	PM19	6C4n	55	--	--	--	--	--	--	--	--	--	--	--	--	--	--
17	PM19	7C5n	66	--	--	--	--	--	--	--	--	--	--	--	--	--	--
18	PM19	8C6n	80+	1.18	24.5	75.5	1.01	17.9	5.02	167	0.847	0.707	10.9	0.420	6.47	2.55	165
Post-Modesto Deposits, 3 Ka																	
19	PM8	A1	32	1.24	28.5	90.6	1.04	17.2	4.66	224	0.825	0.776	12.8	0.487	6.34	2.41	174
20	PM8	2C1	55	1.22	27.7	73.8	0.939	15.1	4.93	223	0.880	0.788	12.8	0.409	6.91	2.58	206
21	PM8	3C2	86	--	--	--	--	--	--	--	--	--	--	--	--	--	--
22	PM8	4C3	76+	1.19	29.9	71.0	1.01	15.6	4.97	264	1.03	0.815	15.3	0.441	11.1	2.49	518
23	PM13	A11	5	--	--	--	--	--	--	--	--	--	--	--	--	--	--
24	PM13	A12	35	--	--	--	--	--	--	--	--	--	--	--	--	--	--
25	PM13	2C1ox	86	--	--	--	--	--	--	--	--	--	--	--	--	--	--
26	PM13	3C2ox	112	--	--	--	--	--	--	--	--	--	--	--	--	--	--
27	PM13	4C3ox	136	--	--	--	--	--	--	--	--	--	--	--	--	--	--
28	PM13	5C4ox	200	--	--	--	--	--	--	--	--	--	--	--	--	--	--
29	PM13	6C5n	720	--	--	--	--	--	--	--	--	--	--	--	--	--	--
30	PM14	A11	3	--	--	--	--	--	--	--	--	--	--	--	--	--	--
31	PM14	2A12	33	1.08	26.1	92.3	0.986	18.4	5.04	180	0.822	0.658	11.3	--	5.60	2.43	165
32	PM14	3C1ox	99	1.19	29.9	82.5	0.939	19.0	5.36	173	1.00	0.765	13.3	--	11.0	2.64	290
33	PM14	4C2ox	130	--	--	--	--	--	--	--	--	--	--	--	--	--	--
34	PM14	5C3ox	175	--	--	--	--	--	--	--	--	--	--	--	--	--	--
35	PM14	6C4ox	200	1.22	34.1	83.2	1.02	19.5	5.40	190	0.986	0.814	15.3	0.440	12.1	2.82	359
36	PM14	7C5n	230+	--	--	--	--	--	--	--	--	--	--	--	--	--	--
37	PM16	A	2	--	--	--	--	--	--	--	--	--	--	--	--	--	--
38	PM16	C1ox	25	--	--	--	--	--	--	--	--	--	--	--	--	--	--
39	PM16	2C2ox	35	--	--	--	--	--	--	--	--	--	--	--	--	--	--
40	PM16	3C3ox	65	--	--	--	--	--	--	--	--	--	--	--	--	--	--
41	PM16	4C4ox	90	--	--	--	--	--	--	--	--	--	--	--	--	--	--
42	PM16	5C5ox	116	--	--	--	--	--	--	--	--	--	--	--	--	--	--
43	PM16	5C6n	236	--	--	--	--	--	--	--	--	--	--	--	--	--	--
44	PM17	A	6	--	--	--	--	--	--	--	--	--	--	--	--	--	--
45	PM17	2C2ox	45	--	--	--	--	--	--	--	--	--	--	--	--	--	--
46	PM17	2C2ox	63	--	--	--	--	--	--	--	--	--	--	--	--	--	--
47	PM17	2C3ox	74	--	--	--	--	--	--	--	--	--	--	--	--	--	--
48	PM17	3C4n	120+	--	--	--	--	--	--	--	--	--	--	--	--	--	--
49	PM18	A	6	0.872	23.0	95.7	1.06	16.6	4.40	178	0.816	0.568	9.15	0.36	6.10	2.20	226
50	PM18	2C1ox	65	1.03	27.7	75.6	1.05	19.3	5.56	152	0.901	0.834	10.9	0.41	6.25	2.77	287
51	PM18	2C2ox	115	--	--	--	--	--	--	--	--	--	--	--	--	--	--
52	PM18	3C3ox	164	--	--	--	--	--	--	--	--	--	--	--	--	--	--
53	PM18	4C4ox	175+	1.05	28.3	87.5	1.09	21.8	5.63	146	0.976	0.848	11.5	0.470	6.66	2.78	292

Supplementary Table 7, Part 2. Total chemical analyses of the fine (less than 47 μm) fraction by instrumental neutron activation--Continued

No.	Sample	Horizon	Basal depth (cm)	Na	Nd	Rb	Sb	Sc	Sm	Sr	Ta	Tb	Th	Tm	U	Yb	Zr
Modesto Formation, upper member, 10 Ka																	
54	M31	A11	20	1.12	26.0	96.5	0.917	18.3	5.19	202	0.915	0.679	11.1	0.390	5.24	2.47	174
55	M31	A12	63	--	--	--	--	--	--	--	--	--	--	--	--	--	--
56	M31	AC	150	--	--	--	--	--	--	--	--	--	--	--	--	--	--
57	M31	2C1	200	1.59	26.4	87.5	0.854	17.2	4.67	158	0.864	0.672	11.4	0.35	3.77	2.22	200
58	M31	3C2	254	1.49	24.2	99.1	0.900	17.0	4.75	180	1.02	--	12.5	0.370	4.51	2.27	277
59	M46	A11p	5	--	--	--	--	--	--	--	--	--	--	--	--	--	235
60	M46	A12p	14	1.34	33.3	118	1.38	21.0	6.15	223	1.14	0.828	17.5	0.500	7.80	3.03	287
61	M46	2A13p	32	--	--	--	--	--	--	--	--	--	--	--	--	--	259
62	M46	3AC	66	1.48	24.7	109	1.01	14.4	4.86	204	1.01	0.653	15.5	0.360	5.98	2.25	222
63	M46	4Cox	250	1.49	26.0	95.0	0.989	14.2	4.62	207	1.01	0.646	15.5	0.360	5.36	2.17	219
Modesto Formation, upper member, 40 Ka																	
64	M12	A11	85	--	--	--	--	--	--	--	--	--	--	--	--	--	160
65	M12	A12	81	2.07	29.3	106	1.01	11.3	5.05	332	1.17	0.669	17.3	0.351	6.42	2.50	308
66	M12	2B21t	102	--	--	--	--	--	--	--	--	--	--	--	--	--	--
67	M12	3B22t	170	1.40	35.8	86.6	0.867	14.7	5.77	212	0.938	0.741	22.8	0.405	6.57	2.55	205
68	M12	4B3	201	--	--	--	--	--	--	--	--	--	--	--	--	--	--
69	M12	5C1	231	1.84	27.2	78.4	0.703	11.5	5.05	293	1.01	0.661	20.1	0.331	6.46	2.27	312
70	M12	6C2	413+	1.54	41.9	142	1.07	13.5	7.81	278	1.14	0.867	51.6	0.450	9.77	2.75	318
Riverbank Formation, upper member, 130 Ka																	
71	R9	A11p	30	1.85	28.0	115	1.00	10.9	5.21	279	1.08	0.691	13.4	0.349	5.08	2.41	267
72	R9	A12p	60	--	--	--	--	--	--	--	--	--	--	--	--	--	256
73	R9	B1	105	--	--	--	--	--	--	--	--	--	--	--	--	--	248
74	R9	2B21	180	--	--	--	--	--	--	--	--	--	--	--	--	--	196
75	R9	2B22	235	1.15	34.8	103	1.02	14.3	5.95	182	1.01	0.673	17.5	0.370	5.44	2.27	159
76	R9	3B3	350	--	--	--	--	--	--	--	--	--	--	--	--	--	158
77	R9	4C	400+	1.40	40.6	89.5	1.10	14.9	7.52	253	1.22	0.873	32.5	0.491	6.69	3.18	271
78	R33	A11	4	1.66	30.3	131	1.15	12.7	5.62	274	1.25	0.679	15.1	0.460	5.38	2.69	310
79	R33	2A12	19	--	--	--	--	--	--	--	--	--	--	--	--	--	--
80	R33	3A3	39	--	--	--	--	--	--	--	--	--	--	--	--	--	--
81	R33	3B21t	62	--	--	--	--	--	--	--	--	--	--	--	--	--	--
82	R33	3B22t	83	--	--	--	--	--	--	--	--	--	--	--	--	--	--
83	R33	3B23t	122	0.937	40.5	97.1	0.968	15.1	6.76	143	1.00	0.709	18.0	0.330	5.77	2.23	170
84	R33	3B31	151	--	--	--	--	--	--	--	--	--	--	--	--	--	--
85	R33	3B32	210	--	--	--	--	--	--	--	--	--	--	--	--	--	--
86	R33	4B33	260	--	--	--	--	--	--	--	--	--	--	--	--	--	--
87	R33	5Cox	300+	0.320	55.1	88.0	0.892	17.5	8.98	110	0.843	0.924	38.7	0.410	11.9	2.63	51
Riverbank Formation, middle member, 250 Ka																	
88	R2	Ap	25	2.16	26.2	103	1.14	9.11	4.92	340	1.21	0.610	16.0	--	5.28	2.46	425
89	R2	B21	81	--	--	--	--	--	--	--	--	--	--	--	--	--	308
90	R2	B22t	185	1.22	29.8	107	1.12	14.1	5.63	156	1.09	0.727	18.8	0.401	6.45	2.40	157
91	R2	B3	386	--	--	--	--	--	--	--	--	--	--	--	--	--	195
92	R2	C1	500	--	--	--	--	--	--	--	--	--	--	--	--	--	177
93	R2	C2n	500+	--	--	--	--	--	--	--	--	--	--	--	--	--	--
94	R10	A	46	1.86	30.6	121	1.04	10.7	5.02	242	1.13	0.649	14.5	0.370	5.17	2.18	221
95	R10	2B10	70	--	--	--	--	--	--	--	--	--	--	--	--	--	293
96	R10	2B21t	140	1.17	38.0	105	1.04	16.0	6.66	169	1.16	0.762	19.2	--	6.10	2.67	223
97	R10	2B22t	210	--	--	--	--	--	--	--	--	--	--	--	--	--	220
98	R10	3B3t	386	1.17	38.7	102	0.974	15.3	6.59	176	0.964	0.716	25.6	0.360	6.52	2.28	143
99	R10	3Cox	500	--	--	--	--	--	--	--	--	--	--	--	--	--	--
100	R32	A11	26	1.86	26.1	107	1.03	10.7	4.93	265	1.09	0.626	14.0	0.350	5.00	2.26	274
101	R32	A12	50	--	--	--	--	--	--	--	--	--	--	--	--	--	--
102	R32	A3	70	--	--	--	--	--	--	--	--	--	--	--	--	--	--
103	R32	B21t	105	--	--	--	--	--	--	--	--	--	--	--	--	--	--
104	R32	B22t	150	1.37	35.6	98.4	1.01	13.6	5.84	188	1.03	0.736	18.9	0.390	5.82	2.20	238
105	R32	B31t	220	--	--	--	--	--	--	--	--	--	--	--	--	--	--
106	R32	2B32	354	--	--	--	--	--	--	--	--	--	--	--	--	--	--
107	R32	3Cox	360+	0.532	49.1	114	0.891	18.3	7.76	118	1.03	0.882	36.6	0.430	10.1	2.52	112

Supplementary Table 7, Part 2. Total chemical analyses of the fine (less than 47 μm) fraction by instrumental neutron activation--Continued

No.	Sample	Horizon	Basal depth (cm)	Na	Nd	Rb	Sb	Sc	Sm	Sr	Ta	Tb	Th	Tm	U	Yb	Zr
Riverbank Formation, lower member, 330 Ka																	
108	R30	Ap	65	1.78	35.0	134	1.13	11.8	5.93	246	1.41	0.811	18.8	0.360	6.34	2.55	278
109	R30	B10	78	--	--	--	--	--	--	--	--	--	--	--	--	--	--
110	R30	B21t	127	1.03	36.1	87.4	0.980	14.8	6.23	144	1.30	0.618	23.5	--	6.05	2.00	157
111	R30	2B22t	179	--	--	--	--	--	--	--	--	--	--	--	--	--	--
112	R30	3B3t	197	--	--	--	--	--	--	--	--	--	--	--	--	--	--
113	R30	3C1ox	220	0.261	47.3	75.5	1.02	18.8	8.29	100	1.02	0.995	32.8	0.500	6.98	2.94	110
Turlock Lake Formation, 600 Ka																	
114	T2	A	31	1.05	29.5	129.	0.959	9.36	4.79	169	1.37	0.703	15.8	0.353	5.25	2.45	414
115	T2	B21	173	--	--	--	--	--	--	--	--	--	--	--	--	--	--
116	T2	2B22	386	1.63	45.0	74.1	1.03	15.0	8.21	254	1.58	1.08	26.1	0.563	6.05	3.79	362
117	T2	3C	417	1.30	57.1	96.2	1.19	12.6	9.92	210	1.17	1.30	26.2	0.487	5.64	3.34	334
118	T6	A11	20	1.78	43.0	126	0.93	14.4	7.43	301	1.37	0.925	20.0	0.510	5.54	3.33	355
119	T6	A12	40	--	--	--	--	--	--	--	--	--	--	--	--	--	298
120	T6	2B21t	90	--	--	--	--	--	--	--	--	--	--	--	--	--	111
121	T6	2B22t	190	0.233	42.2	104	0.940	21.0	7.42	100	1.13	0.822	27.1	0.470	5.45	2.64	110
122	T6	3B+C	370	0.826	64.5	113	1.06	24.1	10.4	199	1.24	1.22	41.6	0.630	8.64	4.21	249
123	T11	A11p	5	--	--	--	--	--	--	--	--	--	--	--	--	--	--
124	T11	2A12p	11	1.60	25.7	131	1.14	9.70	5.19	246	1.31	0.628	17.4	0.420	5.12	2.44	360
125	T11	2A+B	20	--	--	--	--	--	--	--	--	--	--	--	--	--	--
126	T11	2B1t	33	0.786	25.4	96.8	1.23	13.8	4.58	115	1.31	0.495	20.8	0.271	5.30	1.89	235
127	T11	2B2t	80	--	--	--	--	--	--	--	--	--	--	--	--	--	--
128	T11	3B31t	191	--	--	--	--	--	--	--	--	--	--	--	--	--	--
129	T11	4B32t	256	--	--	--	--	--	--	--	--	--	--	--	--	--	--
130	T11	5B+C	292	--	--	--	--	--	--	--	--	--	--	--	--	--	--
131	T11	5C1ox	375	--	--	--	--	--	--	--	--	--	--	--	--	--	--
132	T11	6C2ox	375+	0.216	61.8	79.4	0.881	21.9	10.1	103	1.20	1.07	36.0	0.483	6.47	3.22	110
China Hat gravel member of Laguna Formation, 3,000 Ka																	
133	CH1	A1	12	0.702	25.7	98.5	0.942	9.46	4.38	97.9	1.01	0.718	13.5	0.396	5.22	2.54	412
134	CH1	2AB	53	--	--	--	--	--	--	--	--	--	--	--	--	--	--
135	CH1	2B21t	88	0.524	29.0	73.0	1.16	13.7	4.17	79.1	1.16	0.665	15.8	0.410	5.48	2.33	270
136	CH1	2B22t	140	--	--	--	--	--	--	--	--	--	--	--	--	--	--
137	CH1	2B31	234	--	--	--	--	--	--	--	--	--	--	--	--	--	--
138	CH1	2B32	310	--	--	--	--	--	--	--	--	--	--	--	--	--	--
139	CH1	3B33	350	0.0733	15.9	53.0	1.46	24.6	2.89	45	0.608	0.571	14.0	0.345	6.36	2.10	174
140	CH2	A1	8	0.373	18.9	99.8	0.937	10.3	3.55	100	1.11	0.480	11.8	0.340	4.73	2.03	293
141	CH2	A3	30	--	--	--	--	--	--	--	--	--	--	--	--	--	380
142	CH2	2A+B	50	--	--	--	--	--	--	--	--	--	--	--	--	--	348
143	CH2	2B21t	110	--	--	--	--	--	--	--	--	--	--	--	--	--	254
144	CH2	2B22	170	--	--	--	--	--	--	--	--	--	--	--	--	--	193
145	CH2	2B23	200	0.0335	11.8	35.1	1.06	21.2	2.44	100	0.901	0.454	8.97	0.270	3.13	1.65	127
146	CH2	3B24	290	--	--	--	--	--	--	--	--	--	--	--	--	--	142
147	CH2	3B3	350	0.0580	24.7	33.9	1.34	27.9	5.13	0.00	0.693	0.603	11.9	0.000	3.76	1.85	100
148	CH3	A1	9	0.447	20.9	98.3	0.907	11.1	4.23	100	1.14	0.535	12.5	0.360	4.78	2.22	269
149	CH3	A3	35	--	--	--	--	--	--	--	--	--	--	--	--	--	--
150	CH3	A+B	68	--	--	--	--	--	--	--	--	--	--	--	--	--	--
151	CH3	B2t	105	--	--	--	--	--	--	--	--	--	--	--	--	--	--
152	CH3	B22t	153	--	--	--	--	--	--	--	--	--	--	--	--	--	--
153	CH3	2B23	173	0.0333	14.5	34.9	1.06	19.2	2.59	0.00	1.06	0.313	10.9	0.200	4.29	1.35	77.9
154	CH3	3B24	260	--	--	--	--	--	--	--	--	--	--	--	--	--	--
155	CH3	4B31	340	--	--	--	--	--	--	--	--	--	--	--	--	--	--
156	CH3	5B32	750+	0.0557	38.5	31.7	1.25	25.9	7.29	0.00	0.609	0.705	9.78	0.334	5.58	2.22	140
157	CH4	2B31	750	0.106	31.8	56.5	1.27	29.4	6.67	100	0.778	0.872	12.1	0.51	6.84	2.74	107
158	CH4	4C1ox	1000	0.153	42.9	55.1	1.13	29.2	9.68	100	1.09	1.32	17.4	0.81	7.19	4.40	191

Supplementary Table 8, Part 1. Total chemical analyses of the less-than-2-mm fraction by instrumental neutron activation

[Na values in weight percent; all others in parts per million. Analysts: J. Baker, A. Bartel, D. Burgi, R. Johnson, R. Knight, H.T. Millard, V.G. Mossotti, S. Ramage, B. Scott, J. Taggart, J.S. Wahlberg, and K. Wong]

No.	Sample	Horizon	Basal depth (cm)	Ba	Ce	Co	Cr	Cs	Dy	Eu	Fe	Gd	Hf	K	La	Lu	Mn
Modern River Alluvium																	
1	MRA1	--	--	--	--	--	--	--	--	--	--	--	--	--	--	--	--
2	MRA2	--	--	--	--	--	--	--	--	--	--	--	--	--	--	--	--
3	MRA3	--	--	--	--	--	--	--	--	--	--	--	--	--	--	--	--
4	MRA4	--	--	--	--	--	--	--	--	--	--	--	--	--	--	--	--
Post-Modesto Deposits, .2 Ka																	
5	PM15	A1	4	--	--	--	--	--	--	--	--	--	--	--	--	--	--
6	PM15	2C1ox	19	--	--	--	--	--	--	--	--	--	--	--	--	--	--
7	PM15	3C2ox	42	--	--	--	--	--	--	--	--	--	--	--	--	--	--
8	PM15	4C3ox	47	--	--	--	--	--	--	--	--	--	--	--	--	--	--
9	PM15	5C4ox	51	--	--	--	--	--	--	--	--	--	--	--	--	--	--
10	PM15	6C5ox	51+	--	--	--	--	--	--	--	--	--	--	--	--	--	--
11	PM19	A11	7	--	--	--	--	--	--	--	--	--	--	--	--	--	--
12	PM19	2A12	12	--	--	--	--	--	--	--	--	--	--	--	--	--	--
13	PM19	3C1ox	23	--	--	--	--	--	--	--	--	--	--	--	--	--	--
14	PM19	4C2ox	43	--	--	--	--	--	--	--	--	--	--	--	--	--	--
15	PM19	5C3ox	49	--	--	--	--	--	--	--	--	--	--	--	--	--	--
16	PM19	6C4n	55	--	--	--	--	--	--	--	--	--	--	--	--	--	--
17	PM19	7C5n	66	--	--	--	--	--	--	--	--	--	--	--	--	--	--
18	PM19	8C6n	80+	--	--	--	--	--	--	--	--	--	--	--	--	--	--
Post-Modesto Deposits, 3 Ka																	
19	PM8	A1	32	899	49.4	17.9	110	4.02	4.32	1.12	4.12	5.78	5.82	1.77	25.7	0.328	875
20	PM8	2C1	55	932	51.6	16.4	114	3.80	4.23	1.11	3.91	4.56	6.76	1.53	26.2	0.349	766
21	PM8	3C2	66	--	--	--	--	--	--	--	--	--	--	--	--	--	--
22	PM8	4C3	76+	839	32.7	9.40	58.8	2.70	2.32	0.770	2.34	--	3.12	2.01	17.4	0.184	480
23	PM13	A11	5	--	--	--	--	--	--	--	--	--	--	--	--	--	--
24	PM13	A12	35	--	--	--	--	--	--	--	--	--	--	--	--	--	--
25	PM13	2C1ox	86	--	--	--	--	--	--	--	--	--	--	--	--	--	--
26	PM13	3C2ox	112	--	--	--	--	--	--	--	--	--	--	--	--	--	--
27	PM13	4C3ox	136	--	--	--	--	--	--	--	--	--	--	--	--	--	--
28	PM13	5C4ox	200	--	--	--	--	--	--	--	--	--	--	--	--	--	--
29	PM13	6C5n	720	--	--	--	--	--	--	--	--	--	--	--	--	--	--
30	PM14	A11	3	--	--	--	--	--	--	--	--	--	--	--	--	--	--
31	PM14	2A12	33	--	--	--	--	--	--	--	--	--	--	--	--	--	--
32	PM14	3C1ox	99	--	--	--	--	--	--	--	--	--	--	--	--	--	--
33	PM14	4C2ox	130	--	--	--	--	--	--	--	--	--	--	--	--	--	--
34	PM14	5C3ox	175	--	--	--	--	--	--	--	--	--	--	--	--	--	--
35	PM14	6C4ox	200	--	--	--	--	--	--	--	--	--	--	--	--	--	--
36	PM14	7C5n	239+	--	--	--	--	--	--	--	--	--	--	--	--	--	--
37	PM16	A	2	--	--	--	--	--	--	--	--	--	--	--	--	--	--
38	PM16	C1ox	25	--	--	--	--	--	--	--	--	--	--	--	--	--	--
39	PM16	2C2ox	35	--	--	--	--	--	--	--	--	--	--	--	--	--	--
40	PM16	3C3ox	65	--	--	--	--	--	--	--	--	--	--	--	--	--	--
41	PM16	4C4ox	90	--	--	--	--	--	--	--	--	--	--	--	--	--	--
42	PM16	5C5ox	116	--	--	--	--	--	--	--	--	--	--	--	--	--	--
43	PM16	5C6n	236	--	--	--	--	--	--	--	--	--	--	--	--	--	--
44	PM17	A	6	--	--	--	--	--	--	--	--	--	--	--	--	--	--
45	PM17	2C2ox	45	--	--	--	--	--	--	--	--	--	--	--	--	--	--
46	PM17	2C2ox	63	--	--	--	--	--	--	--	--	--	--	--	--	--	--
47	PM17	2C3ox	74	--	--	--	--	--	--	--	--	--	--	--	--	--	--
48	PM17	3C4n	120+	--	--	--	--	--	--	--	--	--	--	--	--	--	--
49	PM18	A	6	--	--	--	--	--	--	--	--	--	--	--	--	--	--
50	PM18	2C1ox	65	--	--	--	--	--	--	--	--	--	--	--	--	--	--
51	PM18	2C2ox	115	--	--	--	--	--	--	--	--	--	--	--	--	--	--
52	PM18	3C3ox	164	--	--	--	--	--	--	--	--	--	--	--	--	--	--
53	PM18	4C4ox	175+	--	--	--	--	--	--	--	--	--	--	--	--	--	--

Supplementary Table 8, Part 1. Total chemical analyses of the less-than-2-mm fraction by instrumental neutron activation--Continued

No.	Sample	Horizon	Basal depth (cm)	Ba	Ce	Co	Cr	Cs	Dy	Eu	Fe	Gd	Hf	K	La	Lu	Mn
Modesto Formation, upper member, 10 Ka																	
54	M31	A11	20	--	--	--	--	--	--	--	--	--	--	--	--	--	--
55	M31	A12	63	--	--	--	--	--	--	--	--	--	--	--	--	--	--
56	M31	AC	150	--	--	--	--	--	--	--	--	--	--	--	--	--	--
57	M31	2C1	200	--	--	--	--	--	--	--	--	--	--	--	--	--	--
58	M31	3C2	254	--	--	--	--	--	--	--	--	--	--	--	--	--	--
59	M46	A11p	5	--	--	--	--	--	--	--	--	--	--	--	--	--	--
60	M46	A12p	14	--	--	--	--	--	--	--	--	--	--	--	--	--	--
61	M46	2A13p	32	--	--	--	--	--	--	--	--	--	--	--	--	--	--
62	M46	3AC	66	--	--	--	--	--	--	--	--	--	--	--	--	--	--
63	M46	4Cox	250	--	--	--	--	--	--	--	--	--	--	--	--	--	--
Modesto Formation, lower member, 40 Ka																	
64	M12	A11	15	--	--	--	--	--	--	--	--	--	--	--	--	--	--
65	M12	A12	81	902	49.7	5.12	19.9	2.65	2.73	0.855	1.96	2.43	4.04	2.43	25.1	0.189	344
66	M12	2B21t	102	--	--	--	--	--	--	--	--	--	--	--	--	--	--
67	M12	3B22t	170	738	55.6	4.66	30.1	2.57	2.63	0.651	2.63	--	3.51	1.98	29.3	0.199	347
68	M12	4B3	201	--	--	--	--	--	--	--	--	--	--	--	--	--	--
69	M12	5C1	231	870	43.2	5.64	18.3	2.45	2.54	0.859	2.24	4.02	3.13	2.17	22.0	0.179	311
70	M12	6C2	413+	--	--	--	--	--	--	--	--	--	--	--	--	--	--
Riverbank Formation, upper member, 130 Ka																	
71	R9	A11p	30	971	39.8	6.16	36.2	2.38	2.45	0.829	2.07	2.95	4.36	2.47	20.0	0.208	461
72	R9	A12p	60	--	--	--	--	--	--	--	--	--	--	--	--	--	--
73	R9	B1	105	--	--	--	--	--	--	--	--	--	--	--	--	--	--
74	R9	2B21	180	--	--	--	--	--	--	--	--	--	--	--	--	--	--
75	R9	2B22	235	840	49.4	8.69	41.3	2.88	2.5	0.903	2.49	3.1	3.64	2.33	23.6	0.221	523
76	R9	3B3	350	--	--	--	--	--	--	--	--	--	--	--	--	--	--
77	R9	4C	400+	875	43.6	8.81	18.9	3.31	2.56	0.906	2.65	--	2.71	2.25	21.8	0.197	466
78	R33	A11	4	--	--	--	--	--	--	--	--	--	--	--	--	--	--
79	R33	2A12	19	--	--	--	--	--	--	--	--	--	--	--	--	--	--
80	R33	3A3	39	--	--	--	--	--	--	--	--	--	--	--	--	--	--
81	R33	3B21t	62	--	--	--	--	--	--	--	--	--	--	--	--	--	--
82	R33	3B22t	83	--	--	--	--	--	--	--	--	--	--	--	--	--	--
83	R33	3B23t	122	--	--	--	--	--	--	--	--	--	--	--	--	--	--
84	R33	3B31	151	--	--	--	--	--	--	--	--	--	--	--	--	--	--
85	R33	3B32	210	--	--	--	--	--	--	--	--	--	--	--	--	--	--
86	R33	4B33	260	--	--	--	--	--	--	--	--	--	--	--	--	--	--
87	R33	5Cox	300+	--	--	--	--	--	--	--	--	--	--	--	--	--	--
Riverbank Formation, middle member, 250 Ka																	
88	R2	Ap	25	917	34.0	3.88	18.0	1.86	3.45	0.756	1.70	--	4.84	2.54	16.9	0.189	289
89	R2	B21	81	--	--	--	--	--	--	--	--	--	--	--	--	--	--
90	R2	B22t	185	914	53.1	8.09	37.8	2.97	2.86	0.897	2.69	3.41	4.31	2.41	25.4	0.256	467
91	R2	B3	386	--	--	--	--	--	--	--	--	--	--	--	--	--	--
92	R2	C1	500	--	--	--	--	--	--	--	--	--	--	--	--	--	--
93	R2	C2n	500+	1210	18.5	2.63	3.64	3.67	0.982	0.448	0.843	--	1.26	3.54	11.5	0.066	167
94	R10	A	46	--	--	--	--	--	--	--	--	--	--	--	--	--	--
95	R10	2B1	70	--	--	--	--	--	--	--	--	--	--	--	--	--	--
96	R10	2B21t	140	--	--	--	--	--	--	--	--	--	--	--	--	--	--
97	R10	2B22t	210	--	--	--	--	--	--	--	--	--	--	--	--	--	--
98	R10	3B3t	386	--	--	--	--	--	--	--	--	--	--	--	--	--	--
99	R10	3Cox	500	--	--	--	--	--	--	--	--	--	--	--	--	--	--
100	R32	A11	26	--	--	--	--	--	--	--	--	--	--	--	--	--	--
101	R32	A12	50	--	--	--	--	--	--	--	--	--	--	--	--	--	--
102	R32	A3	70	--	--	--	--	--	--	--	--	--	--	--	--	--	--
103	R32	B21t	105	--	--	--	--	--	--	--	--	--	--	--	--	--	--
104	R32	B22t	150	--	--	--	--	--	--	--	--	--	--	--	--	--	--
105	R32	B31t	220	--	--	--	--	--	--	--	--	--	--	--	--	--	--
106	R32	2B32	354	--	--	--	--	--	--	--	--	--	--	--	--	--	--
107	R32	3Cox	360+	--	--	--	--	--	--	--	--	--	--	--	--	--	--
Riverbank Formation, lower member, 330 Ka																	
108	R30	Ap	65	--	--	--	--	--	--	--	--	--	--	--	--	--	--
109	R30	B10	78	--	--	--	--	--	--	--	--	--	--	--	--	--	--
110	R30	B21t	127	--	--	--	--	--	--	--	--	--	--	--	--	--	--
111	R30	2B22t	179	--	--	--	--	--	--	--	--	--	--	--	--	--	--
112	R30	3B3t	197	--	--	--	--	--	--	--	--	--	--	--	--	--	--
113	R30	3C1ox	220	--	--	--	--	--	--	--	--	--	--	--	--	--	--

Supplementary Table 8, Part 1. Total chemical analyses of the less-than-2-mm fraction by instrumental neutron activation--Continued

No.	Sample	Horizon	Basal depth (cm)	Ba	Ce	Co	Cr	Cs	Dy	Eu	Fe	Gd	Hf	K	La	Lu	Mn
Turlock Lake Formation, 600 Ka																	
114	T2	A	31	1210	42.4	10.0	85.6	2.82	1.96	0.543	2.20	2.56	7.31	3.15	16.9	0.178	605
115	T2	B21	173	--	--	--	--	--	--	--	--	--	--	--	--	--	--
116	T2	2B22	386	739	67.1	8.72	36.0	2.35	4.22	1.25	2.85	3.2	6.75	1.89	33.1	0.339	236
117	T2	3C	417	989	31.4	4.33	25.6	2.45	2.48	0.959	2.08	3.03	2.73	2.57	19.9	0.182	210
118	T6	A11	20	--	--	--	--	--	--	--	--	--	--	--	--	--	--
119	T6	A12	40	--	--	--	--	--	--	--	--	--	--	--	--	--	--
120	T6	2B21t	90	--	--	--	--	--	--	--	--	--	--	--	--	--	--
121	T6	2B22t	190	--	--	--	--	--	--	--	--	--	--	--	--	--	--
122	T6	3B+C	370	--	--	--	--	--	--	--	--	--	--	--	--	--	--
123	T11	A11p	5	--	--	--	--	--	--	--	--	--	--	--	--	--	--
124	T11	2A12p	11	--	--	--	--	--	--	--	--	--	--	--	--	--	--
125	T11	2A+B	20	--	--	--	--	--	--	--	--	--	--	--	--	--	--
126	T11	2B1t	33	--	--	--	--	--	--	--	--	--	--	--	--	--	--
127	T11	2B2t	80	--	--	--	--	--	--	--	--	--	--	--	--	--	--
128	T11	3B31t	191	--	--	--	--	--	--	--	--	--	--	--	--	--	--
129	T11	4B32t	256	--	--	--	--	--	--	--	--	--	--	--	--	--	--
130	T11	5B+C	292	--	--	--	--	--	--	--	--	--	--	--	--	--	--
131	T11	5C1ox	375	--	--	--	--	--	--	--	--	--	--	--	--	--	--
132	T11	61C2ox	375+	--	--	--	--	--	--	--	--	--	--	--	--	--	--
China Hat gravel member of Laguna Formation, 3000 Ka																	
133	CH1	A1	12	666	50.6	7.73	112	3.10	3.18	0.770	2.63	3.5	9.36	1.39	22.3	0.332	342
134	CH1	2A8	53	--	--	--	--	--	--	--	--	--	--	--	--	--	--
135	CH1	2B21t	88	549	64.4	18.4	107	3.77	3.50	0.854	4.17	3.59	8.06	1.14	26.4	0.306	603
136	CH1	2B22t	140	--	--	--	--	--	--	--	--	--	--	--	--	--	--
137	CH1	2B31	234	--	--	--	--	--	--	--	--	--	--	--	--	--	--
138	CH1	2B32	310	--	--	--	--	--	--	--	--	--	--	--	--	--	--
139	CH1	31B33	350	615	24.5	7.54	120	2.48	2.37	0.623	5.40	3.94	3.08	1.14	18.6	0.270	127
140	CH2	A1	8	--	--	--	--	--	--	--	--	--	--	--	--	--	--
141	CH2	A3	30	--	--	--	--	--	--	--	--	--	--	--	--	--	--
142	CH2	2A+B	50	--	--	--	--	--	--	--	--	--	--	--	--	--	--
143	CH2	2B21t	110	--	--	--	--	--	--	--	--	--	--	--	--	--	--
144	CH2	2B22	170	--	--	--	--	--	--	--	--	--	--	--	--	--	--
145	CH2	2B23	200	--	--	--	--	--	--	--	--	--	--	--	--	--	--
146	CH2	3B24	290	--	--	--	--	--	--	--	--	--	--	--	--	--	--
147	CH2	311B3	350+	--	--	--	--	--	--	--	--	--	--	--	--	--	--
148	CH3	A1	9	--	--	--	--	--	--	--	--	--	--	--	--	--	--
149	CH3	A3	35	--	--	--	--	--	--	--	--	--	--	--	--	--	--
150	CH3	A+B	68	--	--	--	--	--	--	--	--	--	--	--	--	--	--
151	CH3	B2t	105	--	--	--	--	--	--	--	--	--	--	--	--	--	--
152	CH3	B22t	153	--	--	--	--	--	--	--	--	--	--	--	--	--	--
153	CH3	2B23	173	--	--	--	--	--	--	--	--	--	--	--	--	--	--
154	CH3	311B24	260	--	--	--	--	--	--	--	--	--	--	--	--	--	--
155	CH3	4V831	340	--	--	--	--	--	--	--	--	--	--	--	--	--	--
156	CH3	5B32	750+	--	--	--	--	--	--	--	--	--	--	--	--	--	--
157	CH4	2B31	750	--	--	--	--	--	--	--	--	--	--	--	--	--	--
158	CH4	4C1ox	1000	--	--	--	--	--	--	--	--	--	--	--	--	--	--

Supplementary Table 8, Part 2. Total chemical analyses of the less-than-2-mm fraction by instrumental neutron activation

[Na values in weight percent; all others in parts per million. Analysts: J. Baker, A. Bartel, D. Burgi, R. Johnson, R. Knight, H.T. Millard, V.G. Mossotti, S. Ramage, B. Scott, J. Taggart, J.S. Wahlberg, and K. Wong]

No.	Sample	Horizon	Basal depth (cm)	Na	Nd	Rb	Sb	Sc	Sm	Sr	Ta	Tb	Th	Tm	U	Yb	Zr
Modern River Alluvium																	
1	MRA1	--	--	--	--	--	--	--	--	--	--	--	--	--	--	--	--
2	MRA2	--	--	--	--	--	--	--	--	--	--	--	--	--	--	--	--
3	MRA3	--	--	--	--	--	--	--	--	--	--	--	--	--	--	--	--
4	MRA4	--	--	--	--	--	--	--	--	--	--	--	--	--	--	--	--
Post-Modesto Deposits, .2 Ka																	
5	PM15	A1	4	--	--	--	--	--	--	--	--	--	--	--	--	--	--
6	PM15	2C1ox	19	--	--	--	--	--	--	--	--	--	--	--	--	--	--
7	PM15	3C2ox	42	--	--	--	--	--	--	--	--	--	--	--	--	--	--
8	PM15	4C3ox	47	--	--	--	--	--	--	--	--	--	--	--	--	--	--
9	PM15	5C4ox	51	--	--	--	--	--	--	--	--	--	--	--	--	--	--
10	PM15	6C5ox	51+	--	--	--	--	--	--	--	--	--	--	--	--	--	--
11	PM19	A11	7	--	--	--	--	--	--	--	--	--	--	--	--	--	--
12	PM19	2A12	12	--	--	--	--	--	--	--	--	--	--	--	--	--	--
13	PM19	3C1ox	23	--	--	--	--	--	--	--	--	--	--	--	--	--	--
14	PM19	4C2ox	43	--	--	--	--	--	--	--	--	--	--	--	--	--	--
15	PM19	5C3ox	49	--	--	--	--	--	--	--	--	--	--	--	--	--	--
16	PM19	6C4n	55	--	--	--	--	--	--	--	--	--	--	--	--	--	--
17	PM19	7C5n	66	--	--	--	--	--	--	--	--	--	--	--	--	--	--
18	PM19	8C6n	80+	--	--	--	--	--	--	--	--	--	--	--	--	--	--
Post-Modesto Deposits, 3 Ka																	
19	PM8	A1	32	1.35	23.6	93.6	0.995	16.9	4.76	227	0.864	0.628	10.3	0.362	6.03	2.31	167
20	PM8	2C1	55	1.58	22.9	87.1	0.903	16.1	4.92	258	0.911	0.535	11.2	0.429	5.77	2.15	223
21	PM8	3C2	66	--	--	--	--	--	--	--	--	--	--	--	--	--	--
22	PM8	4C3	76+	1.96	14.2	80.7	0.526	0.890	2.96	302	0.611	0.335	6.75	--	3.85	1.26	89.2
23	PM13	A11	5	--	--	--	--	--	--	--	--	--	--	--	--	--	--
24	PM13	A12	35	--	--	--	--	--	--	--	--	--	--	--	--	--	--
25	PM13	2C1ox	86	--	--	--	--	--	--	--	--	--	--	--	--	--	--
26	PM13	3C2ox	112	--	--	--	--	--	--	--	--	--	--	--	--	--	--
27	PM13	4C3ox	136	--	--	--	--	--	--	--	--	--	--	--	--	--	--
28	PM13	5C4ox	200	--	--	--	--	--	--	--	--	--	--	--	--	--	--
29	PM13	6C5n	720	--	--	--	--	--	--	--	--	--	--	--	--	--	--
30	PM14	A11	3	--	--	--	--	--	--	--	--	--	--	--	--	--	--
31	PM14	2A12	33	--	--	--	--	--	--	--	--	--	--	--	--	--	--
32	PM14	3C1ox	99	--	--	--	--	--	--	--	--	--	--	--	--	--	--
33	PM14	4C2ox	130	--	--	--	--	--	--	--	--	--	--	--	--	--	--
34	PM14	5C3ox	175	--	--	--	--	--	--	--	--	--	--	--	--	--	--
35	PM14	6C4ox	200	--	--	--	--	--	--	--	--	--	--	--	--	--	--
36	PM14	7C5n	239+	--	--	--	--	--	--	--	--	--	--	--	--	--	--
37	PM16	A	2	--	--	--	--	--	--	--	--	--	--	--	--	--	--
38	PM16	C1ox	25	--	--	--	--	--	--	--	--	--	--	--	--	--	--
39	PM16	2C2ox	35	--	--	--	--	--	--	--	--	--	--	--	--	--	--
40	PM16	3C3ox	65	--	--	--	--	--	--	--	--	--	--	--	--	--	--
41	PM16	4C4ox	90	--	--	--	--	--	--	--	--	--	--	--	--	--	--
42	PM16	5C5ox	116	--	--	--	--	--	--	--	--	--	--	--	--	--	--
43	PM16	5C6n	236	--	--	--	--	--	--	--	--	--	--	--	--	--	--
44	PM17	A	6	--	--	--	--	--	--	--	--	--	--	--	--	--	--
45	PM17	2C2ox	45	--	--	--	--	--	--	--	--	--	--	--	--	--	--
46	PM17	2C2ox	63	--	--	--	--	--	--	--	--	--	--	--	--	--	--
47	PM17	2C3ox	74	--	--	--	--	--	--	--	--	--	--	--	--	--	--
48	PM17	3C4n	120+	--	--	--	--	--	--	--	--	--	--	--	--	--	--
49	PM18	A	6	--	--	--	--	--	--	--	--	--	--	--	--	--	--
50	PM18	2C1ox	65	--	--	--	--	--	--	--	--	--	--	--	--	--	--
51	PM18	2C2ox	115	--	--	--	--	--	--	--	--	--	--	--	--	--	--
52	PM18	3C3ox	164	--	--	--	--	--	--	--	--	--	--	--	--	--	--
53	PM18	4C4ox	175+	--	--	--	--	--	--	--	--	--	--	--	--	--	--

Supplementary Table 8, Part 2. Total chemical analyses of the less-than-2-mm fraction by instrumental neutron activation--Continued

No.	Sample	Horizon	Basal depth (cm)	Na	Nd	Rb	Sb	Sc	Sm	Sr	Ta	Tb	Th	Tm	U	Yb	Zr
Modesto Formation, upper member, 10 Ka																	
54	M31	A11	20	--	--	--	--	--	--	--	--	--	--	--	--	--	--
55	M31	A12	63	--	--	--	--	--	--	--	--	--	--	--	--	--	--
56	M31	AC	150	--	--	--	--	--	--	--	--	--	--	--	--	--	--
57	M31	2C1	200	--	--	--	--	--	--	--	--	--	--	--	--	--	--
58	M31	3C2	254	--	--	--	--	--	--	--	--	--	--	--	--	--	--
59	M46	A11p	5	--	--	--	--	--	--	--	--	--	--	--	--	--	--
60	M46	A12p	14	--	--	--	--	--	--	--	--	--	--	--	--	--	--
61	M46	2A13p	32	--	--	--	--	--	--	--	--	--	--	--	--	--	--
62	M46	3AC	66	--	--	--	--	--	--	--	--	--	--	--	--	--	--
63	M46	4Cox	250	--	--	--	--	--	--	--	--	--	--	--	--	--	--
Modesto Formation, lower member, 40 Ka																	
64	M12	A11	15	--	--	--	--	--	--	--	--	--	--	--	--	--	--
65	M12	A12	81	2.31	21.2	95.4	0.695	4.89	3.77	370	0.895	0.373	9.81	0.20	3.20	1.42	120
66	M12	2B21t	102	--	--	--	--	--	--	--	--	--	--	--	--	--	--
67	M12	3B22t	170	1.98	24.0	82.5	0.448	7.29	4.14	313	0.778	0.436	13.6	0.271	3.95	1.37	132
68	M12	4B3	201	--	--	--	--	--	--	--	--	--	--	--	--	--	--
69	M12	5C1	231	2.40	19.2	85.6	0.494	5.21	3.03	421	0.726	0.318	11.1	--	3.11	1.15	88.1
70	M12	6C2	413+	--	--	--	--	--	--	--	--	--	--	--	--	--	--
Riverbank Formation, upper member, 130 Ka																	
71	R9	A11p	30	1.94	18.8	96.4	0.491	5.41	3.46	300	0.817	0.321	12.0	0.170	3.18	1.20	132
72	R9	A12p	60	--	--	--	--	--	--	--	--	--	--	--	--	--	148
73	R9	B1	105	--	--	--	--	--	--	--	--	--	--	--	--	--	127
74	R9	2B21	180	--	--	--	--	--	--	--	--	--	--	--	--	--	124
75	R9	2B22	235	1.60	22.8	93.5	0.534	7.06	3.92	254	0.862	0.380	9.42	--	2.84	1.25	111
76	R9	3B3	350	--	--	--	--	--	--	--	--	--	--	--	--	--	101
77	R9	4C	400+	2.38	20.0	83.0	0.614	7.86	3.49	418	0.570	0.369	11.3	--	2.47	1.25	863
78	R33	A11	4	--	--	--	--	--	--	--	--	--	--	--	--	--	168
79	R33	2A12	19	--	--	--	--	--	--	--	--	--	--	--	--	--	--
80	R33	3A3	39	--	--	--	--	--	--	--	--	--	--	--	--	--	--
81	R33	3B21t	62	--	--	--	--	--	--	--	--	--	--	--	--	--	--
82	R33	3B22t	83	--	--	--	--	--	--	--	--	--	--	--	--	--	--
83	R33	3B23t	122	--	--	--	--	--	--	--	--	--	--	--	--	--	127
84	R33	3B31	151	--	--	--	--	--	--	--	--	--	--	--	--	--	--
85	R33	3B32	210	--	--	--	--	--	--	--	--	--	--	--	--	--	--
86	R33	4B33	260	--	--	--	--	--	--	--	--	--	--	--	--	--	--
87	R33	5Cox	300+	--	--	--	--	--	--	--	--	--	--	--	--	--	61
Riverbank Formation, middle member, 250 Ka																	
88	R2	Ap	25	1.87	18.8	89.4	0.533	3.58	3.09	308	0.819	0.332	8.85	0.192	2.61	1.23	158
89	R2	B21	81	--	--	--	--	--	--	--	--	--	--	--	--	--	143
90	R2	B22t	185	1.43	23.9	99.8	0.674	6.80	4.32	253	0.929	0.397	11.2	--	3.84	1.71	134
91	R2	B3	386	--	--	--	--	--	--	--	--	--	--	--	--	--	98
92	R2	C1	500	--	--	--	--	--	--	--	--	--	--	--	--	--	77
93	R2	C2n	500+	2.60	7.20	136	0.829	1.63	1.21	451	0.271	0.098	5.22	--	1.66	0.421	53
94	R10	A	46	--	--	--	--	--	--	--	--	--	--	--	--	--	--
95	R10	2B1	70	--	--	--	--	--	--	--	--	--	--	--	--	--	149
96	R10	2B21t	140	--	--	--	--	--	--	--	--	--	--	--	--	--	--
97	R10	2B22t	210	--	--	--	--	--	--	--	--	--	--	--	--	--	124
98	R10	3B3t	386	--	--	--	--	--	--	--	--	--	--	--	--	--	--
99	R10	3Cox	500	--	--	--	--	--	--	--	--	--	--	--	--	--	--
100	R32	A11	26	--	--	--	--	--	--	--	--	--	--	--	--	--	186
101	R32	A12	50	--	--	--	--	--	--	--	--	--	--	--	--	--	--
102	R32	A3	70	--	--	--	--	--	--	--	--	--	--	--	--	--	--
103	R32	B21t	105	--	--	--	--	--	--	--	--	--	--	--	--	--	--
104	R32	B22t	150	--	--	--	--	--	--	--	--	--	--	--	--	--	173
105	R32	B31t	220	--	--	--	--	--	--	--	--	--	--	--	--	--	--
106	R32	2B32	354	--	--	--	--	--	--	--	--	--	--	--	--	--	--
107	R32	3Cox	360+	--	--	--	--	--	--	--	--	--	--	--	--	--	101
Riverbank Formation, lower member, 330 Ka																	
108	R30	Ap	65	--	--	--	--	--	--	--	--	--	--	--	--	--	--
109	R30	B10	78	--	--	--	--	--	--	--	--	--	--	--	--	--	--
110	R30	B21t	127	--	--	--	--	--	--	--	--	--	--	--	--	--	--
111	R30	2B22t	179	--	--	--	--	--	--	--	--	--	--	--	--	--	--
112	R30	3B2c	197	--	--	--	--	--	--	--	--	--	--	--	--	--	--
113	R30	3C1ox	220	--	--	--	--	--	--	--	--	--	--	--	--	--	--

Supplementary Table 8, Part 2. Total chemical analyses of the less-than-2-mm fraction by instrumental neutron activation--Continued

No.	Sample	Horizon	Basal depth (cm)	Na	Nd	Rb	Sb	Sc	Sm	Sr	Ta	Tb	Th	Tm	U	Yb	Zr
Turlock Lake Formation, 600 Ka																	
114	T2	A	31	0.812	13.3	124	0.547	4.31	2.42	197.	0.780	0.285	8.54	--	2.29	1.12	228
115	T2	B21	173	--	--	--	--	--	--	--	--	--	--	--	--	--	--
116	T2	2B22	386	1.94	30.8	79	0.587	8.23	5.50	313.	0.986	0.598	16.1	--	3.53	1.90	214
117	T2	3C	417	1.97	22.0	109	0.550	3.81	3.64	324.	0.822	0.371	11.6	0.177	2.49	1.16	86.5
118	T6	A11	20	--	--	--	--	--	--	--	--	--	--	--	--	--	123
119	T6	A12	40	--	--	--	--	--	--	--	--	--	--	--	--	--	147
120	T6	2B21t	90	--	--	--	--	--	--	--	--	--	--	--	--	--	77
121	T6	2B22t	190	--	--	--	--	--	--	--	--	--	--	--	--	--	76
122	T6	3B+C	370	--	--	--	--	--	--	--	--	--	--	--	--	--	70
123	T11	A11p	5	--	--	--	--	--	--	--	--	--	--	--	--	--	--
124	T11	2A12p	11	--	--	--	--	--	--	--	--	--	--	--	--	--	166
125	T11	2A+B	20	--	--	--	--	--	--	--	--	--	--	--	--	--	--
126	T11	2B1t	33	--	--	--	--	--	--	--	--	--	--	--	--	--	144
127	T11	2B2t	80	--	--	--	--	--	--	--	--	--	--	--	--	--	--
128	T11	3B31t	191	--	--	--	--	--	--	--	--	--	--	--	--	--	--
129	T11	4B32t	256	--	--	--	--	--	--	--	--	--	--	--	--	--	--
130	T11	5B+C	292	--	--	--	--	--	--	--	--	--	--	--	--	--	--
131	T11	5C1ox	375	--	--	--	--	--	--	--	--	--	--	--	--	--	--
132	T11	61C2ox	375+	--	--	--	--	--	--	--	--	--	--	--	--	--	83
China Hat gravel member of Laguna Formation, 3,000 Ka																	
133	CH1	A1	12	0.453	22.4	78.8	0.822	7.91	3.65	65.1	0.882	0.460	10.1	0.38	3.73	1.90	292
134	CH1	2A8	53	--	--	--	--	--	--	--	--	--	--	--	--	--	--
135	CH1	2B21t	88	0.341	23.2	66.2	1.12	12.2	4.08	--	1.08	0.454	12.6	0.16	4.42	2.03	241
135	CH1	2B22t	140	--	--	--	--	--	--	--	--	--	--	--	--	--	--
137	CH1	2B31	234	--	--	--	--	--	--	--	--	--	--	--	--	--	--
138	CH1	2B32	310	--	--	--	--	--	--	--	--	--	--	--	--	--	--
139	CH1	31B33	350	0.067	15.1	49.3	1.27	22.2	2.85	77.3	0.722	0.335	9.99	--	4.25	1.49	142
140	CH2	A1	8	--	--	--	--	--	--	--	--	--	--	--	--	--	--
141	CH2	A3	30	--	--	--	--	--	--	--	--	--	--	--	--	--	--
142	CH2	2A+B	50	--	--	--	--	--	--	--	--	--	--	--	--	--	--
143	CH2	2B21t	110	--	--	--	--	--	--	--	--	--	--	--	--	--	--
144	CH2	2B22	170	--	--	--	--	--	--	--	--	--	--	--	--	--	--
145	CH2	2B23	200	--	--	--	--	--	--	--	--	--	--	--	--	--	--
146	CH2	3B24	290	--	--	--	--	--	--	--	--	--	--	--	--	--	--
147	CH2	311B3	350+	--	--	--	--	--	--	--	--	--	--	--	--	--	--
148	CH3	A1	9	--	--	--	--	--	--	--	--	--	--	--	--	--	--
149	CH3	A3	35	--	--	--	--	--	--	--	--	--	--	--	--	--	--
150	CH3	A+B	68	--	--	--	--	--	--	--	--	--	--	--	--	--	--
151	CH3	B2t	105	--	--	--	--	--	--	--	--	--	--	--	--	--	--
152	CH3	B22t	153	--	--	--	--	--	--	--	--	--	--	--	--	--	--
153	CH3	2B23	173	--	--	--	--	--	--	--	--	--	--	--	--	--	--
154	CH3	311B24	260	--	--	--	--	--	--	--	--	--	--	--	--	--	--
155	CH3	4VB31	340	--	--	--	--	--	--	--	--	--	--	--	--	--	--
156	CH3	5B32	750+	--	--	--	--	--	--	--	--	--	--	--	--	--	--
157	CH4	2B31	750	--	--	--	--	--	--	--	--	--	--	--	--	--	--
158	CH4	4C1ox	1000	--	--	--	--	--	--	--	--	--	--	--	--	--	--

